Electrochemical Energy Reviews (2018) 1:483–530
https://doi.org/10.1007/s41918-018-0014-z

REVIEW ARTICLE

Recent Progresses in Electrocatalysts for Water Electrolysis

Muhammad Arif Khan[1,2] · Hongbin Zhao[1] · Wenwen Zou[1] · Zhe Chen[1] · Wenjuan Cao[1] · Jianhui Fang[1] · Jiaqiang Xu[1] · Lei Zhang[1,3] · Jiujun Zhang[1,4]

Received: 5 June 2018 / Revised: 26 June 2018 / Accepted: 3 July 2018 / Published online: 28 July 2018

Abstract
The study of hydrogen evolution reaction and oxygen evolution reaction electrocatalysts for water electrolysis is a developing field in which noble metal-based materials are commonly used. However, the associated high cost and low abundance of noble metals limit their practical application. Non-noble metal catalysts, aside from being inexpensive, highly abundant and environmental friendly, can possess high electrical conductivity, good structural tunability and comparable electrocatalytic performances to state-of-the-art noble metals, particularly in alkaline media, making them desirable candidates to reduce or replace noble metals as promising electrocatalysts for water electrolysis. This article will review and provide an overview of the fundamental knowledge related to water electrolysis with a focus on the development and progress of non-noble metal-based electrocatalysts in alkaline, polymer exchange membrane and solid oxide electrolysis. A critical analysis of the various catalysts currently available is also provided with discussions on current challenges and future perspectives. In addition, to facilitate future research and development, several possible research directions to overcome these challenges are provided in this article.

Keywords Electrocatalysts · Water electrolysis · Hydrogen generation · Energy storage · Proton exchange membrane · Alkaline media · Solid oxide electrolysis · Oxygen evolution · Hydrogen evolution

PACS 81.16.Hc- Catalytic methods

1 Introduction

Energy is a necessity for the economic and social development of the world, and currently, ~65% of the global energy demand is fulfilled by non-renewable fossil fuels [1–3]. This fossil fuel consumption emits harmful greenhouse gasses such as CO_2 gas, causing global warming and inducing a series of associated environmental damages. To deal with the diminishing supply of fossil fuels and the increase in CO_2 emissions, at least 10 TW of renewable energy must be produced by 2050 [4–7], with sources from solar, wind, hydroelectricity, biomass, ocean thermal and sea wave/tide, etc. In conjunction to the exploration of renewable energy sources, energy storage technologies must be developed as well. Currently, there are several viable energy storage technologies with electrochemical technology being recognized as the most feasible and effective method in the storage and conversion of renewable energy. Electrochemical technologies include methods such as batteries, electrolysis, compressed air, fly wheels, pumped hydroelectricity, magnetic superconductors. Because H_2 is the ultimate energy carrier in which produced H_2 can be converted to electricity by using fuel cell technologies, the use of renewable electricity to electrolyse water for the production of hydrogen (H_2) is the ultimate method of energy storage among the different available electrochemical energy technologies. Therefore, the development of water electrolysis technologies for H_2 production is of great urgency and importance [8–10].

✉ Hongbin Zhao
hongbinzhao@shu.edu.cn

✉ Jiujun Zhang
jiujun@shaw.ca; jiujun.zhang@i.shu.edu.cn

1 Department of Chemistry, College of Sciences, Shanghai University, Shanghai 200444, China

2 School of Materials Science and Engineering, Shanghai University, Shanghai 200444, China

3 Energy, Mining and Environment, National Research Council of Canada, Vancouver V6T 1W5, Canada

4 Institute for Sustainable Energy, Shanghai University, Shanghai 200444, China

1.1 Hydrogen Production from Different Fuel Sources

Hydrogen, possessing the highest specific energy content of 122 kJ g^{-1}, has a 2.5 times higher specific energy content than hydrocarbons. Currently, the total global hydrogen production is about 500 billion cubic metre (b m^3), of which the majority is used in ammonia synthesis, petroleum refining and metal refining [11]. Hydrogen can be produced from many sources, and the various sources for hydrogen energy production along with associated advantages and disadvantages are provided in Table 1 [12–16]. The ratio of hydrogen production from various sources are roughly 48% from natural gas, 30% from oils, 18% from coal and only 4% from electrolysis [8, 9].

1.2 Hydrogen Production from Water Electrolysis

In terms of environmental impact and sustainability, water electrolysis is the best method of hydrogen production because it utilizes renewable H_2O and the only by-product is pure oxygen, which has no negative environmental effects. In addition, the consumed electricity in the electrolysis process can come from sustainable sources such as solar, wind, biomass. In electrolysis, water molecules are split into hydrogen and oxygen through the application of electricity and the cost of H_2 energy production is mainly determined by the cost of electricity [4, 15, 17]. In Table 2, [17, 18] present and future costs of hydrogen production from electrolysis using different electricity sources are compared, and environmental impacts of the various electrolysis techniques are listed.

From Table 2, it can be seen that electrolysis using hydropower is the most reliable method of hydrogen production with the lowest production costs. Although hydrogen is a sustainable alternative for fossil fuels, challenges associated with this strategy remain. These challenges mainly include the high cost of production and the difficulty in storage due to the impossible liquification of hydrogen at room temperature [8, 18, 19].

Table 1 Hydrogen production from various sources and associated process mechanisms, efficiencies, costs as well as advantages/disadvantages [12–16]

Source	Mechanism	Advantages	Disadvantages	Hydrogen cost ($ kg^{-1})	Efficiency %
Steam methane reforming (SMR)	Bio gas + steam → $H_2 + CO_2$	Most developed technology Existing infrastructure	Geopolitical tension Pollution (CO, CO_2) Unstable supply	2.27	74~85
Gasification of coal	$C_2H_4 + O_2 \rightarrow CO + H_2$		Along with H_2, the production of heavy oils, petroleum and coke can occur H_2 production depends on season	1.48	60~75
Hydrogen from biomass		Less expensive Dependent on renewable sources Other useful products can be obtained such as adhesives, polymers, fertilizers.	Not entirely clean source because of methane gas as by-product Risk of deforestation Inefficient as compared to fossil fuels	2.05	35~50
Nuclear energy		Less carbon production	Mining and processing of uranium Disposal of radioactive waste Potential for accidents	4~7	45~50
Water electrolysis	$2H_2O \rightarrow 2H_2 + O_2$	Zero emission Proven technology Existing infrastructure By-product is O_2	Transportation problem Storage problem Applicable only to special purposes	10~23	40~60

Table 2 Comparison of various electricity sources for water electrolysis [17, 18]

Electricity source	Present cost ($ kg^{-1})	Future cost ($ kg^{-1})	Efficiency %	CO_2 emission (kg CO_2 kg^{-1} H_2)
Wind	7~11	3~4	21	0
Solar	10~30	3~4	20	0
Hydro	1.4	–	25	0
Nuclear	4.15~7	2.45~2.63	45	0

1.3 Classification of Water Electrolysis Technologies

Water electrolysis can be classified into three main types depending on the types of electrolyte, operating temperatures and ionic agents. As shown in Fig. 1, the three types of electrolysis technologies are (a) alkaline electrolysis, (b) solid oxide electrolysis and (c) proton exchange membrane electrolysis. Table 3 lists the three types of water electrolysis technologies, their corresponding operation temperature ranges, as well as their advantages and disadvantages.

1.3.1 Alkaline Electrolysis Cell (AEC)

Troostwijik and Diemann first discovered the electrolysis phenomenon in 1789 [20, 21], and currently, the most mature hydrogen production technology is alkaline electrolysis (Fig. 1a) [22], which is being used on a global commercial scale. In alkaline electrolysis, two electrodes are immersed in a liquid alkaline solution of 20%~30% KOH caustic soda. At the anode, water oxidation occurs to produce O_2; and at the cathode, water reduction occurs to produce H_2. A diaphragm is present in the middle to separate the product gases from each other, avoiding the mixing of hydrogen with oxygen [23]. Alkaline electrolysis possesses several drawbacks such as limited electrolysis current densities, low partial loads and low operating pressures, which can lead to low energy efficiencies [24].

1.3.2 Solid Oxide Electrolysis Cell (SOEC)

The first ever solid oxide electrolysis cell (SOEC) was reported in the 1980s by Donitz and Erdle. Currently, the technology is still immature and further research is required. However, SOECs have been demonstrated to possess high hydrogen production efficiencies [25] and scientists believe that they have the potential to be applied on a commercial scale. Currently, the major focus in SOEC development is the exploration of novel, low-cost and durable materials [26].

1.3.3 Proton Exchange Membrane Electrolysis Cell (PEMEC)

To address the challenges of alkaline electrolysis cells, polymer membrane electrolysis was developed in 1960 for space applications [27]. This concept was further advanced by the use of solid sulphonated polystyrene membranes as an

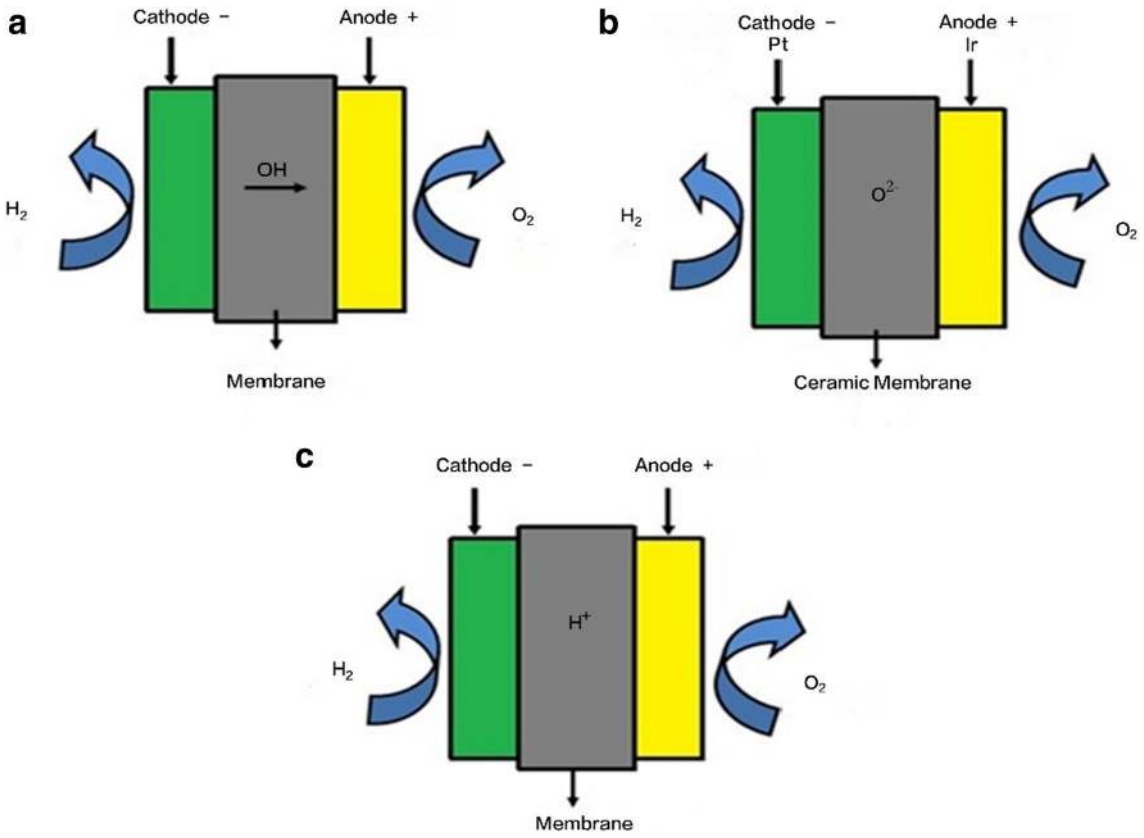

Fig. 1 Schematic illustration of **a** alkaline electrolysis, **b** solid oxide electrolysis, **c** proton exchange membrane electrolysis

Table 3 Comparison of the three types of technology for water electrolysis [27–29]

Type of electrolysers	Operating temperature (°C)	Advantages	Disadvantages
Alkaline	40~90	Developed technology	Current density is low
		Less expensive catalysts	Low partial load range
		Long-term stability	Liquid electrolyte can cause corrosion
		Cheap	Crossover of gases
Solid oxide	500~1000	100% efficiency	Laboratory-scale production
		Non-noble catalysts	Bulky system
		Possible high-pressure operation	Brittle system because of ceramic catalysts
			Operation at elevated temperatures
Proton exchange membrane	20~100	High current density	Mostly precious metal catalysts
		High gas purity	Corrosive acidic environment
		High voltage efficiency	
		Component design	
		Good partial load range	

electrolyte. These types of membranes, known as polymer electrolyte membranes or solid polymer electrolyte membranes, are used for water electrolysis in PEMECs [27–31] and can be as low as 20~300 μm in thickness, resulting in many advantages such as low gas crossover, high proton conductivity, high-pressure operations and very compact designs.

1.4 Electrocatalysis of Water Electrolysis Reactions

In water electrolysis, water reduction at the cathode to produce H_2 and water oxidation at the anode to produce O_2 are in general kinetically sluggish, leading to low energy efficiencies. Therefore, electrocatalysts are necessary at the electrodes to speed up reaction kinetics. Electrocatalysis in water electrolysis is the biggest challenge for both low-temperature alkaline electrolysis and proton exchange membrane electrolysis. Although great progress has been made in recent years, catalyst performances are still insufficient in terms of both catalytic activity and stability. To facilitate the research and development of advanced electrocatalysts, this article will review the most recent progresses in catalyst synthesis, characterization and performance [32, 33].

1.4.1 Electrochemical Reactions in Water Electrolysis

With regard to the catalytic process of water electrolysis, the overall reaction consists of two electrochemical half-reactions. These two reactions are the oxygen evolution reaction (OER) at the anode and the hydrogen evolution reaction (HER) at the cathode [32–34]. At the anode, water is oxidized to produce O_2 as expressed by reactions (1)–(3) for the three types of water electrolysis indicated in Fig. 1:

$$2H_2O \rightarrow O_2 + 4H^+ + 4e^-\text{(Proton exchange membrane electrolysis at low temperatures)} \quad (1)$$

$$4OH^- \rightarrow 2H_2O + O_2 + 4e^-\text{(Alkaline electrolysis at low temperatures)} \quad (2)$$

$$2O^{2-} \rightarrow O_2 + 4e^-\text{(Solid oxide electrolysis at high temperatures)} \quad (3)$$

At the cathode, water is reduced to produce H_2 as expressed by reactions (4)–(6) for three types of water electrolysis indicated in Fig. 1:

$$2H^+ + 2e^- \rightarrow H_2\text{ (Proton exchange membrane electrolysis at low temperatures)} \quad (4)$$

$$2H_2O + 2e^- \rightarrow H_2 + 2OH^-\text{(Alkaline electrolysis at low temperatures)} \quad (5)$$

$$H_2O + 2e^- \rightarrow H_2 + O^{2-}\text{(Solid oxide electrolysis at high temperatures)} \quad (6)$$

The overall reaction of the three electrolysis processes can all be expressed as Eq. (7) with a standard cell voltage of 1.23 V:

$$2H_2O \rightarrow O_2 + 2H_2 \quad (7)$$

Here, it should be emphasized that the standard cell voltage of 1.23 V is in the case of standard thermodynamic conditions (1.0 atm and 25 °C), and not for other conditions.

Regarding the OER and HER kinetics, the OER is normally much slower than the HER, as indicated by the higher overpotential of the OER at the anode than that of the HER at the cathode. However, the overpotentials of the OER and the HER can both contribute to the limitations of overall energy efficiency for water electrolysis [35–37].

To reduce overpotentials and improve energy efficiencies, both OER and HER kinetics must be increased by using electrocatalysts in the electrolysis process, and in general, both OER and HER electrocatalysts are applied onto their corresponding electrodes. In latter sections of this article, these electrocatalysts will be reviewed in detail, and their properties and performance will be discussed.

1.4.2 Requirements for Electrocatalysts for Water Electrolysis

As discussed above, although the energy efficiency of water electrolysis is based on both the OER and the HER, the contribution of the OER is much greater than that of the HER. This is because the reaction overpotential of the OER is much higher than that of the HER. This higher overpotential is mainly caused by the multi-electron transfer reaction of the OER, involving several multi-step element reactions in which one rate-determining step dominates the overall reaction rate. Therefore, the role of an electrocatalyst is to speed up this rate-determining step, resulting in higher OER or HER rates and, subsequently, higher energy efficiencies [35, 36, 38–40].

In general, electrocatalysts for water electrolysis should possess several properties: (1) a highly active surface that provides good accessibility to reactants and can assist in the fast removal of products; (2) a high electrical conductivity; (3) be chemically/electrochemically/mechanically stable; and (4) provide low intrinsic overpotentials for OERs and/or HERs [41, 42].

For alkaline electrolyte electrolysis, the need for catalysts is not as critical as those of acidic electrolyte electrolysis (proton exchange membrane electrolysis) or solid oxide electrolysis. For example, less expensive transition metal oxides can be extensively used as catalysts for alkaline electrolysis, but expensive noble metal catalysts are required for proton exchange membrane electrolysis.

2 Electrocatalysts for OER in Alkaline Electrolysis

2.1 Noble Metal Catalysts

The most commonly used metals for noble metal catalysts are Ir and Ru because of their high stability, low Tafel value and small overpotential. Pt and Pd have also been used but their performance is lower in which the order of performance for these metals are as follows: Ru > Ir > Pt > Pd. Although Ru demonstrates superior performance, its practical applicability is hindered by its lower stability as compared with the other catalysts [43, 44]. In addition, Ir and Ru oxides (RuO_2 and IrO_2) are much more active and stable in basic media than their pure metal counterparts because pure Ir and Ru are more soluble than oxides in basic electrolytes, leading to decreased stability and potential in basic electrolytes for commercial scale applications [45–49].

In general, porous structures with extremely large specific surface areas can offer numerous benefits for charge and mass transport in electrochemistry. Therefore, noble metal catalysts, possessing porous structures, demonstrate good catalytic activities for OERs [50–52]. To synthesize porous noble metal catalysts, template synthesis routes have been adopted by researchers and the most commonly used templates are polymeric or inorganic beads such as polystyrene (PS), and poly (methyl methacrylate) or silica spheres. For example, in a study conducted by Lee et al. [53], catalytic performances were increased by decorating Ir onto the surface of carbon with Ir and graphene oxide (GO) as precursors and polystyrene (PS) as the template (Fig. 2a–e). In this process, the GO was deposited onto the surface of the PS, and Ir ions were adsorbed onto the surface of the GO. And in addition to the intrinsically high conductivity of the GO, the addition of the GO increased the electrochemical surface area of the resulting catalyst by 6 orders of magnitude, resulting in enhanced catalytic performances in which a current density of 89.99 mA cm^{-2} was obtained at a potential of 1.6 V in their testing.

Because the use of noble metals can increase the cost of hydrogen energy production, reducing the usage quantity of such noble metal-based catalysts is necessary for OER processes to become more economical. Based on this, an effective strategy is to use metal nanoparticles (NPs), such as Ag, Au, Pt, Ru, RuO_2, Ir, IrO_2 and NiRuP, to coat the surface of carbon. The reason for this is because researchers have found that the electrocatalytic properties of NPs are far more superior to bulk systems. Furthermore, performances can be further improved if bimetallic NPs were formed on carbon surfaces, in which the catalytic performance improvements can be attributed to the generation of NPs forming active sites for rapid water dissociation and fast electron transfer [54–57].

In a recent study by Li et al. [58], efforts were made to enhance the intrinsic activity and durability of an Ir and Ru oxide-based catalyst in which a discontinuous IrO_2 layer was supported on the surface of RuO_2@Ru. Here, outstanding OER activities were observed because of a combination of high activities from both RuO_2 and IrO_2. In this study, as shown in Fig. 3a, $RuCl_3$ was reduced to metallic Ru, which initiated the synthesis process, acting as a support for the H_2IrCl_6 precursor. The supported IrO_2–RuO_2@Ru was subsequently obtained through hydrolysis and thermal treatment and in electrochemical testing, achieved a current density of 10 mA cm^{-2} with an overpotential of only 281 mV, which was superior to alloyed Ir_3RuO_2 and IrO_2 crystals.

In another example, Liyanage et al. [59] developed a synthesis process to prepare ternary metal phosphide

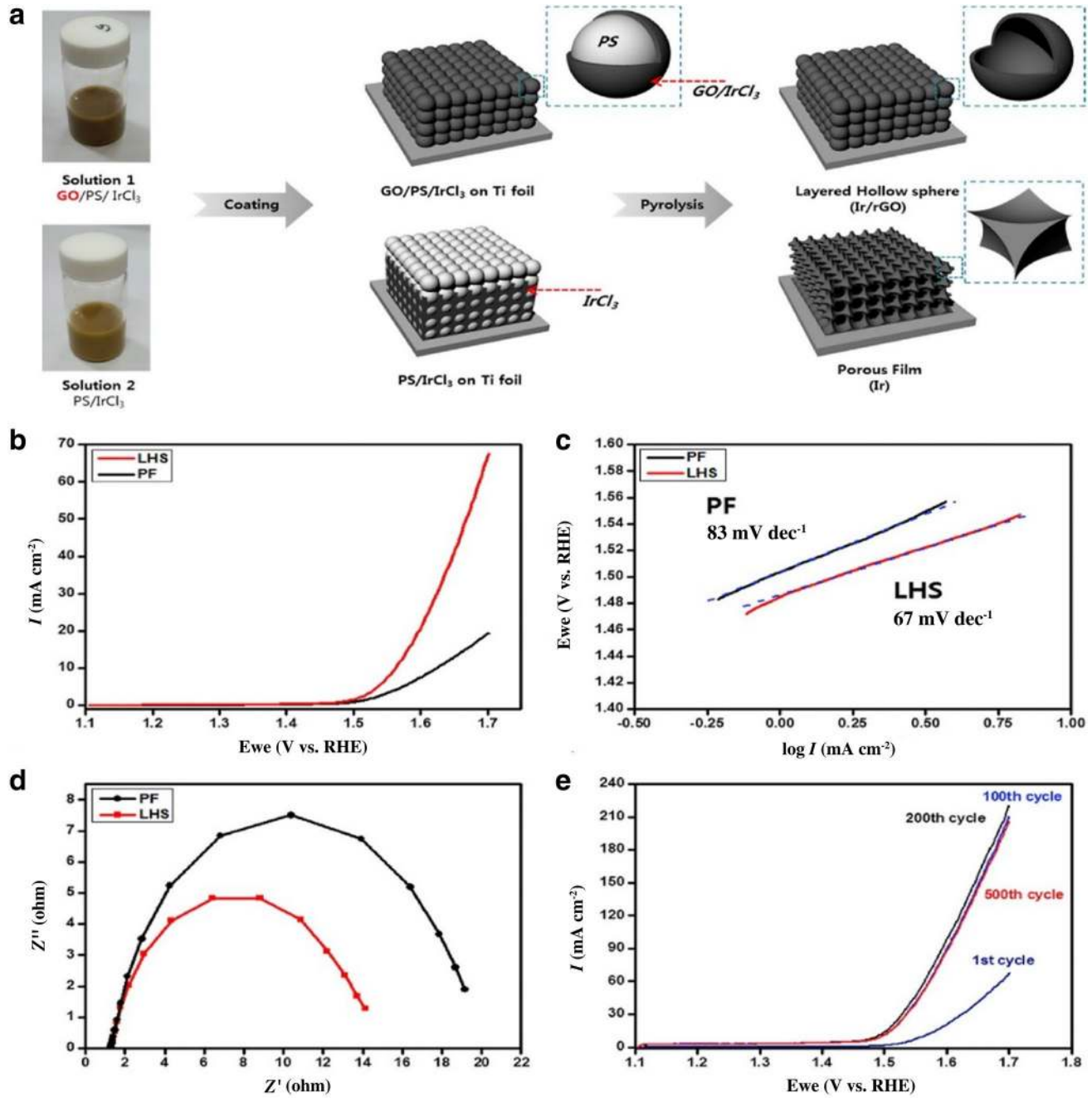

Fig. 2 **a** Schematic illustration of the formation of a layered hollow sphere electrode and a porous film electrode. **b** OER activity comparison between layered hollow spheres (LHS) and porous film (PF) electrodes. **c** Tafel plots. **d** Electrochemical impedance spectroscopy (EIS) of the LHS and PF electrodes. **e** OER activity of the LHS electrode according to cycle numbers [53]

nanoparticles ($Ni_{2-x}Ru_xP$) to create an efficient, low-cost noble metal catalyst for the OER. This composite of Ru and highly active but inexpensive Ni metal was considered by the researchers to be a state-of-the-art catalyst for the OER and its morphology was evaluated by using the TEM. The corresponding images of each composition are shown in Fig. 3b. In the evaluations of this catalyst, the Ni-rich composite was found to possess a spherical morphology that shifted from spherical to elongated nanoparticles with increasing Ru amounts. The catalyst also demonstrated an OER activity comparable to that of RuO_2 and IrO_2 (an overpotential of 340 mV at a current density of 10 mA cm^{-2}) (Fig. 3c).

Although the various strategies of decreasing noble metal loading and changing morphologies by using templates are shown to provide improvements, they are still not effective enough because the cost of noble metals are ever-increasing.

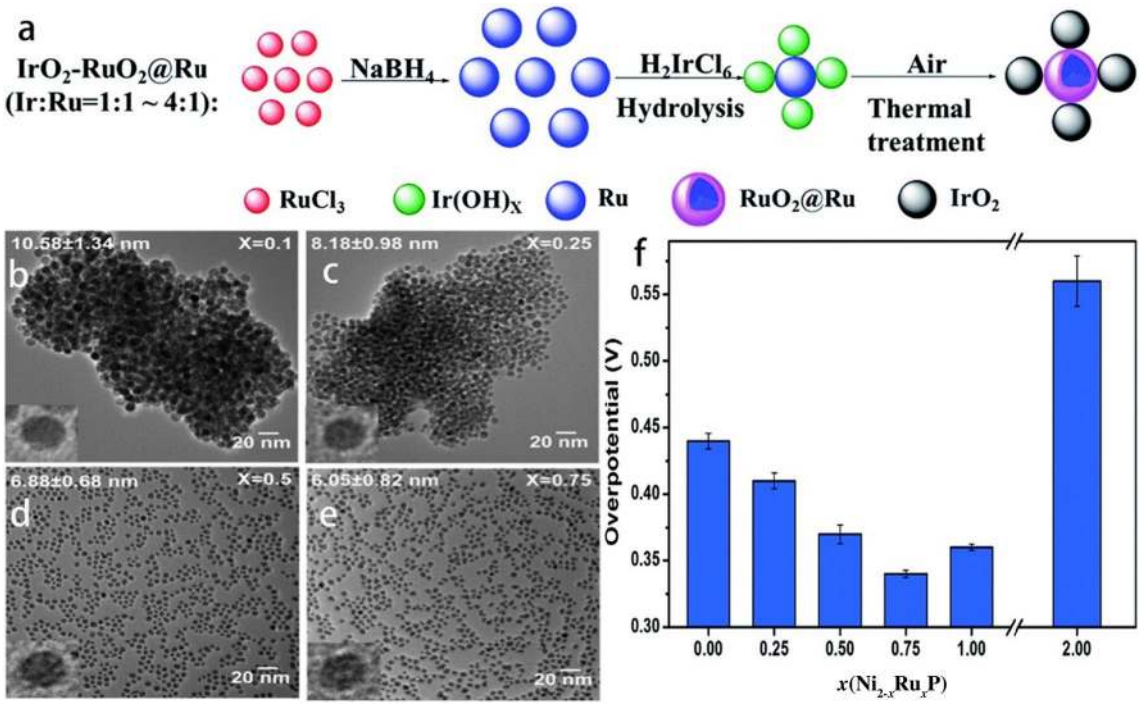

Fig. 3 **a** Schematic illustration of the synthesis of IrO_2–RuO_2@Ru nanocatalysts [58]. **b**–**e** TEM images for $Ni_{2-x}Ru_xP$ nanoparticles. **f** Changes in overpotential (at 10 mA cm^{-2}) for different compositions of $Ni_{2-x}Ru_xP$ in 1.0 M KOH [59]

As an alternative to address the issue of cost, non-noble metal catalysts need to be explored as OER catalysts for alkaline water electrolysis.

2.2 Non-noble Metal Catalysts

Although noble metal compounds are the most efficient catalysts for the OER, their high cost is a major obstacle towards commercialization and widespread application. The short-term solutions such as the lowering of noble metal loading have shown promise, they are not effective because the price of noble metals is ever-increasing, essentially nullifying the improvements of decreased metal loading. Alternatively, an effective approach towards this problem is the replacement of noble metals with non-noble metals. And in recent years, transition metal compounds such as Ni, Co, and Fe compounds, being highly abundant, inexpensive, corrosion resistant and highly active in alkaline environments, have been extensively explored as OER catalysts and are steadily replacing noble metals. In 2017, a comparative study by Huang et al. [59] revealed that Ni-based compounds are more promising as non-noble metal OER catalysts, and in 2008, Jiang et al. [60] found that the order of the electrocatalytic performances of transition metal compounds was in the order of Ni > Co > Fe [60, 61].

Transition metal compounds are also promising in OER catalyst applications because of their variable oxidation states, presence of 3*d* electrons and morphological properties. In addition, the performance of these compounds can be further enhanced by changing their particle sizes, surface areas and microstructures. As for Ni-based OER catalysts, they are in the form of oxides, hydroxides and double hydroxides and the various compounds studied recently are NiP, Ni_3Fe, $NiFe(OH)_2$, N-doped NiFe, NiS, NiFe-LDHs, NiFe oxide, $NiCo_2O_4$, Fe-doped $NiCo_2O_4$ and $NiCoO_2$. Some of these catalysts with their performance values are provided in Table 4. In addition to Ni, this article will also discuss cobalt (Co)- and manganese (Mn)-based compounds.

2.2.1 Nickel Oxides

Nickel oxides are good candidates for the OER [62–65] because these catalysts are resistant to corrosion in alkaline media. In addition, enhancements in the performance of these catalysts can be made by changing their particle size, surface area and microstructure, which motivated researchers to discover new methods to enhance electrocatalytic OER activities as well.

As an example, Arciga-Duran et al. [61] obtained NiO films for testing through the electrodeposition of Ni using an electrolyte solution containing glycine at different pH levels. In their resulting SEM images, the researchers found that by increasing the pH level of the electrolyte solution through the addition of glycine, the grain size of the NiO

film decreased from 170 to 70 nm, and that oxygen vacancies increased from 25% to 36%. The researchers attributed this to the combustion of occluded glycine. The researchers also obtained the best OER performances from the NiO film catalysts that were obtained at pH levels greater than 5, achieving a current density of 1 mA cm^{-2} with an overpotential of 450 mV.

Electrodes possessing 3D structures can also provide high electrical conductivities, large surface areas and high stability. Because of this, nickel foam (NF), a 3D electrode substrate with a long-range porous structure, can potentially facilitate the enhancement of charge transfer and mass transport. Based on this, Babar et al. [62] developed a novel thermal oxidation method to produce a 3D porous NiO electrocatalyst on a nickel foam (NF) substrate that achieved a high electrocatalytic activity with a low Tafel slope value of 54 mV dec^{-1} and an overpotential value of 310 mV to reach a current density of 10 mA cm^{-2} (Fig. 4g–h). In this study, XRD analysis revealed that the degree of crystallinity on the 3D porous electrocatalyst can increase with increasing thermal oxidation temperatures. Furthermore, the interconnected nanowalled structure of the catalyst, as confirmed by the FESEM shown in Fig. 4a–f, was found to thicken with increasing thermal oxidation temperatures.

For nickel oxide electrocatalysts, the use of nickel in higher electronic states, such as Ni^{3+}, usually resulted in optimal OER performances [62]. Based on this, Zhang et al. [63] assembled Fe-doped NiO_x catalysts from ultrathin nanosheets containing trivalent (Ni^{3+}) active centres. Here, XPS analysis confirmed the presence of Ni^{3+} active sites and the incorporation of Fe and Ni was found to result in an increase in oxygen vacancies. And because of this, the OER activity of the assembled Fe-doped NiO_x catalyst was found to be superior to NiO_x catalysts without Fe doping. The effects of Fe doping were also reported by Wu et al. [64] based on a Fe-doped mesoporous NiO catalyst synthesized through a facile solvothermal method. Here, the well-connected 3D porous nanosheet array structure of the prepared catalyst provided many active sites and Fe doping resulted in the modification of the NiO electronic structure through activating Ni centres (Fig. 5a–c). The resulting catalyst demonstrated enhanced OER activities with a low overpotential value of 206 mV and a Tafel slope 49.4 mV dec^{-1} to reach a current density of 10 mA cm^{-2}.

The OER performance of nickel oxides can be further improved by the introduction of other metals (Co, Fe or Mn) to form binary metal oxides and their composites (e.g. $NiCoO_2$, $NiCo_2O_4$ [66–77], $NiMnO_4$ [78] and NiFe oxides) [79–86]. These materials are referred to by researchers as spinel oxides and can demonstrate superior performances as OER catalysts. And of these spinel oxides, the effects of synthesis routes and calcination temperatures have been extensively studied for $NiCo_2O_4$ [65–76], in which several synthesis methods, including coprecipitation by using NaOH, thermal decomposition of hydroxides, microemulsion, and sol–gel, have been evaluated. Here, it was found that optimal catalytic performances can be obtained from catalysts obtained through the coprecipitation method under an optimal temperature of 325 °C. The reason calcination temperatures have such significant effects on performance is that at insufficient temperatures, samples remain as a mixture of two individual oxides and at high temperatures, sintering occurs, causing a decrease in active surface areas [72]. For example, Chen et al. [66] fabricated 3D $NiCo_2O_4$ core–shell nanowires using a simple two-step wet chemical method on a flexible conductive carbon cloth substrate and obtained a catalyst with high surface areas, enhanced charge transfers and 3D conductive pathways, all of which collectively contributed towards a high OER performance [67].

Numerous studies have provided evidence that catalyst morphology is a crucial factor for performance enhancement [66, 67, 70, 71, 73]. Based on this, Yan et al. [76] fabricated a $MnO_2/NiCo_2O_4$ catalyst supported on the nickel foam (NF) through the hydrothermal method which provided high catalytic activities and found that the NF support can provide a 3D skeleton, facilitating the utilization of active surface areas and mass transfers of the electrolyte. The researchers also found that the synergetic effect between MnO_2 and $NiCo_2O_4$ is another factor contributing towards high catalytic activities in which the vertically aligned $NiCo_2O_4$ nanoflakes on the surface of the Ni foam can provide more exposed active sites, further interconnecting with each other to form a hierarchical structure which can act as a precursor for the dispersion of MnO_2 layers (Fig. 5d–g). And because of these beneficial morphological properties, the OER performance of this catalyst in alkaline media was found to be superior with an overpotential value of 340 mV at a current density of 10 mA cm^{-2}. Figure 6 shows the SEM images of $NiCo_2O_4$ with different morphologies.

In conclusion, through extensive research, mono-oxides, bimetallic oxides (spinal oxides), ternary oxides and other composites/hybrids of nickel have been proven to be promising materials for OERs in alkaline electrolyte solutions (Table 4).

2.2.2 Ni-Based LDHs

Ni-based layered double hydroxides (LDHs) have also been explored as suitable candidates for catalysing the OER in water-splitting applications [87–94]. Despite having low electric conductivities, LDHs possess special structures that are helpful in the enhancement of OER performances, and among all LDHs catalysts, NiFe-LDH catalysts have been found to possess the best performances. For example, Yan et al. [87] synthesized a high-performing NiFe-layered double hydroxide using a cost-effective method which contained coprecipitation followed by delamination (Fig. 7d).

Table 4 Non-noble metal OER catalysts in alkaline media

Material	Electrolyte	Overpotential (mV)	Tafel value (mV dec^{-1})	Current density (mA cm^{-2})	References
NiO film	1 M NaOH	450	96	1	[62]
NiO/NF	1 M KOH	310	54	10	[63]
Fe–NiO	1 M KOH	310	49	10	[64]
Fe–NiO/NF	1 M KOH	206	49.4	10	[65]
$NiCo_2O_4/Ti_4O_7$	1 M KOH	–	64	10	[66]
$NiFeO_2$	0.1 M KOH	329	–	2	[79]
$NiCoO_2$ nanowires	1 M KOH	303	57	10	[75]
Fe–$NiCo_2O_4$	0.1 M KOH	350	27	10	[68]
NiFeO	1 M KOH	300	–	10	[85]
$MnO_2/NiCo_2O_4$	1 M KOH	340	–	10	[77]
$NiO/NiFe_2O_4$	1 M KOH	302	42	10	[80]
Ni_3Fe	1 M KOH	248	98	10	[105]
NiFe	1 M KOH	–	90	10	[106]
Boron-doped NiFe	1 M KOH	350	40	10	[107]
NiFe	1 M KOH	257	–	10	[108]
N-doped NiFe	1 M KOH	360	–	10	[110]
NiCo@NC	1 M KOH	–	100	10	[109]
NiFe-LDHs	1 M KOH	350	47	12.8	[88]
NiFe-LDHs	1 M KOH	240	–	20	[90]
3D NiFe-LDHs	0.1 M KOH	435	–	10	[89]
NiFe/RGO	1 M KOH	245	–	10	[92]
NiFeAl LDHs	1 M KOH	304	57	20	[87]
NiFe-LDHs	1 M KOH	210	39	10	[91]
Ni–P foam	1 M KOH	350	–	10	[98]
Ni_2P	1 M KOH	290	–	10	[95]
Fe–NiP/NF	1 M KOH	192	50	10	[103]
NiP_2/CC	1 M KOH	310	–	20	[97]
FeNiP	1 M KOH	156	66	10	[100]
Co_3O_4 nanostructure	1 M KOH	356	–	10	[130]
Co_3O_4 crystalline	1 M KOH	–	49	10	[127]
Co_3O_4 nanosheet	1 M KOH	330	72	20	[131]
Fe–Co_3O_4	0.1 M KOH	420	–	10	[135]
$CoFe_2O_4$	1 M KOH	490	54.2	10	[133]
Porous Co_3O_4	0.1 M KOH	306	65	10	[137]
$ZnCo_2O_4$	0.1 M KOH	306	65	10	[139]
$CoWO_4$	1 M KOH	389	59.4	10	[134]
Co@Co_3O_4	1 M KOH	309	51	10	[145]
Co_3O_4 NPs/G	0.1 M KOH	435	–	10	[140]
$Co_3O_4/CoMoO_4$	0.1 M KOH	375	67	10	[143]
Co–N/C Co_3O_4	0.1 M KOH	318	63	10	[142]
CoP polyhedron	0.1 M KOH	300	57	10	[148]
Co_2P needles	1 M KOH	–	127	10	[149]
Co_2P NWs	1 M KOH	400	57	10	[150]
CoFeP	1 M KOH	267	30	10	[156]
CoP_2/RGO	1 M KOH	–	25.6	10	[158]
CoS	1 M KOH	267	30	10	[163]
Co_9S_8/NS–CN	0.1 M KOH	271	64.8	10	[165]
Fe–$CoSe_2$	1 M KOH	330	82	10	[170]
Mn–CoN	1 M KOH	265	–	10	[168]
Mn_2O_3	1 M KOH	427	–	10	[177]

Table 4 (continued)

Material	Electrolyte	Overpotential (mV)	Tafel value (mV dec^{-1})	Current density (mA cm^{-2})	References
Ni–Mn_3O_4	1 M KOH	283	165	10	[180]

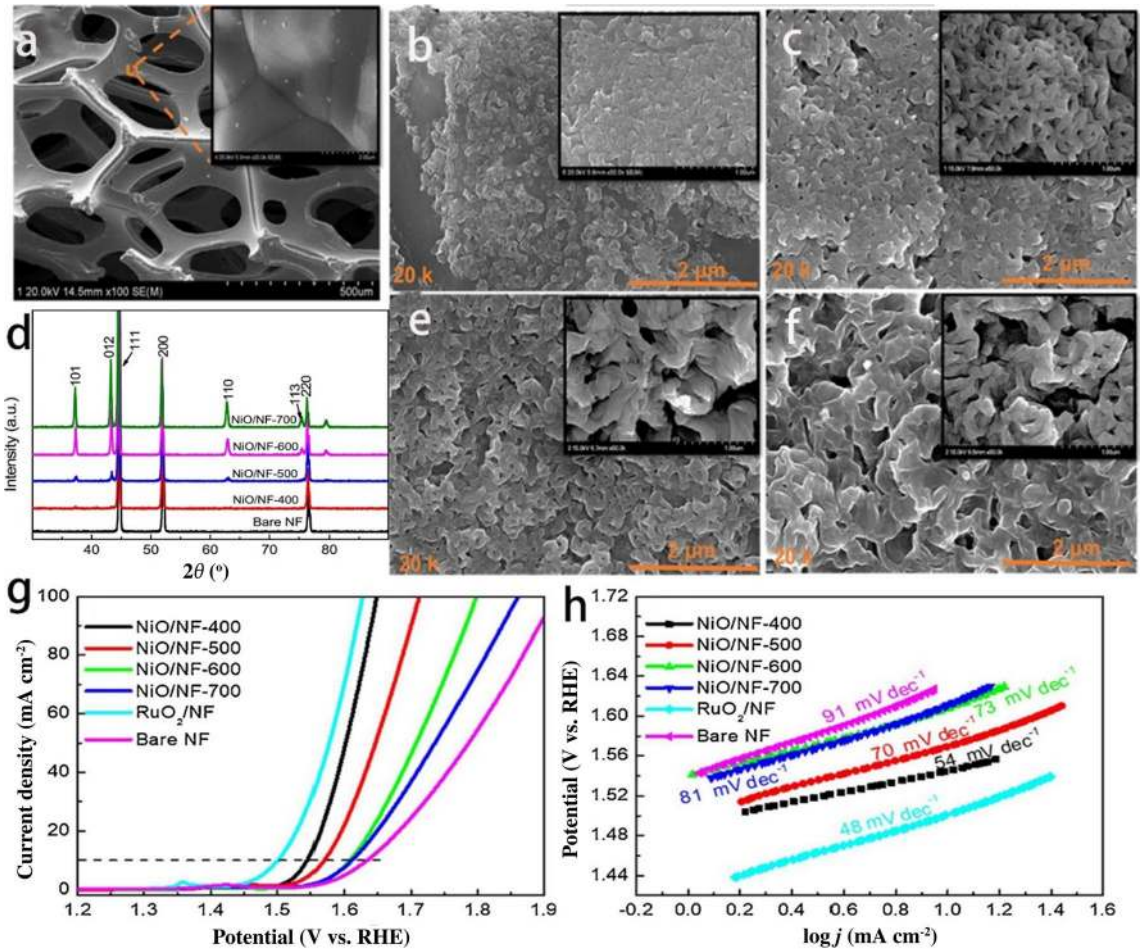

Fig. 4 **a**–**f** XRD pattern of NiO/NF and SEM images at different temperatures. **g** OER polarization curves. **h** Tafel plots [63]

The observed high electrocatalytic activity of this LDH was attributed to its nanosheet array structure in which the delamination step can prevent the agglomeration of the nanosheets. In this study, a comparative analysis was also made between four different LDHs, namely NiFe-LDH, CuFe-LDH, CoFe-LDH and ZnFe-LDH, among which, NiFe-LDH demonstrated the highest OER performance with a Tafel slope value of 47 mV dec^{-1} (Fig. 7b, c) [88]. Another drawback of LDHs is that they possess significantly higher charge densities because of the barriers between layers of nanosheets. To modify this, Li et al. [88] designed an atomically thin layered NiFe-LDH to synergistically incorporate the effects of released carbonate anions and butanol. Based on this, the obtained catalyst gained a 3D porous structure which in combination with the atomically thin layered LDHs nanosheets, enhanced electrocatalytic activities.

In general, graphene-based electrocatalysts possess desired activities for OER applications but is hindered because of their chemical inertness. However, if combined with LDHs, the properties of graphene and LDHs complement each other, increasing performances [94]. And because the chemical reactivity of graphene can be improved by combining with LDHs that possess high chemical reactivity, a new field of hybrid compounds as OER catalysts is emerging. Xia et al. [93] suggested that this enhanced catalytic activity can be attributed to the promising synergetic effects between NiFe and the reduced graphene oxide (RGO), in which the RGO layer can facilitate the uniform deposition of NiFe, providing electrochemical pathways and high surface

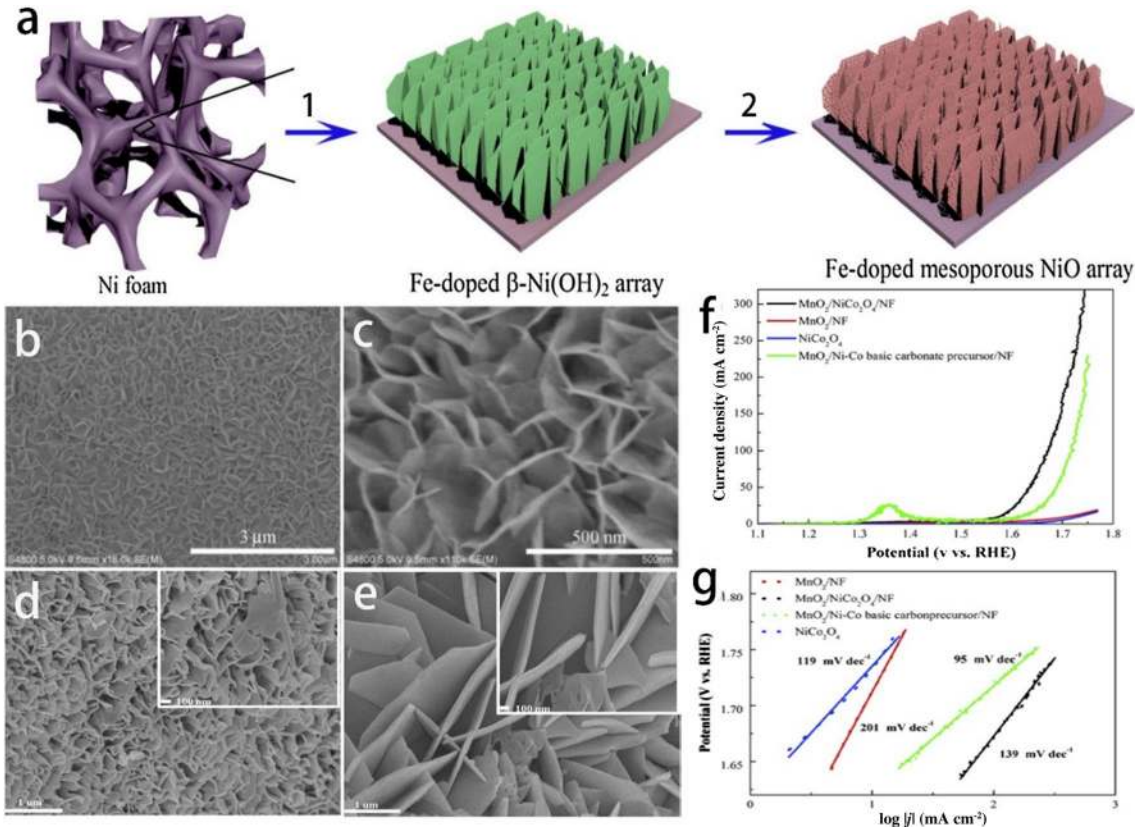

Fig. 5 **a** Graphical representation of the formation process of the Fe-doped NiO mesoporous nanosheets array. **b–c** FESEM images of $Fe_{11\%}$–NiO/NF with low and high magnifications [65]. **d** SEM image of Ni–Co basic carbonate precursor. **e** SEM image of MnO_2/$NiCo_2O_4$/NF. **f–g** Linear sweep voltammetry (LSV) and Tafel slopes of $NiCo_2O_4$/NF [77]

areas to the loaded NiFe. The researchers here demonstrated this by synthesizing a graphene-/Ni–Fe-layered double-hydroxide composite and found that the obtained catalyst provided good stability (up to 1000 cycles), satisfactory electrocatalytic property (overpotential of 245 mV at a current density of 10 mA cm^{-2}) and a high faradic efficiency of 97% [93]. Based on these results, this composite shows promise in future commercial scale applications because of its high stability, activity and low cost. The synthesis process of the composite is illustrated in Fig. 7a.

Despite promising performances, Ni-based LDHs still face challenges such as low electrical conductivities for electron transportation. This problem can be reduced, however, through coupling with carbon nanotubes, graphene-like networks or exfoliation. Nevertheless, there is much need for further developments in LDHs to achieve desirable electrocatalytic performances.

2.2.3 Ni Phosphides

Ni-based phosphides are generally employed as HER catalysts in alkaline water electrolysis; however, inspired by the promising HER activities of these catalysts, researchers have started to investigate their OER activities as well and have obtained promising results demonstrating that these Ni-based phosphides have potential as OER catalysts [95–99]. In one example, Stern et al. [94] reported Ni_2P as an OER catalyst in alkaline media in which the researchers adopted two separate synthesis routes. One route involved a thermal reaction between NaH_2PO_2 and $NiCl_2{\cdot}6H_2O$ at 250 °C resulting in poly-dispersed nanoparticles of about 50 nm in size. The other route resulted in Ni_2P nanowires which were with an average of 11 nm in size fabricated by heating nickel acetylacetone in a solution of oleic acid, trioctylamine and tri-*n*-octylphosphine at 320 °C. The second method proved to be more suitable for the synthesis of Ni_2P giving more uniform particle size. In this study, the researchers found that as an OER catalyst, Ni_2P provided superior performances comparable with state-of-the-art catalysts such as nickel oxides and spinal oxides with an overpotential of only 290 mV being required to reach a current density of 10 mA cm^{-2}.

Further enhancements in the electrocatalytic activity of Ni phosphides can be made by the introduction of doping elements. For example, a facile and safe sol–gel method was developed by Liu et al. [95] for the synthesis of Ni_2P

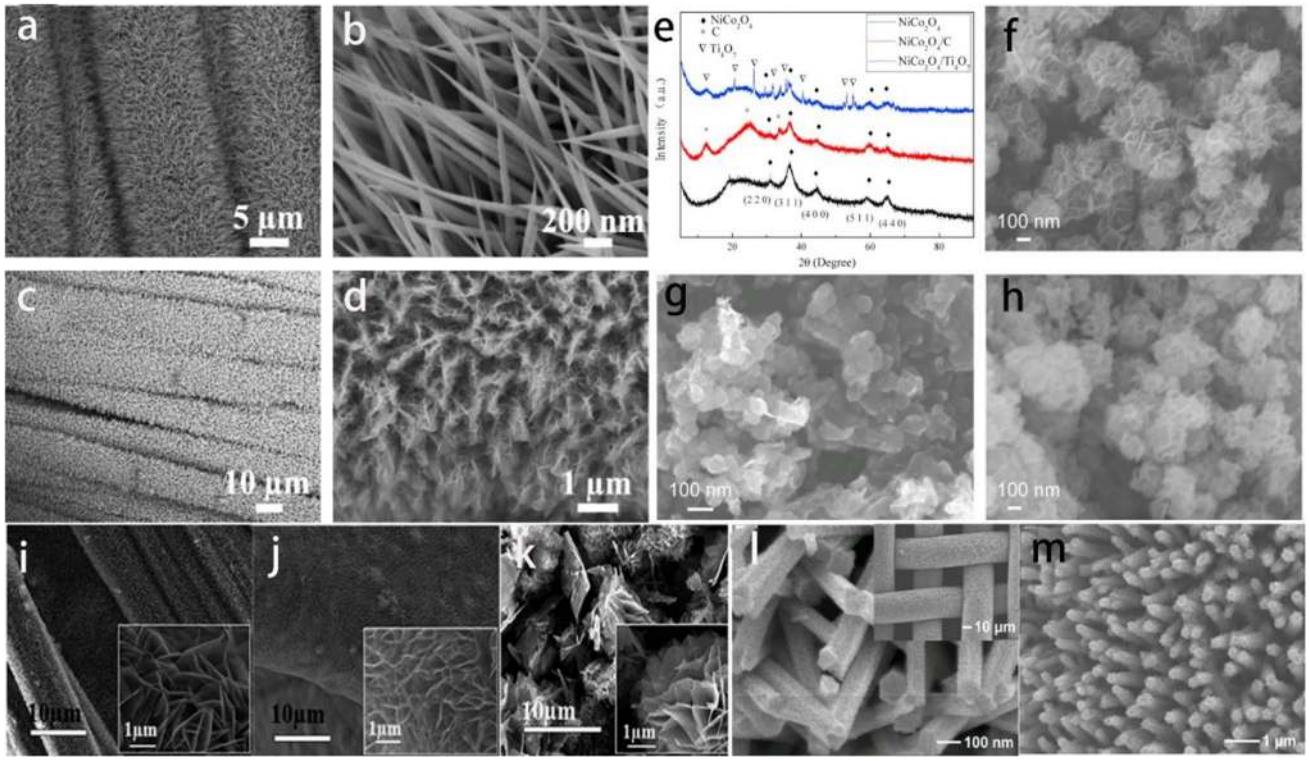

Fig. 6 **a**–**d** SEM images of $NiCo_2O_4$ nanowire arrays [67]. **e**–**h** XRD patterns and SEM images of $NiCo_2O_4$, $NiCo_2O_4$/C and $NiCo_2O_4/Ti_4O_7$ [66]. **i**–**k** SEM images of $NiCo_2O_4$/CP, $NiCo_2O_4$/NF and $NiCo_2O_4$ nanosheets [70]. **l**–**m** SEM and TEM images of $NiCo_2O_4$/SSL [71]

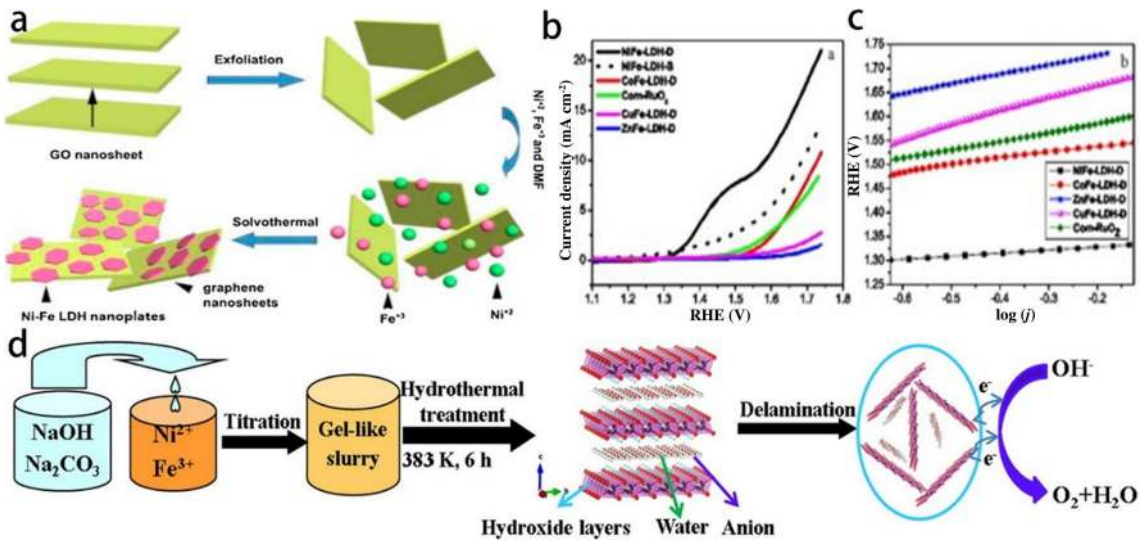

Fig. 7 **a** Schematic illustration of the formation of the RGO–Ni–Fe LDH [94]. **b** LSV of the as-prepared LDHs, the NiFe-LDH-D (NiFe-LDHs after delamination), the NiFe-LDH-B (bulk NiFe-LDHs without delamination) and commercial RuO_2. **c** Tafel plot of the NiFe-LDHs and commercial RuO_2. **d** Schematic procedure of the facile and cost-effective synthesis of NiFe-LDH nanosheets [88]

nanocatalyst. Here, Fe doping was conducted to enhance the catalytic activity of the Ni phosphide and the resulting Fe-doped Ni_2P catalyst outperformed the catalytic performances of simple Ni phosphides, and commercial RuO_2, producing a small Tafel slope value of 50 mV dec^{-1} and an overpotential of only 292 mV. These findings may provide a new pathway for the development of new OER materials [96].

Despite these promising results, however, further improvements in catalytic activity and the development of cost-effective methods for Ni phosphides synthesis are still required. Wang et al. [97] attempted to tackle these issues by synthesizing a novel 3D porous self-supported Ni–P foam as an efficient OER catalyst. In their study, binder-free and P-enriched nickel diphosphide nanosheet arrays were fabricated on the surface of carbon cloth. Here, obtained SEM images revealed a well-preserved 3D structure for the NiP_2/CC (Fig. 8a–f) that resulted in high OER performances because of the considerable number of exposed active sites (Fig. 8l, m).

Research has shown that a combination of two metals in a compound can enhance catalytic activities because of the synergetic effects between them. Based on this, bimetallic Ni phosphides (FeNiP, NiCo, FeNiP) are gaining increasing attention as efficient OER catalysts [60, 100–104]. For example, Xiao et al. [103] studied a bimetallic iron nickel phosphide (FeNiP/NF) on Ni foam as a potential OER catalyst, in which the role of the Ni foam was not only to act as a substrate but also as a slow releasing Ni source. In the obtained SEM micrographs shown in Fig. 8, the formation of nanosheets can be clearly seen and the colour changes indicate the successful modification of the catalyst. In this study, the researchers found that the combined effects of the bimetallic composite, the metallic phosphide and the electrode fabrication method collectively contributed to a high OER activity with an overpotential of just 192 mV to reach a current density of 10 mA cm^{-2}. The schematic illustration of this synthesis process is shown in Fig. 8k.

2.2.4 Ni-Based Alloys

The alloying of Ni with other transition metals can enhance OER performances, and various alloys have been synthesized and studied in which Ni alloys with Co and Fe were found to be particularly effective in enhancing OER performances [105–120]. The reason for this enhancement is the combination of two transition metals that can synergistically provide better electrocatalytic properties than their individual components. Based on this, Bandal et al. [104] developed a facile method to synthesize Ni_3Fe alloy catalysts with a bicontinuous (BC) structure [105] through the coprecipitation of metal salts with EDA. In this study, SEM micrographs revealed the uniform formation of a highly porous and bicontinuous structure with interconnected pores which are helpful in reducing mass transfer resistances (Fig. 9f–h). The obtained Ni_3Fe-BC also possessed a high BET surface area of 62 mg cm^{-2}, allowing it to provide greater numbers of active sites. These factors subsequently were found to contribute to a high catalytic activity with an overpotential value of only 248 mV to achieve a current density of 10 mA cm^{-2}. A schematic illustration of the synthesis process is shown in Fig. 9e.

Further catalytic performance improvements of these Ni alloys can also be achieved by metallic or non-metallic elemental doping. In one example, Yang et al. [107] developed

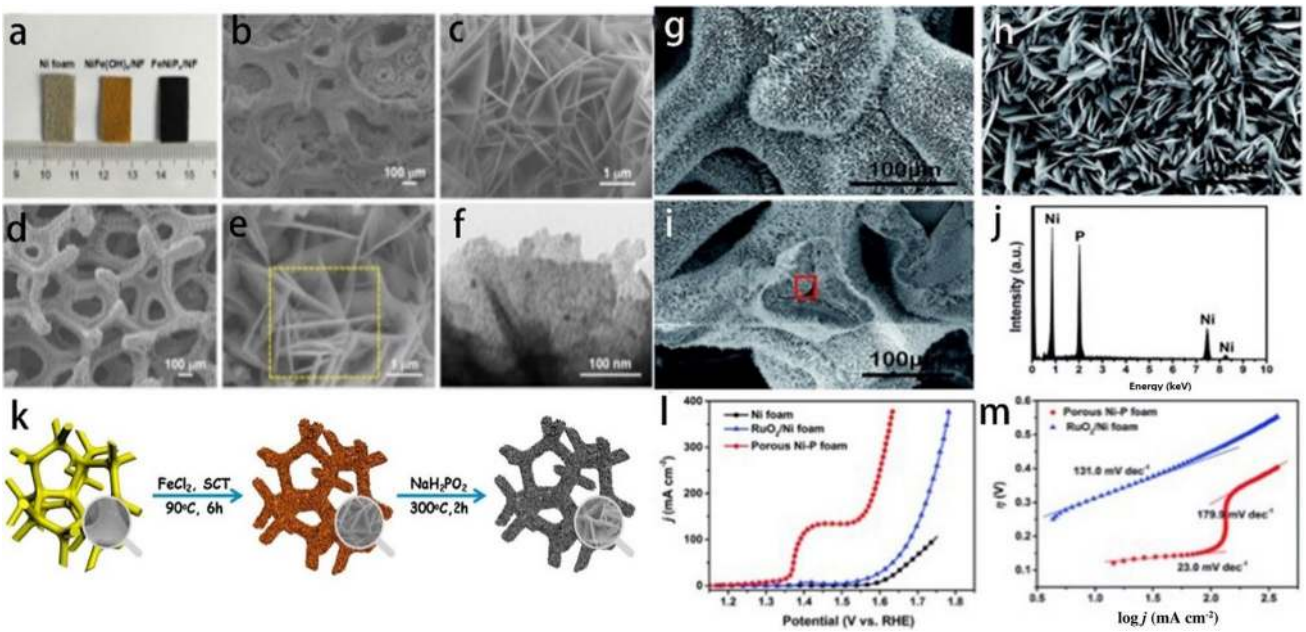

Fig. 8 **a–f** SEM images of FeNiP. **g–i** Low and high-magnification top-view SEM images of the as-fabricated self-supported porous Ni–P foam. **j** EDX spectrum taken from the rectangular region. **k** Schematic illustration of the formation of $FeNiP_x$/NF. **l–m** Polarization curve and Tafel plot of Ni–P [98, 103]

a novel magnetic field-assisted method for the synthesis of boron-doped NiFe alloys. In this study, the researchers found that the addition of $NaBH_4$ as a boron doping source decreased the magnetic moment of the intermediate product, resulting in a high specific surface area for the obtained nanochains. SEM images of the nanochains before and after boron doping are shown in Fig. 9a–d. Various other alloys including NiCo, NiMo and Ni–B have also been explored as OER catalysts with promising results [112, 115, 116].

Ternary metal alloys have also been applied as OER catalysts. For example, Rosalbino et al. [112] tested the electrocatalytic performance of NiCoM alloys (in which M = Cr, Mn or Cu) in 1 M NaOH solution and found that catalytic activities increased because of the combination of *d*-orbital of Ni with the *d*-orbital of Cr, Mn and Cu. This also increases the electrical conductivity. One issue associated with these alloys is the low electrical conductivity, however, but this can be addressed by the introduction of hybrid materials. Research has shown that Ni alloys within hybrid compounds can possess significantly better performances than that of single metal hybrid materials. Such enhancements in catalytic activity are thought to be caused by synergetic effects in these hybrid alloys [119]. For example, Yu et al. [120] reported the synthesis of a NiCo alloy encapsulated in nitrogen-doped carbon nanotubes (NCNTs) using a one-pot pyrolysis method. The resulting hybrid alloy was revealed to possess a nanotube structure as confirmed by SEM and TEM analysis in which the presence of stripes at the CNT compartments attributed to the entrapment of graphene sheets within the CNTs. In addition, the catalyst synthesized at a pyrolysis temperature of 800 °C possessed the lowest onset potential and therefore the highest activity as confirmed by electrochemical tests, achieving a low overpotential of 41 mV at a current density of 10 mA cm^{-2}.

Aside from Ni-based oxides, LDHs, phosphides and alloys, Ni-based sulphides and selenides are also capable of catalysing OER reactions in alkaline media [121–126].

2.2.5 Cobalt Oxides

OER catalysts for alkaline electrolysis can also include transition metal oxides, such as RuO_2, IrO_2, PtO_2, MnO_2 and Co_3O_4. Noble metal oxides, despite being more active, are not suitable for commercial applications because of high costs. Therefore, the development of non-noble metal oxides as OER catalysts for alkaline electrolysis has become the focus of many researchers [127, 128].

Of these non-noble metal oxides, Co-based oxides have been found to be very promising as an OER catalyst because the microstructure of Co_3O_4 can have profound influences on the performance of these catalysts [127–131]. A comparative study was conducted by Koza et al. [128] for the electrodeposition of crystalline Co_3O_4 onto stainless steel-type electrodes and they found from the obtained XRD patterns that by increasing reflux temperatures, the crystallite size

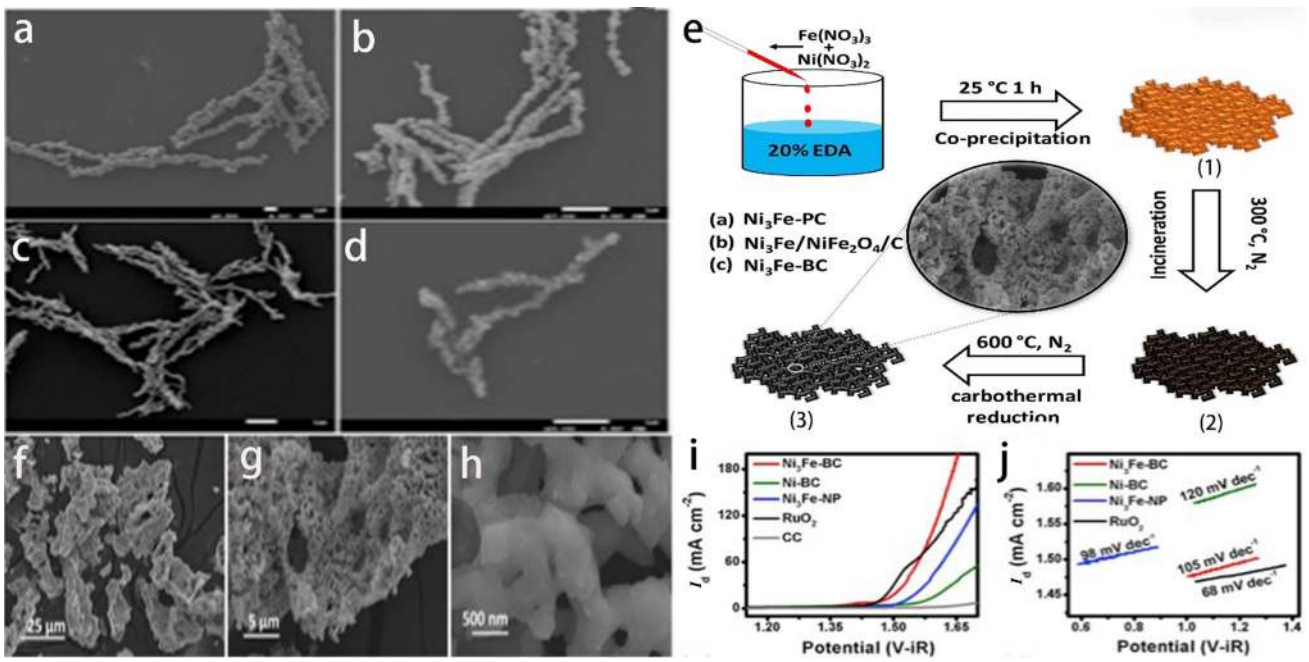

Fig. 9 **a–d** SEM images and magnetic behaviours of Fe/Ni nanochains before and after boron doping. **e** Schematic representation of an experimental method used for the synthesis of Ni_3Fe-BC. **f–h** SEM images of Ni_3Fe-BC. **i–j** Polarization curve and Tafel plot [105, 107]

of the catalysts can increase from 2 nm (at 50 °C) to 26 nm (at 103 °C). In addition, the crystalline Co_3O_4 obtained at 103 °C produced a Tafel slope of 49 mV dec^{-1}, whereas the amorphous film deposited at 50 °C only produced a Tafel slope of 36 mV dec^{-1} [128]. In another example, Sun et al. [129] synthesized a catalyst composed of atomically thin layered Co_3O_4 porous sheets with a thickness of 0.45 nm and a pore occupancy of roughly 30% and found that the resulting catalyst sheets exhibited an electrocatalytic current density of 341.7 mA cm^{-2}, which was about 50 times higher than that of the bulk.

Ranaweera et al. [129] also developed a facile binder-free method for the synthesis of flower-shaped Co_3O_4 nanostructures in which the resulting catalyst provided a high OER activity with an overpotential value of 356 mV to reach a current density of 10 mA cm^{-2} (Fig. 10g, h). Here, SEM micrographs of the resulting Co_3O_4 catalyst at different magnifications confirmed a flower-shaped morphology (Fig. 10e, f) in which the researchers attributed the observed high electrocatalytic activity to the nanoporous structure and the direct contact between the Co_3O_4 and the Ni foam. This binder-free and cost-effective approach towards the synthesis of nanoporous materials has great potential for large-scale industrial applications [130].

The incorporation of other transition metals with Co-based oxides into composites can also increase OER performances because of enhanced electrical conductivities [39, 132–139]. In one example, Zhu et al. [134] composited Fe, Ni and Fe/Ni into mesoporous Co_3O_4 [135] and observed an unusual synergetic effect in which the pore size distribution of Fe increased from 3~15 to 3~18 nm for the resulting Fe/Co_3O_4. Because of this increase, this obtained composite catalyst achieved a current density of 10 mA cm^{-2} with a lower overpotential value of 380 mV as compared with 420 mV for mesoporous Co_3O_4. Similar synergetic effects were also observed for spinal metal oxides such as $MnCo_2O_4$ and $ZnCo_2O_4$ [132, 139]. The special morphology of $ZnCo_2O_4$ is shown in Fig. 10a–d, i–n along with its electrochemical performance.

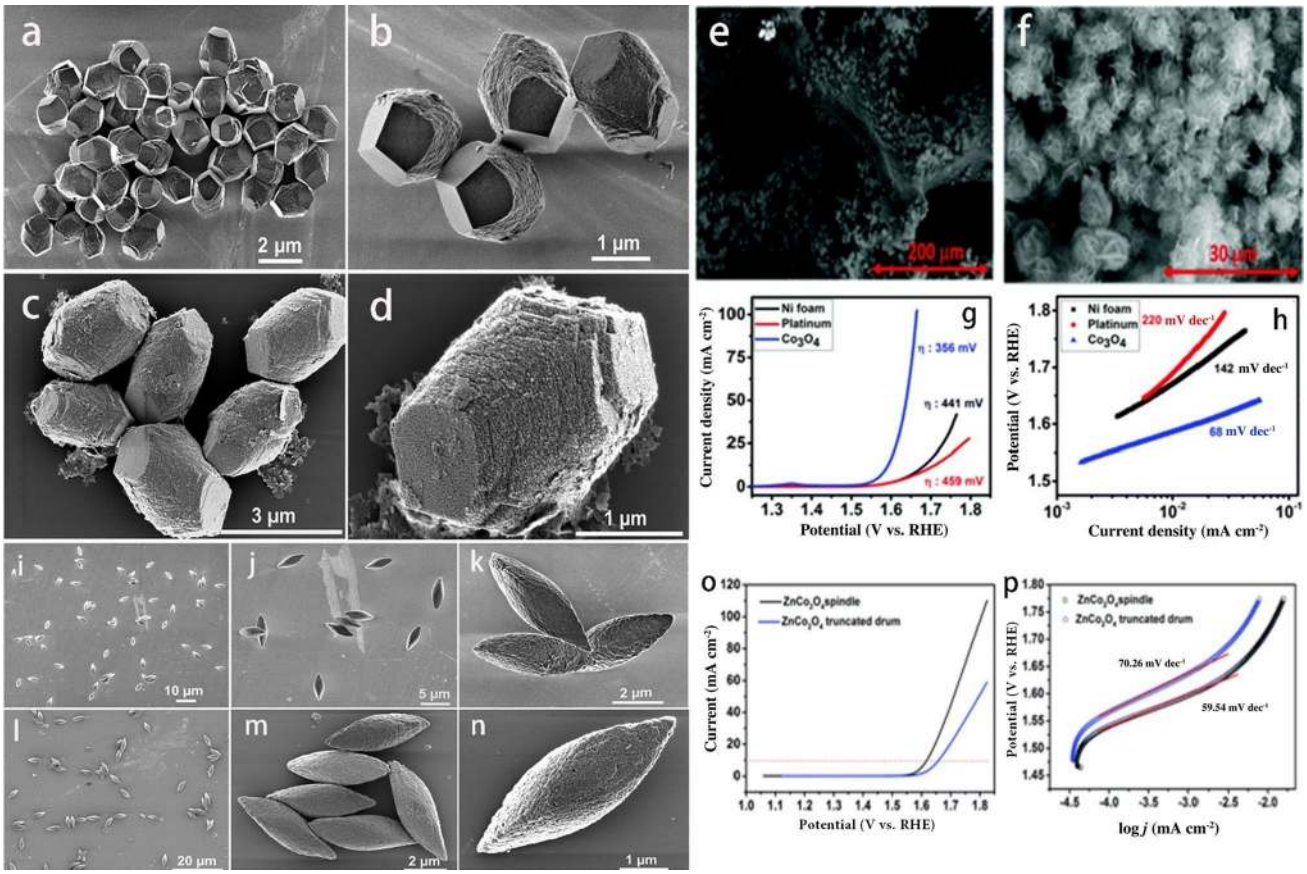

Fig. 10 **a–d** SEM images of truncated drum-shaped $ZnCo_2O_4$ precursors and porous $ZnCo_2O_4$ truncated drums obtained by annealing at 400 °C for 2 h. **i–n** SEM images of spindle-like $ZnCo_2O_4$ precursors and porous $ZnCo_2O_4$ microspindles obtained by annealing. **o–p** LSV curves obtained at a sweep rate of 5 mV s^{-1} and Tafel plots of the OER currents [139]. **e–f** SEM images of synthesized Co_3O_4 at various magnifications. **g–h** OER polarization curves and Tafel slopes [130]

Despite promising results, further OER performance improvements of Co_3O_4 catalysts are needed to overcome issues of low intrinsic conductivity and thermal stability. In this regard, hybrid materials using graphite and graphene as supports are of prime interest [140–147]. This is because they possess a high surface area, high mechanical strength and high chemical stability, making it a suitable candidate as the substrate for the fabrication of composite oxides. For example, Suryanto et al. [139] fabricated a composite of graphene/Co_3O_4 using a controlled layer-by-layer method [140] and found that this strategy enhanced OER activities because of the synergetic effects between the conductive graphene and Co_3O_4, resulting in more exposed active sites. Therefore, hybrid compounds possess immense potential for OER catalyst applications in alkaline media.

2.2.6 Cobalt Phosphides

Transition metal phosphides are another important class of compounds for OER catalysis in alkaline media. And although Co phosphides, possessing different morphologies with Co oxides and Co hydroxides which are mainly used as OER catalysts, are mainly used as HER catalysts, their high HER performances have led researchers to explore their viability as OER catalysts as well [148–150]. For example, Liu et al. [148] reported the development of a regular hollow polyhedron CoP electrocatalyst for OER using Co-centred metal organic frameworks (MOFs) as a template and cobalt as the raw material, with the resulting catalyst being found to be capable of catalysing both HER and OER reactions. In this study, SEM micrographs confirmed the retention of the hollow polyhedron shape of CoP, in which the as-synthesized CoP hollow polyhedron provided both a large specific surface area and a high porosity that can offer more active sites. In electrochemical testing, it was found that the resulting catalyst only required an overpotential of 400 mV to achieve a current density of 10 mA cm^{-2} (Fig. 11a–d). This low-cost and simple synthesis method based on MOFs as a template can be extended to other OER catalysts with different morphologies and structures as well. In another example, Dutta et al. [148] fabricated a needle-like 1D structured Co_2P to enhance catalytic performances in which they found that the activity of the catalyst is a surface phenomenon, in which changing the shape has immense effects on performance [149]. CoP with different morphologies (including bimetallic phosphides) can also be obtained such as nanowires, nanocubes [151–153].

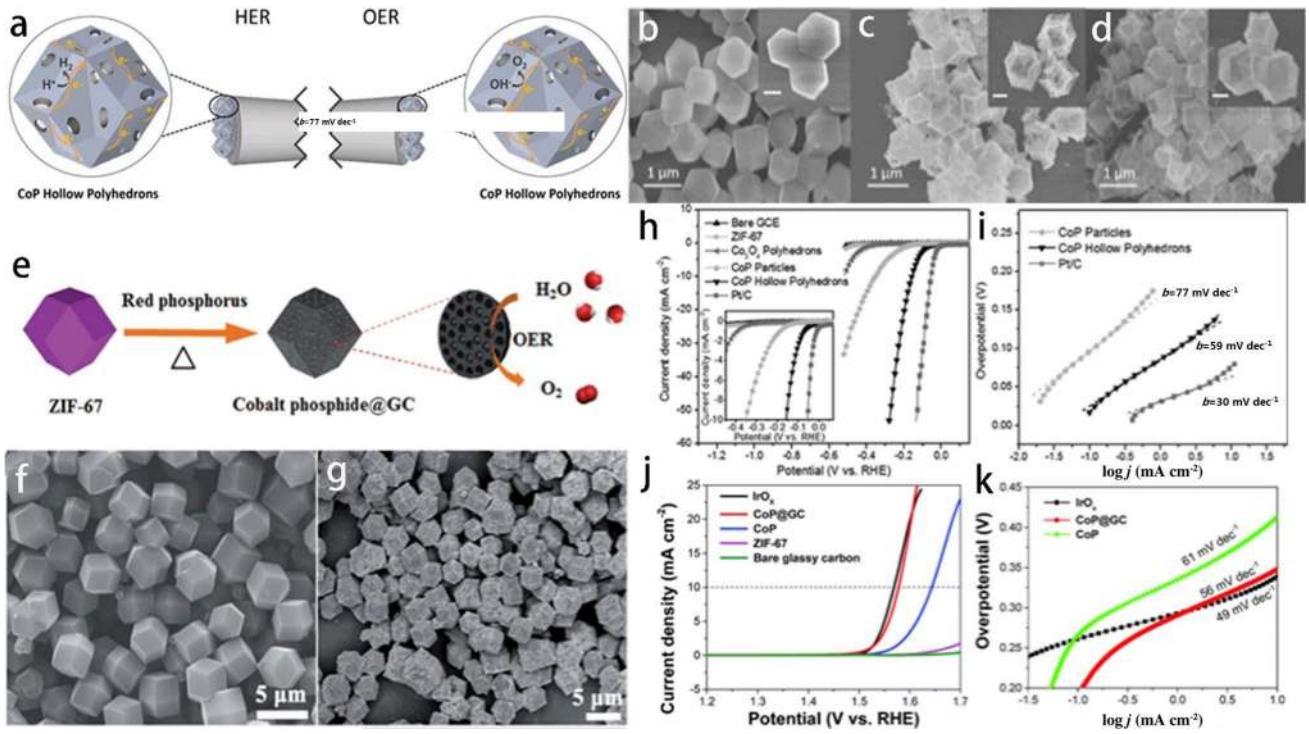

Fig. 11 **a** Schematic diagram to illustrate the HER and OER catalytic principles of CoP hollow polyhedrons. **b–d** Low- and (inset) high-magnification SEM images of ZIF-67, Co_3O_4 polyhedron and CoP hollow polyhedron. **h–i** Polarization curve and Tafel slope [148]. **e** Schematic illustration of the preparation process of the hybrid composite. **f–g** FESEM images of the preformed ZIF-67 precursor and hybrid composite. **j–k** Polarization curve and Tafel slope [162]

The introduction of other metals to obtain bimetallic phosphides (CoNiP, CoFeP, CoFePO, CoMnP) is another helpful method to improve catalytic performances in which the combination of structural and compositional effects can provide more opportunities for tailored electrocatalytic properties [102, 154–157]. For example, Fu et al. [154] synthesized a Co–Ni phosphide (CoNiP) catalyst using a hard template method and found that the obtained catalyst possessed a highly ordered mesoporous structure with large mesopores. In 1 M KOH solution, the synthesized catalyst demonstrated improvements in catalytic performance because of the synergetic effects between Co and Ni. Following this approach, more bimetallic phosphides have also been developed such as CoFe and CoMnP [154] with promising results.

Cobalt phosphide hybrid materials have also been widely employed as OER catalysts because of the synergetic effects between the components. Hybrid composites include CoP_2/RGO, CoP/C, MnO_2–CoP_3/Ti, CoP@CoPNG, FeCo and CoP/GC [158–162]. In one example, Wang et al. [158] synthesized a novel OER catalyst based on the CoP_2/RGO using a phosphidation method and achieved a current density of 10 mA cm^{-2} with a low Tafel slope value of 96 mV dec^{-1}. Here, the increase in catalytic activity was attributed to the synergetic effects between RGOs and CoP_2, which combined the high intrinsic conductivity of the RGO with CoP_2 [158]. In another example, a novel cobalt phosphide/graphitic carbon polyhedral hybrid composite was formed by Wu et al. [161] using pyrolysis and phosphidation of Co-based zeolitic imidazolate frameworks (ZIF-67). Here, SEM images confirmed the presence of the polyhedral structure of the template even after high-temperature phosphidation at 700 °C (Fig. 11f, g). The schematic illustration of the synthesis process and electrocatalytic performances is shown in Fig. 11e.

Other Co-based compounds that can be used as OER catalysts include sulphides [163–165], nitrides [166–168] and selenides [169, 170]. These compounds, such as CoS, Co_3O_4/CoS_2, Co_9S_8/N–S CNS, Co_4N, CoFeN@MWCNTs, CoSe, Fe-doped CoS [171], Fe-doped CoSe, CoFeS, Mn-doped CoN, and CoS_2/CNTs [172], have also been explored with promising results. In summary, Co-based compounds, including oxide, phosphide, nitride, selenide, sulphide and hybrid forms, possess enormous potential for OER catalysis in alkaline media.

2.2.7 Mn Oxides

Aside from Ni- and Co-based compounds, manganese oxides have recently also gained attention as viable candidates to replace noble metals catalysts and are being widely studied for their OER activities. For manganese oxides, the electrochemical and physicochemical properties are highly dependent on morphology and crystallographic nature [173–180]. Therefore, to study the effects of structure on OER activity, Meng et al. [177] synthesized four different crystal lattices of MnO_2, including α, β, σ-MnO_2 and amorphous MnO_2 (AMO), and analysed them. Here, XRD patterns confirmed the amorphous nature of the AMO with three weak peaks and SEM images revealed aggregated particles of less than 50 nm. In the obtained results, as shown in Fig. 12b, g–j, σ-MnO_2 exhibited a nanostructured flower-like morphology composed of nanoplates (500 nm × 20 nm), whereas β-MnO_2 and α-MnO_2 possessed morphologies of nanorods and nanofibres, respectively. Electrochemical measurements were subsequently conducted and revealed that σ-MnO_2 produced the lowest overpotential (490 mV) as compared with the other crystallographic structures at a current density of 10 mA cm^{-2}. In another study to further investigate the effects of structure on OER activities, Maruthapandian et al. [179] synthesized manganese oxides with different morphologies on the surface of Ti foil. In this study, the reactions were carried out at 40, 70 and 90 °C, and the corresponding morphologies of the samples obtained at these temperatures were in the structures of cotton wool, nanosheets and nanoarrays, respectively. The OER performance testing was conducted and the researchers found that the superior performance was obtained with the nanowire structure as compared with the other two morphologies (cotton wool and nanosheet arrays). From these two examples, it is clear that the morphology of Mn-based oxides is key to OER activities. In addition, like Ni and Co, bimetallic oxides of Mn are also more electrochemically active than the corresponding single metal oxides and these bimetallic oxides include MnCrO, MnFeO and Ni-doped Mn_3O_4 [178–184].

The intrinsically low electrical conductivity of manganese oxides can also be improved by using carbon as a support and through incorporating other metals to form binary metallic oxides for the fabrication of nanostructured oxides. For example, Bhandary et al. [178] combined both of these concepts and electrosynthesized MnFe oxide layers onto the surface of porous carbon paper [179]. In this study, SEM micrographs revealed a nanostructured flower-like morphology (Fig. 12c–f) and the obtained catalyst demonstrated high electrochemical activities for both ORRs and OERs. XRD analysis was conducted to confirm the phase structure of the resulting Mn_2O_3 and the observed diffraction peaks were in good agreement with standard Mn_2O_3/C cubic.

The effects of doping on the OER performance of manganese oxides have also been reported by Maruthapandian et al. [179] in which in their study, a catalyst composed of 10 wt% Ni in Mn_2O_3 (an optimum value) demonstrated an improved OER performance with an overpotential value of only 283 mV and a Tafel slope value of 165 mV dec^{-1}

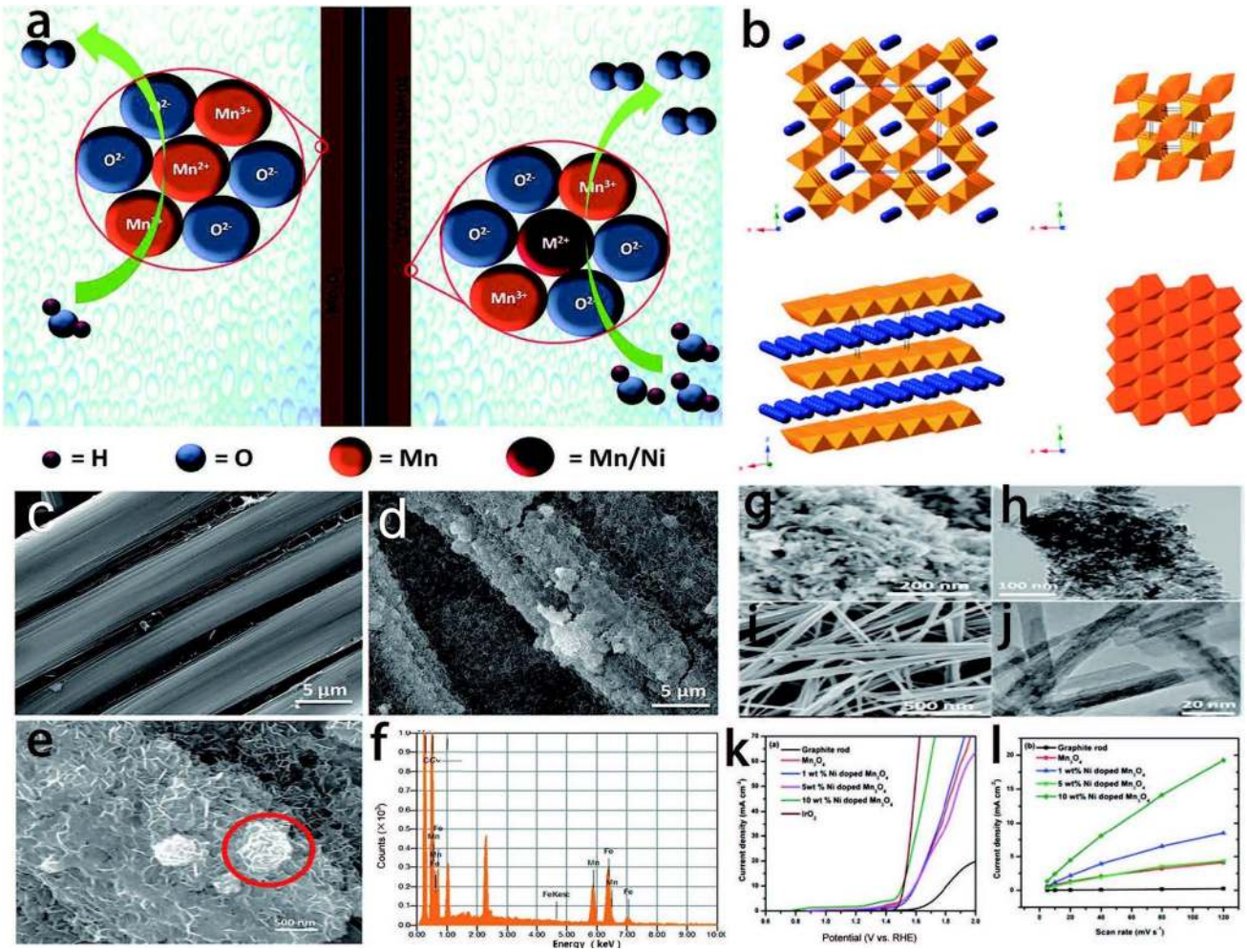

Fig. 12 **a** Schematic illustration of the catalytic activity of Mn_3O_4 and 10 wt% Ni-doped Mn_3O_4. **k–l** LSV and capacitive current density profiles [180]. **b** Structures of manganese oxide. **g–j** SEM images of MnO_2 [178]. **c–f** SEM images and EDX results of MnFe oxide [179]

to reach a current density of 10 mA cm^{-2}. This increased catalytic activity might be because of the improved absorption/desorption of hydroxide and oxyhydroxide atoms associated with the intermediates, as well as the improved electron transport between the electrolyte/active materials of the Mn_3O_4/electrode surface, along with the increased surface area and active sites. The schematic illustration of the catalytic activity is shown in Fig. 12a. This finding into the doping of non-precious metals into Mn_3O_4 can be helpful in lowering the costs of OER catalysts.

In addition to Ni-, Co- and Mn-based compounds, Fe and Cu compounds have also been reported to be favourable choices for OER [185–189]. As a result, transition metals have enormous potential to replace noble metals for OERs in alkaline electrolysis, reducing costs and providing promising applications in water electrolysis.

2.3 Catalysts for OER in Proton Exchange Membrane Electrolysis (PEM Electrolysis)

2.3.1 Noble Metal Catalysts

PEM electrolysis is another emerging field for energy storage and conversion. Although this technology has been commercially available for about 10 years, expensive materials are normally required to achieve higher efficiencies and longer lifetimes than alkaline technologies. Despite this, PEM electrolysis possesses several advantages such as high current density, high degree of gas purity and high operating safety because of a solid polymer electrolyte separator. Therefore, areas of interest for researchers in PEM electrolysis include material and component development [190].

As for the OER catalyst of PEM electrolysis, commonly used catalysts include oxides of Ir and Ru, with ruthenium oxides showing more promise than iridium oxides in terms of performance. For example, Song et al. [191] conducted a comparative analysis of Ir, Ru and their corresponding oxides as OER catalysts in PEM electrolysis and found that although RuO_2 possessed better electrocatalytic performances than Ir and Ir oxide, it was unstable in acidic media. And despite IrO_2 possessing lower electrocatalytic performances than RuO_2, it was highly stable up to 10000 cycles. The researchers also found that the performance of IrO_2 can be further enhanced through modifying the synthesis method by using colloidal iridium hydroxide hydrate as a precursor, which permits a lower heat treatment temperature. Other noble metal and composite-based catalysts used as OER catalysts in PEM electrolysis are Ir, Pt, Ag, IrO_2/Pt and NPG/IrO_2 (nanoporous gold/IrO_2).

One of the main challenges for OER catalysis in PEM electrolysis is the cost, and various efforts have been taken and new strategies have been developed to reduce the cost of the catalysts. These include the reduction in catalyst loading, the increase in catalytic activity through increasing surface areas, the synthesis of nanosized Ir oxides [191, 192]. Different support materials for enhancing the catalytic performance of these noble metal catalysts have also been explored including carbon-based materials (graphene) and Ebonex materials for nanosized noble catalysts.

In general, preparation methods and experimental conditions greatly influence both catalyst material activity and stability [192] with several research groups publishing results on the synthesis of different Ebonex-supported electrocatalysts (Pt, Co, PtCo, Ir, PtIr, etc.) as well as their characterization and application in low-temperature hydrogen energy systems. The different preparation methods that have been reported in these studies include boron hydride wet chemical reduction, impregnation sol–gel deposition, thermal decomposition of metal salts and electroplating [193].

2.3.2 Non-noble Metal Catalysts

Commonly used noble metal catalysts for OERs in PEM electrolysis such as Ir and Ru possess the lowest overpotentials, with Ir-based catalysts possessing better stability than Ru-based catalysts, resulting in their high demand. However, to reduce the cost of catalysts, different strategies have been employed, including the exploration of non-precious metal catalysts with high activity and durability. However, it is unlikely that a completely non-noble metal-based catalyst will ever be identified for PEM systems. Therefore, the most feasible method is to decrease noble metal loading.

One strategy to decrease noble metal loading is to dope noble catalysts with non-precious elements that can in turn improve stability because of the resulting changes in electronic structure. In this way, the OER performance of the multi-metallic catalyst is not only dominated by the intrinsic properties of the components, but also by their synergistic effects, crystallite phases, surface properties, sizes, shapes and pore structures, all of which can be determined by preparation methods. In the literature, many important doping elements including fluorine, tin, tantalum, molybdenum and manganese have been explored and have shown promise [194–200]. For example, a novel dopant/alloying element (fluorine) for noble metal oxide electrocatalysts was developed by Kadakia et al. [195] to determine the effects of fluorine doping. In their study, the fluorine content on a pre-treated Ti foil was varied from 5% to 30% through the thermal decomposition of a homogeneous mixture of $IrCl_4$ and NH_4F in ethanol–DI water solution. XRD patterns of the resulting thin-film IrO_2 with different fluorine contents revealed a rutile-type structure that was like that of RuO_2. In the subsequent electrochemical testing, an increase in electrochemical performances was observed with increasing fluorine content up to 10 wt%, beyond which a decrease in specific surface area and electrocatalytic activity was observed. According to the researchers, this decrease in specific surface area might be related to the exothermic reaction of NH_4F burning, which occurs during the formation of the catalyst powder. The heat released during this process could also cause the agglomeration of IrO_2F composites, also resulting in decreased specific surface areas [195].

Studies have also revealed that the stability of IrO_2 and RuO_2 can be improved through doping with other oxides such as SnO_2, Co_3O_4, MnO_2 and Ta_2O_5 [201–203]. However, increases in concentration of these inexpensive oxides can lead to decreases in active surface area and electrical conductivity. Recently, Kadakia et al. [196] reported that the doping of solid solutions of IrO_2 and corrosion-resistant oxides (SnO_2, Nb_2O_5) with fluorine can result in improved electrochemical activities and durability as well as the reduction of IrO_2 loading. The researchers here suggested that this increased activity might be due to the increase in electrical conductivity with the shifting of the *d*-band centre towards pure IrO_2. A similar strategy was adopted for F-doped (SnRu) O_2 in the same study and the observed Tafel slope value for 10 wt% F was found to be 65 mV dec^{-1} at a current density of 10 mA cm^{-2} (Fig. 13f–h).

Another method to develop low-cost Ir-based catalysts for OERs is the use of a high specific surface area support for the electrocatalyst. By using a support, the agglomeration of the electrocatalyst can be minimized, which increases active surface areas. In this method, the support material should be electrically conductive, chemically stable, inexpensive and readily available. In addition, the particle size difference of the supported and unsupported nanoparticles should not allow for the penetration of large particles into the catalyst layer. Synergetic effects arising from the addition of support

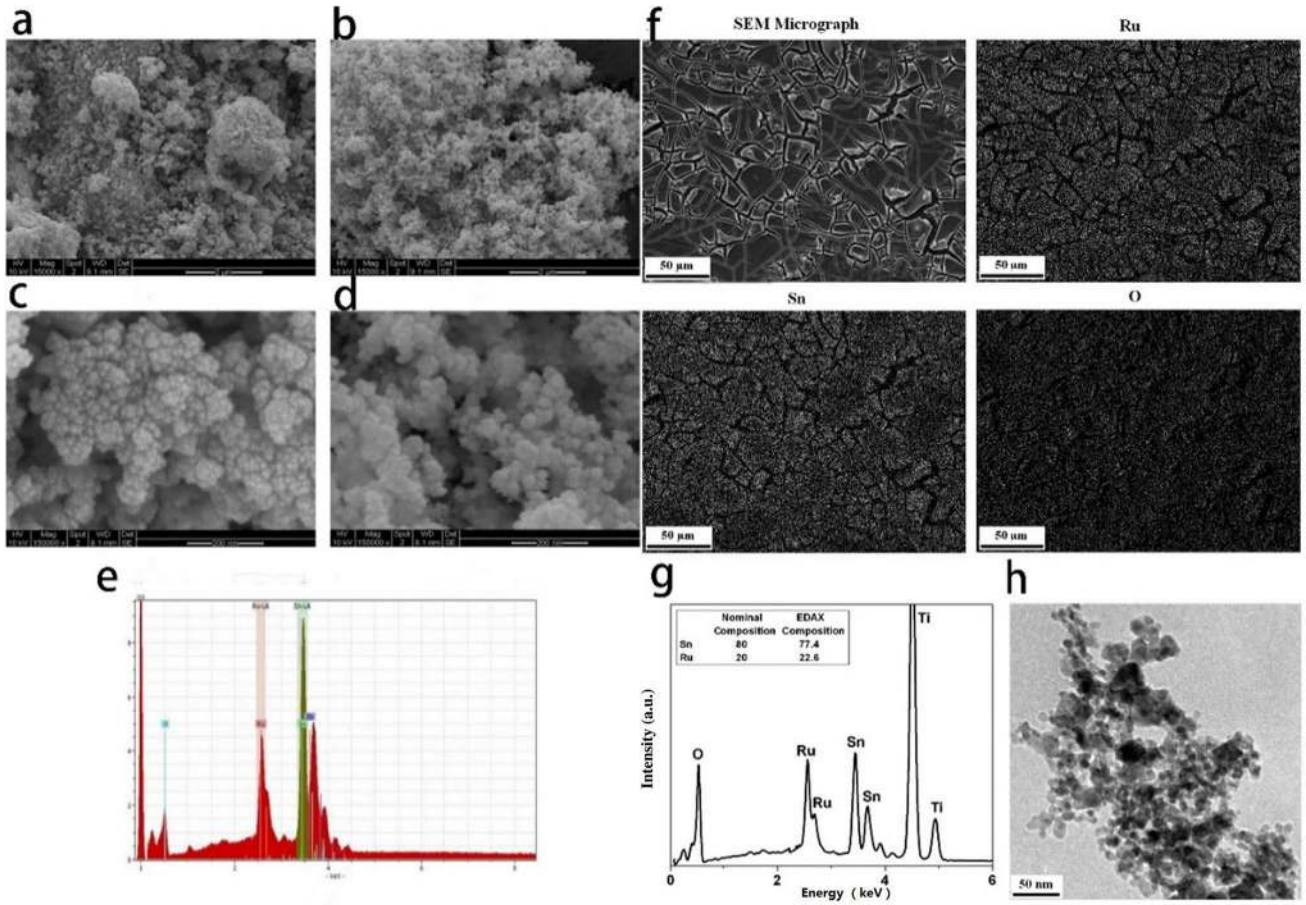

Fig. 13 **a–d** SEM images of RuO_2/ATO×15000, ATO×15000, RuO_2/ATO×150000 and ATO×150000. **e** EDX spectrum of RuO_2/ATO [197]. **f** SEM micrograph along with X-ray mapping of Ru, Sn and O. **g** EDAX of $(Sn_{0.8}Ru_{0.2})$ O_2/10F film. **h** TEM bright field image of $(Sn_{0.8}Ru_{0\cdot2})$ O_2:10 F film showing the presence of fine nanoparticles [204]

materials can also influence electrochemical performances of the catalyst [200, 204–207]. Based on this concept of using supports, Wu et al. [203] used Sb-doped SnO_2 as a support for RuO_2 catalysts and found that with the Ru deposition, the particle size of the antimony-doped tin oxide (ATO) increased from 30~40nm to 40~50 nm (Fig. 13a–e). The researchers also found that because of the support material, the agglomeration of RuO_2 was prevented. In this study, RuO_2, despite having insufficient stabilities for OER, was picked because it exhibits less overpotential than IrO_2 and is several times cheaper. The electrochemical properties of RuO_2 can also be improved by using SnO_2 as a support because of its semiconductor nature. The reason Sb-doped SnO_2 was used instead of SnO_2 in this study is because Sb-doped SnO_2 possesses higher electrical conductivity than SnO_2 because of the pentavalent nature of Sb. A similar approach has also been adopted for IrO_2 [200].

Alternatively, if metal oxides with low electrical conductivities were used as support materials, it can cause an increase in noble metal loading. To overcome this issue, transition metal carbides have attracted much attention as support materials and as electrocatalysts [208–211] and many different metal carbides such as TiC, SiC–Si and TaC have been studied as support materials for IrO_2. For example, Karimi et al. [208] conducted a comparative analysis of six different metal carbides as support materials, including TaC, NbC, TiC, WC, NbO and Sb_2O_5–SnO_2, and numerous factors were evaluated for OER catalyst applications such as surface area, IrO_2 loading and conductivity. Here, the results revealed that to choose a good support for Ir electrocatalysts, both OER activity and support surface areas are important and must be taken into consideration.

The above discussions into non-noble metals for PEM electrolysis clearly indicate that pure non-noble metals are not suitable for OERs; while non-noble metals should be used as dopants or support materials for noble metals. In addition, non-precious transition metal oxides such as niobium oxide (Nb_2O_2), tin oxide (SnO_2), tantalum oxide (Ta_2O_5) and titanium oxide (TiO_2) can be used as catalyst compositing materials to decrease overall operational costs.

However, these non-precious transition metal oxides do not show any activity for OER in PEM electrolysis. And because of this, the goal of achieving non-noble metal catalysts for the OER in PEM electrolysis is still not practical.

2.4 Catalysts for OER in Solid Oxide Electrolysis

2.4.1 Noble Metal Catalysts

A solid oxide electrolysis cell (SOEC) is the reverse mode of a solid oxide fuel cell (SOFC). In SOECs, the oxygen evolution reaction occurs at the anode which is the cathode in SOFCs and the limiting component of SOECs is the anode. In general, the performance of the anode OER process needs to be improved and one method of improving OERs is the addition of noble metals such as Pd, Pt or Ag to the anode. However, the catalytic effects of the addition of small amounts of noble metals have not been explored much and very few literature sources are available [212–214].

And in one of the few sources addressing the addition of a small amount of noble metal to form catalysts, Erning et al. [212] reported that the addition of small amounts of palladium (Pd) can activate the catalytic process in which the addition of small amounts of Pd (0.1 mg cm^{-2}) to $La_{0.84}Sr_{0.6}MnO_3$ (LSM) was found to decrease the activation energy from 200 to 100 kJ mol^{-1}. However, this study was conducted on an SOFC rather than on an SOEC. In another study conducted by Sahibzada et al. [214], $La_{0.6}Sr_{0.4}Co_{0.2}Fe_{0.8}O_3$ cathode (LSCF) performances were improved through adding small amounts of Pd as a promotor in which the addition of Pd was found to decrease the overall cell resistance by 15%.

However, despite these promising findings, these noble metal-doped compounds are not suitable choices for SOECs and alternative low-cost and efficient materials need to be developed for high-temperature operating SOECs.

2.4.2 Non-noble Metal Catalysts

Barium–strontium–cobalt–ferro (BSCF) perovskite-type catalysts have been shown to possess high catalytic activities for SOFC cathodes; in addition, these perovskites also possess potential for applications as the anode in SOECs [214]. For example, Bo et al. [215] reported a novel combustion method for the development of a BSCF oxygen electrode for use as an anode and the resulting anodic material demonstrated lower area specific resistance (*ASR*) values of 0.66 Ω cm^2 at 750 °C, 0.27 Ω cm^2 at 800 °C and 0.077 Ω cm^2 at 850 °C, which were lower than commonly used LSM, LSC and LSCF. In their study, XRD analysis confirmed the presence of single-phase perovskites at a calcination temperature of 900 °C and the HRTEM identified the presence of monodispersed particles with an average size less than 20 nm. In addition, the presence of barium, strontium, cobalt, iron and oxygen was also analysed through EDX elemental techniques. Here, the exceptionally high catalytic activity of BSCF was thought to be responsible for the low *ASR* values.

The LSCF is another important class of perovskites used as electrode materials for both SOFCs and SOECs [216–219]. For example, Fan et al. [219] reported an infiltration method for the development of $La_{0.6}Sr_{0.4}Co_{0.2}Fe_{0.8}O_{3-\sigma}$ (LSCF)–YSZ (yttria-stabilized zirconia) as an oxygen electrode. In this study, SEM micrographs showed that the unmodified Y_2O_3-stabilized zirconia (YSZ) backbone possessed a clean surface and clearly visible grain boundaries (Fig. 14h–l) and that after infiltration, nanosized LSCF particles were uniformly distributed on the surface of the porous YSZ.

A novel bifunctional $SrCo_{0.8}Fe_{0.1}Ga_{0.1}$ (SCFG) electrode material was also developed by Meng et al. [220] that could work simultaneously in both SOFCs and SOECs. In their study, the researchers used a sol–gel method to synthesize a perovskite doped with Ga^{3+} to form SCFG. And because of the modification of this material, the electrical conductivity of the resulting SCFG achieved a maximum value of 319 S cm^{-1} at 600 °C. In addition, the maximum power density reached 1044, 836 and 586 mW cm^{-2} at 750, 700 and 650 °C, respectively, and a hydrogen production rate of 22.9 mL m^{-1} cm^{-2} was achieved at a cell voltage of 2 V for an SOEC.

In another study, Boulfrad et al. [221] added small amounts of $Ce_{0.9}Gd_{0.1}O_{2-\sigma}$ (CGO) to $(La_{0.15}Sr_{0.25})_{0.97}Cr_{0.5}Mn_{0.5}O_3$ (LSCM) to overcome the poor ionic conductivity of LSCM in applications as an anode material. In this study, the catalyst was pre-coated with 5 wt% Ni from nitrates and an increase in catalytic performance was observed with polarization resistances decreasing from about 0.60 Ω cm^2 to 0.38 Ω cm^2 at 900 °C. This increase in catalytic activity was attributed to the presence of Ni nanoparticles as shown in Fig. 14k–m.

Studies have also reported that metallic ratios and temperature have profound influences on the microstructure, composition and electrochemical property of perovskites [222, 223]. Based on this, the effects of Ni/Co ratios were evaluated in a recent study by Chrzan et al. [220] for a yttria-stabilized zirconia backbone with a $Ce_{0.8}Gd_{0.2}0_{1.95}$ barrier layer and a $LaNi_{1-x}Co_xO_{3-\sigma}$ ($x = 0.4$–0.7) catalyst for application in SOECs in which the electrochemical results in the study demonstrated that the lowest polarization resistance (67 Ω cm^2 at 600 °C) can be obtained at a Ni:Co ratio of 1:1 ($LaNi_{0.5}Co_{0.5}O_{3-\sigma}$).

To address the low melting temperature and high activity of bismuth-based oxides, Ai et al. [224]

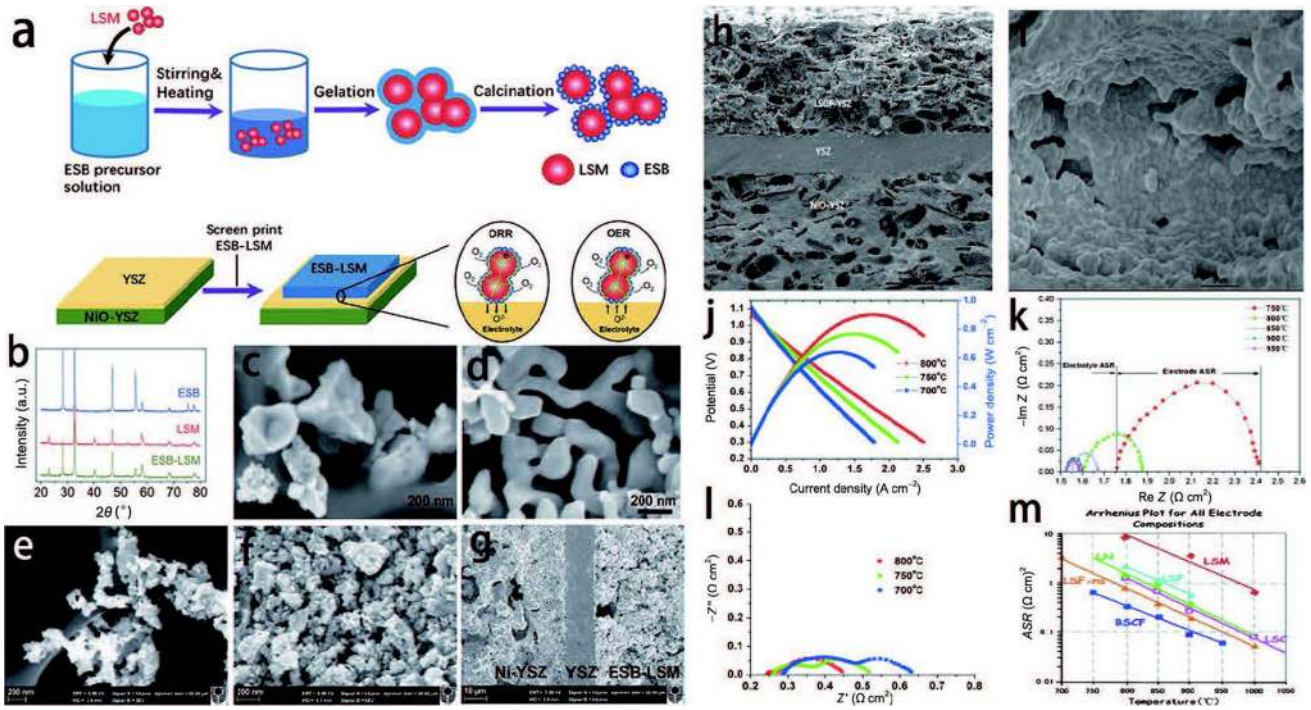

Fig. 14 **a** Schematic of the synthesis of nanostructured ESB decorated LSM (ESB–LSM) powder by using the gelation process and direct assembly of the ESB–LSM electrode on a Ni–YSZ anode-supported YSZ electrolyte cell. **b** XRD patterns of ESB, LSM and ESB–LSM powders. **c–e** SEM micrographs of the as-prepared ESB, LSM and ESB–LSM powders. **f** Surface of a directly assembled ESB–LSM electrode. **g** Cross section of a Ni–YSZ anode [224]. **h–i** SEM micrographs of the fractured cross section of LSCF-infiltrated NiO–YSZ/YSZ/LSCF–YSZ RSOFC and porous YSZ backbone. **j** Plots of voltage and power density versus current density curves. **l** Nyquist electrochemical impedance spectra (EIS) plots at open circuit [219]. **k–m** EIS analyses of BSCF and *ASR* comparisons with other oxygen electrodes [215]

successfully synthesized a 40 wt% $Er_{0.4}Bi_{1.6}O_3$ decorated with $La_{0.76}Sr_{0.19}MnO_{3+\sigma}$ (ESB–LSM) using a new gelation method. In this method, the pre-sintering step at conventional elevated temperatures was prevented and subsequently, these modifications led to improved current densities with peak power densities of 1.62, 0.32, 0.17, 0.40 and 0.20 W cm^{-2} being achieved at 750, 700, 650, 600 and 550 °C, respectively.

Overall, the performance of anodic catalysts for SOECs is highly dependent on the composition of the different metals, the pre-treatment method, the combustion temperature and the synthesis method. And based on the discussions above for SOEC oxygen electrodes, electrode materials can be classified into three main categories: (1) noble metals such as Pt or Ag that can be used as oxygen electrode in SOECs but are very expensive and difficult to apply commercially; (2) ceramic electrodes such as SFM, LSV, LSCM and LSM that possess good ionic and electrical conductivities but are catalytically slow and unstable; and (3) composite electrodes such as Ni–YSZ, NI–SDC, LSC–YSZ and LSM–YSZ that possess enhanced catalytic activities and thermal expansions matching with electrolytes [221–230].

3 Electrocatalysts for HER

3.1 Catalysts for HER in Alkaline Electrolysis

3.1.1 Noble Metal Catalysts

The hydrogen evolution reaction (HER) is the other necessary reaction at the cathode in water electrolysis in which platinum (Pt)- and palladium (Pd)-based catalysts are commonly used. However, the commercial application of these noble metal-based catalysts is hindered by high costs and scarcity [231, 232]. To overcome this challenge, researchers have attempted to disperse Pt-based catalysts onto the surface of various supports in the form of single atoms or sub-nanometric clusters. For example, the support that is commonly used for the dispersion of Pt is carbon black. There are two issues associated with the support strategy, however, one of which is the unfavourable changes to the electronic and geometric properties of Pt, and the other is the possible detachment of particles from the support, with both issues causing dramatic decreases to Pt catalyst activities [233–237]. In this regard, carbon nanotubes (CNTs) have

been explored and have shown promise as a support for Pt-based nanoparticles (NPs) with additional treatment, such as nitrogen doping, which can activate the pie electrons in the conjugated carbon, as shown in Fig. 15a, c–h. In one example, Ma et al. [235] synthesized a catalyst composed of Pt-based nanoparticles supported on bamboo-like CNTs which demonstrated a high catalytic property (with an overpotential of 40 mV and a Tafel slope of 33 mV dec^{-1}) that was near the activity of commercially available 20 wt% Pt/C.

Other than the use of carbon black and CNTs as supports to stabilize noble metal catalysts, reducible metal oxides, due to their strong interactions with metal, can also be used as supports to effectively stabilize noble metals in their oxidized state. This effect of strong metal–support interactions (SMSI) can also be seen in electrocatalysis [238–241]. For example, Wang et al. [239] synthesized ultrafine and stable Pt nanoclusters with a trigonal prismatic coordination cage with sulphur atoms on the edges and their electrochemical tests indicated that the synthesized Pt NCs possessed high electrocatalytic performances towards HERs with low overpotentials and high current densities. This observed high catalytic activity was attributed to the highly active surface of the ultrafine Pt NCs and the synergistic effects between Pt NCs and the cage matrix [241]. The schematic illustration of the process used by Wang et al. is shown in Fig. 15b. In addition, Cheng et al. [231] reported the synthesis of sub-nanometric Pt clusters which were uniformly distributed on the surface of a TiO_2 support that demonstrated high stability and enhanced mass activity. Here, the high stability of the prepared PtO_x/TiO_2 was attributed to the strong interactions between PtO_x and the TiO_2 support, and in comparison with commercially available Pt/C, the supported PtO_x provided a 8.4 times enhanced mass activity and improved stability for the HER [231].

Up to now, Pt-based catalysts are the most efficient catalysts for HER; however, low earth abundance and high cost have prohibited their large-scale commercial application. Because of this, researchers are now devoting efforts to find alternative materials to be used as HER catalysts in water electrolysis.

3.1.2 Non-noble Metal Catalysts

Transition metal compounds including Ni compounds (alloys, phosphides, sulphides), Co compounds (phosphides and sulphides) and Mo compounds (sulphides and nitrides) are of prime importance as HER catalysts, and their electrocatalytic performances are provided in Table 5.

3.1.2.1 Ni-Based Alloys According to the Sabatier principle of electrocatalysis, the efficiency of a catalyst is dependent on the heat of absorption of the reaction intermediate on the

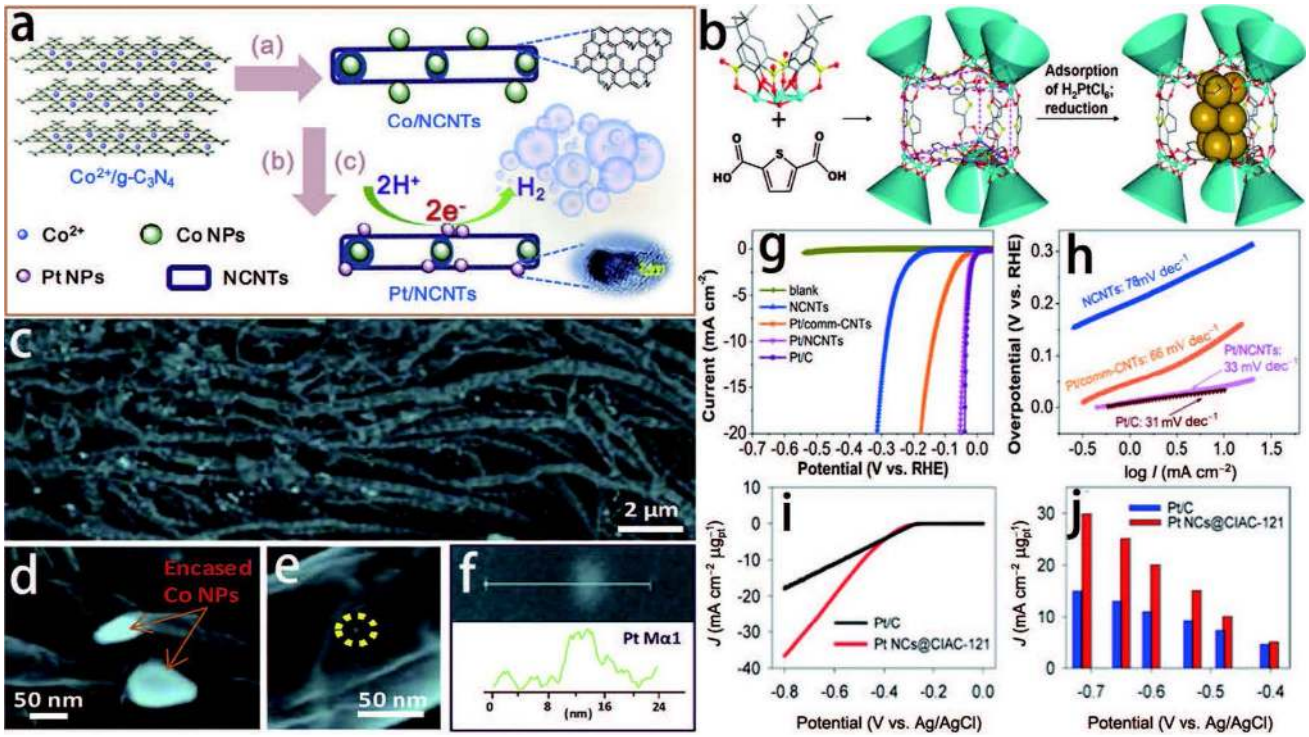

Fig. 15 **a** Schematic illustration for the preparation of Pt NPs bonding to NCNTs (Pt/NCNTs). **c–f** High- and low-magnification SEM images of Co NP@CNTs. **g–h** Polarization curve and Tafel slope [237]. **b** Illustration of the assembly of trigonal prismatic $\{Ni_{24}\}$ coordination cages (CIAC-121) and the fabrication of ultrafine Pt NCs [241]

electrode surface [242]. In the case of HER catalytic activity, the activity is observed to follow a volcano-type relation in which the hydrogen binding free energy should be closest to that of state-of-the-art Pt catalysts (ΔG_H approximately zero). Therefore, the incorporation of other metals to Ni (smaller values of ΔG_H as compared with other earth abundant metals) to form alloys such as NiCo, NiMo, NiCu and ternary metal alloys such as NiMoZn is a promising method to produce electrocatalysts with enhanced HER performances. In addition, synergetic effects can be observed if two transition metals are combined, increasing conductivity [242–254], making Ni–Co alloys efficient electrocatalysts due to improved intrinsic catalytic activities and corrosion resistance behaviours in alkaline media. For example, Sun et al. [243] reported the synthesis of mesoporous NiCo alloys through the electroless deposition method by using different compositions of lyotropic liquid crystals (LLC) as the mesoporous template. Here, SEM and TEM images confirmed a highly ordered mesoporous structure for the $Ni_{58}Co_{42}$ (Fig. 16b–e, j) alloy which provided the highest electrocatalytic activity with an overpotential value of 52 mV and a Tafel slope of 60 mV dec^{-1}. This improved electrocatalytic activity in the study was attributed by the researchers to the synergetic effects between Ni and Co as well as to the enlarged exposure of catalytically active sites. Similarly in another study, ternary metal alloys (NiCoP) were synthesized by Yang et al. [248] using Ni foam as a substrate and the resulting alloy only required an overpotential value of 107 mV and a Tafel slope of 62 mV dec^{-1} to achieve a current density of 10 mA cm^{-2}. The catalysis model of the synthesized NiCoP is shown in Fig. 16a.

Yin et al. [250] also reported that the composition and morphology of alloy catalysts for HER are tuneable by using the galvanostatic method and is highly dependent on applied currents. In their obtained SEM images, as shown in Fig. 16f–i, it can be seen that through increasing current

Table 5 HER catalysts in alkaline media

Material	Electrolyte	Overpotential (mV)	Tafel slope (mV dec^{-1})	Current density (mA cm^{-2})	References
Ni/Co	1 M NaOH	–	60	10	[243]
Ni/Co–NC	1 M KOH	68	180	10	[244]
Ni/Mo	1 M NaOH	–	–	–	[245]
Ni/Mn	1 M KOH	–	58.97	10	[247]
NiCoP	1 M KOH	107	62	10	[248]
Ni–S–Fe	1 M KOH	222	84.6	10	[257]
Ni_2P pea pod	1 M KOH	60	54	10	[258]
NiP_2 nanosheets	1 M KOH	75	–	10	[259]
Ni_2P NPs	1 M KOH	138	–	10	[261]
Mn–NiP_2	1 M KOH	69	–	10	[263]
Ni–Fe–P	1 M KOH	–	64.6	10	[264]
W–Ni_2P	1 M KOH	110	39	10	[267]
NiS_2/CC	1 M KOH	243	104	10	[271]
Ni_3S_2 NWs	1 M KOH	200	–	10	[273]
NiS/MoS/C	1 M KOH	117	58	10	[274]
V–NiS	1 M KOH	125	–	10	[276]
CoP nanotubes	1 M KOH		60	10	[284]
3D CoP NWs	1 M KOH	–	65	10	[278]
Co_2P NRs	1 M KOH	45	67	10	[285]
CoP NPs WS_2	1 M KOH	50	64.3	10	[286]
Co_9S_8–NSG	1 M KOH	65	84	10	[298]
Co_9S_8–NiS	1 M KOH	163	83	10	[301]
MoS_2 nanoplates	1 M KOH	90	53	10	[306]
MoS_2/Ti	1 M KOH	108	52	10	[309]
MoS_2/C_3N_4	1 M KOH	153	43	10	[310]
MoS_2/CB	1 M KOH	–	39	10	[312]
MoP/CC	1 M KOH	87	61	10	[325]
MoP NA/CC	1 M KOH	124	58	10	[328]
MoO_2/MoC/C	1 M KOH	233	–	10	[329]
N–Mo_2C	1 M KOH	52	49.7	10	[335]

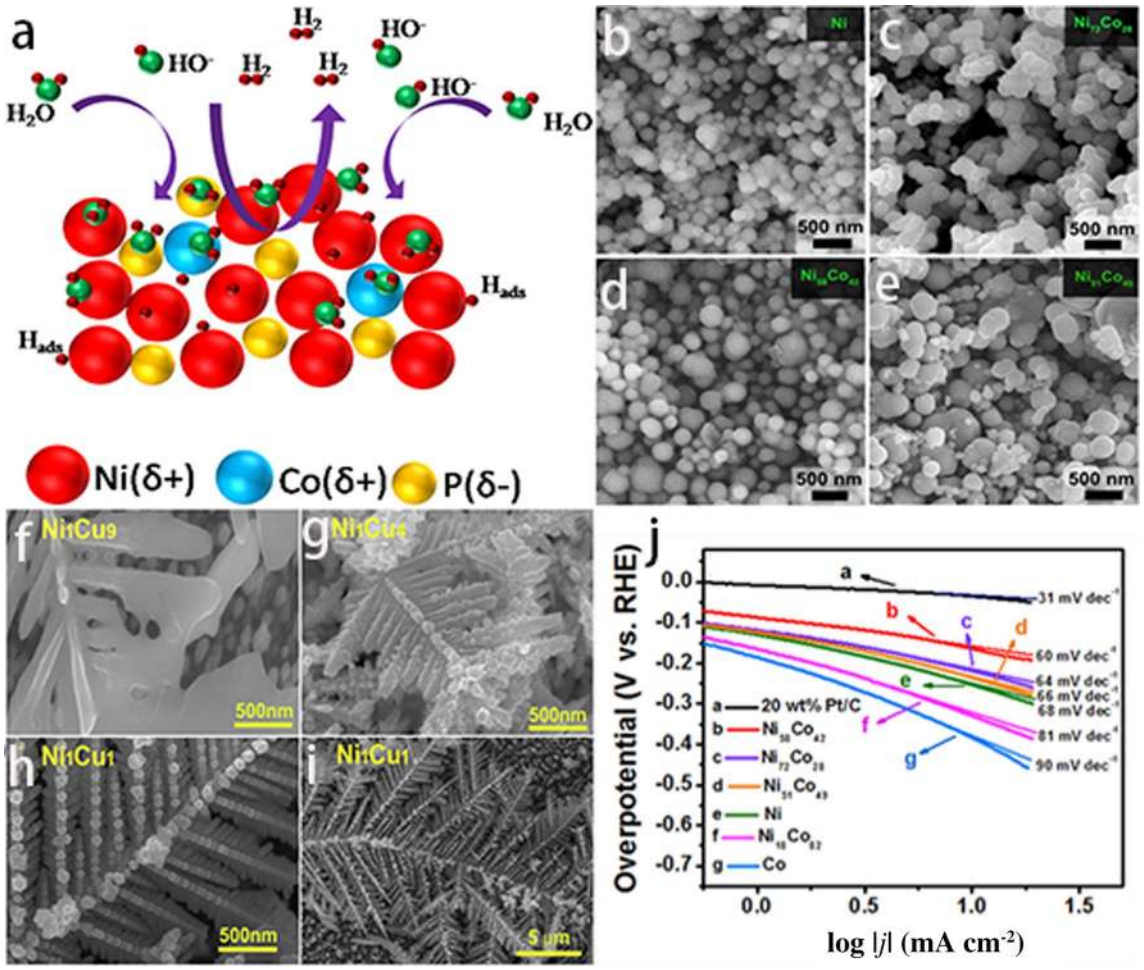

Fig. 16 **a** Schematic illustration of electrocatalytic HER on the surface of catalysts in alkaline media [248]. **b**–**e** SEM images of mesostructured $Ni_{100-x}Co_x$ alloys prepared from different LLC compositions. **j** Tafel plot of NiCo [243]. **f**–**i** FESEM micrographs of the Ni_xCu_y alloys prepared under deposition conditions [251]

densities, the branches of the trunk become thicker, denser and more symmetrical and that the NiCu alloy with a 1:1 composition possessed the highest catalytic activity. In another study conducted by Wu et al. [253], electrodeposition was used to synthesize ternary alloys of Ni–S–Fe by using Cu foil as a substrate. Here, the synergetic effects of Ni and Fe, combined with the increased surface areas of Ni–S–Fe along with the effects of Fe doping, resulted in high HER performances compared with Ni–S alloys with a small overpotential value of 222 mV and a Tafel slope of 84.5 mV dec^{-1}.

Although the intrinsic and extrinsic activities of Ni catalysts in HER applications can be improved through alloying with other earth abundant non-noble metals or through synthesizing nanostructured materials, cathodes based on these Ni catalysts still face several issues, such as cathodic fouling by the electrodeposition of trace metals present in the electrolyte, unsatisfactory structures and poor long-term stability [255–257]. Therefore, further enhancements in alloy-based Ni catalysts are needed to overcome these challenges.

3.1.2.2 Ni-Based Phosphides Transition metal phosphides (TMPs) are another important class of compounds that can be used as electrocatalysts for HERs in alkaline electrolysis. These phosphides possess high electrocatalytic activity, long-term stability and bifunctional properties as both HER and OER catalysts. For HERs, transition metal phosphides are more suitable for application because of their higher electrical conductivities as compared with corresponding transition metal oxides (TMOs). And because of this desirable property, Ni-based phosphides are gaining immense importance as HER catalysts [258–263]. In one example, a novel cost-effective method was developed for the synthesis of nickel phosphide nanoparticles by Bai et al. [256] in which glucose was used as a carbon source and $NiNH_4PO_4H_2O$ nanorods as a precursor. The resulting nanoparticles in this study were found to be encapsulated in carbon fibres and enhanced catalytic activities were observed because of the increase in surface areas and active sites, providing a low overpotential value of 60 mV and a Tafel slope

of 54 mV dec^{-1} with a current density of 10 mA cm^{-2}. The schematic illustration of the synthesis method is shown in Fig. 17a.

The interfacing of Ni-based phosphides with carbon materials is useful in increasing performances because carbon materials possess high electrical conductivities and large surface areas. As an example, Jeoung et al. [258] synthesized Ni_2P nanoparticles (NPs) entrapped in 3D graphene through the thermal conversion of a coordinated compound followed by phosphidation. The schematic illustration of the synthesis process is shown in Fig. 17b. In this study, TEM images confirmed a uniform distribution of Ni NPs throughout the graphene matrix with an average diameter of 5 nm (Fig. 17c–f) and XRD confirmed a single-phase cubic structure for the NiO. In the resulting catalyst, the graphitic layer can stabilize the large surface areas of the Ni_2P NPs and facilitate electron transfer because of the contact between them. In addition, the graphene can act as both a protective layer and an enhancing matrix for the catalytically active Ni_2P NPs. As a result, the catalyst provided a high electrocatalytic activity with a Tafel slope value of 56 mV dec^{-1}. Further improvements in electrocatalytic activity can also be achieved through doping NiP_2 with Mn and compared with pure NiP_2, doped nickel phosphides

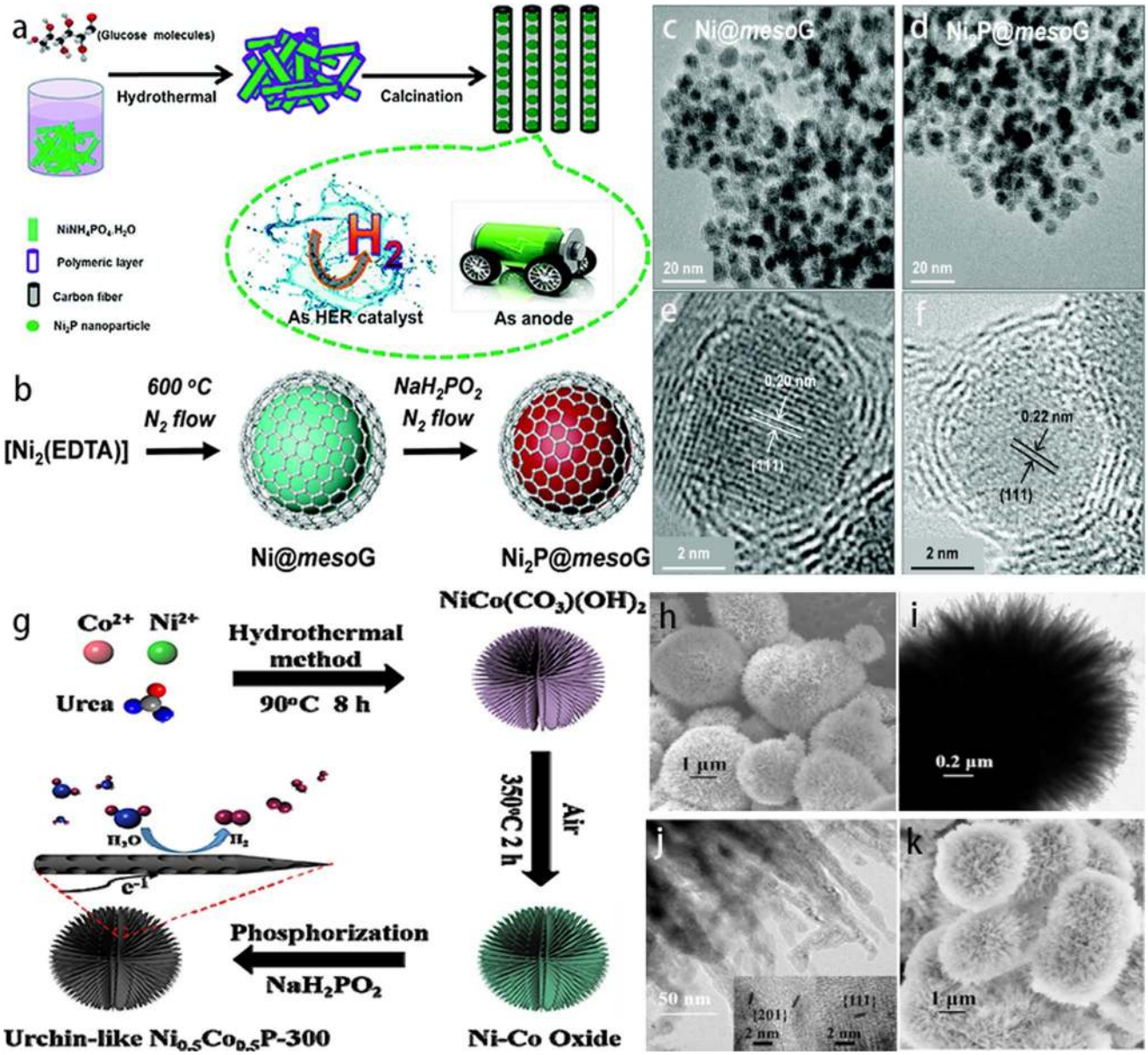

Fig. 17 **a** Schematic illustration of the synthesis process for the peapod-like Ni_2P/C nanocomposite [258]. **b** Schematic illustration of the Ni_2P NPs entrapped in 3D mesoporous graphene (Ni_2P@mesoG). **c–f** TEM and HRTEM images of the Ni@mesoG and the Ni_2P@mesoG [260]. **g** Schematic illustration of the synthesis process for urchin-like porous $Ni_{0.5}Co_{0.5}P$-300. **h–k** SEM and TEM images of $Ni_{0.5}Co_{0.5}P$-300 [268]

possess higher performances because of lower neutral hydrogen absorption free energies [263].

One disadvantage of using carbon materials in alkaline conditions, however, is the degradation of the carbon material which leads to low electrocatalytic performances as a result of the loss in reaction kinetics and oxygen mass transport. Here, the corrosion of carbon black is one of the main degradation processes in cathodic environments, leading to lowered performances due to decreased active surface areas.

Bimetallic phosphides such as NiFeP, $NiPS_3$, W–NiP, NiCoP and NiCoP/NF and NiCoP@CNT/NF have also been employed as HER catalysts because they are generally more effective than their single metal phosphides [264–270]. For example, Li et al. [268] reported the synthesis of highly dispersed NiCoP nanoparticles on the surface of Ni foam modified with carbon nanotubes that possessed more active sites. In the SEM micrographs, the electrodeposition of NiCoP on the surface of the CNT/NF was confirmed and resulted in a novel urchin-like morphology (Fig. 17h–k) that provided more exposed active sites, leading to improved catalytic activities. A schematic illustration of the synthesis process is shown in Fig. 17g.

3.1.2.3 Ni-Based Chalcogenides Ni-based chalcogenides (Ni sulphides and selenides) have also shown high catalytic activities towards HERs. These chalcogenides include NiS_2, 3D Ni_3S_2, NiS–MoS_2, Ni–Co–MoS, V-doped NiS, NiSe, NiSe@CoP, Ni–W–S and Ni–S–CeO_2 [271–278]. Among these chalcogenides, Ni sulphides are important because they are highly abundant and possess high intrinsic activities and good electrical transport abilities. In one example, Yang et al. [272] fabricated a 3D Ni_3S_2 nanofilm on a nanoporous copper substrate (Ni_3S_2@NPC) and the resulting catalyst demonstrated high catalytic activities in both acidic and alkaline media, with an overpotential value of 91.6 and 60.8 mV, respectively. The researchers conducted DFT studies to illustrate the electronic structure and relative density states of the rhombohedral crystal planes, and here, XRD patterns of the template were used as a reference and highlighted the characteristic peaks of the rhombohedral crystal plane. Density functional theory calculations were also performed to demonstrate the electronic band structure and relevant density of the rhombohedral Ni_3S_2 states. As shown in Fig. 18a, b–e, the nickel sulphides in the catalyst exist in a cubic-type structure in which nickel atoms are tetrahedrally bonded to the body-centred cubic sulphur atoms.

Another potential method to improve Ni sulphide performances towards HERs is to dope them with other elements. Based on this, Shang et al. [274] obtained vanadium (V)-doped NiS nanowires supported on Ni foam through in situ cathodic activation (ISCA) in which the formation of nanowires enlarged active surface areas, exposed more sites and allowed for faster electrolyte diffusions to the active surfaces

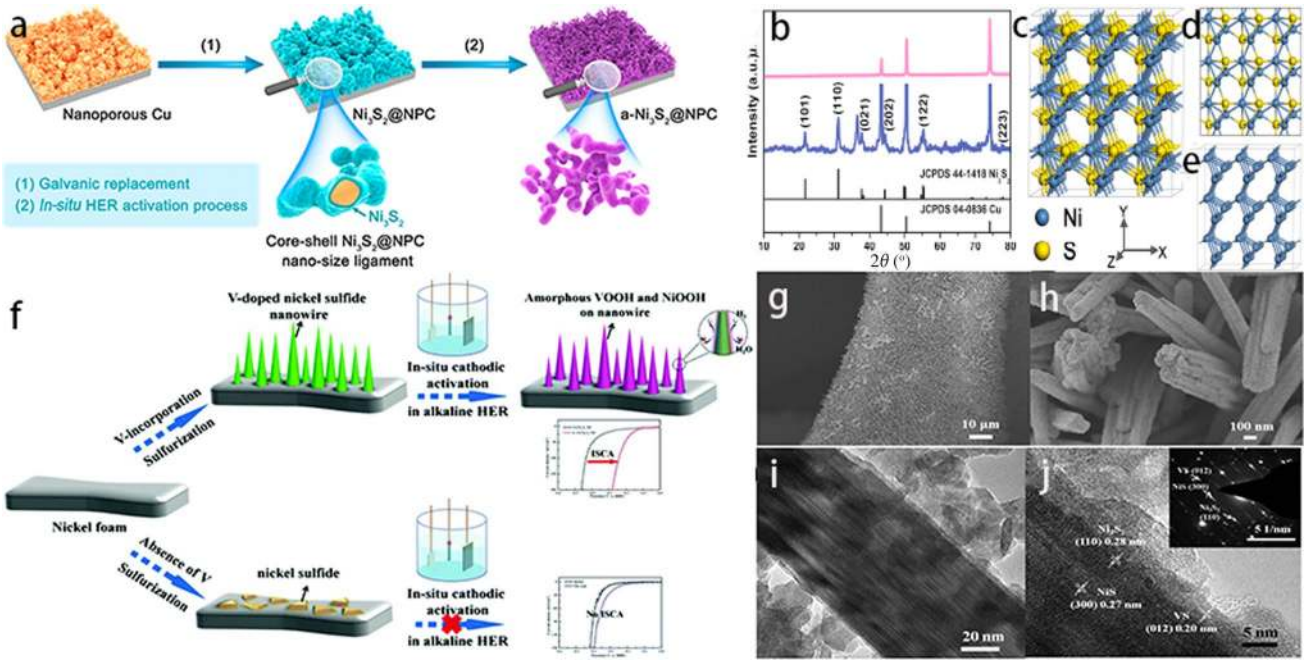

Fig. 18 **a** Schematic illustration showing the fabrication process of the nanoporous Ni_3S_2@NPC electrode and its in situ activation process during HER electrolysis. **b** XRD patterns of bare NPC (pink line) and the Ni_3S_2@NPC (navy line). **c**–**d** Front and top views of the Ni_3S_2 supercell (3 × 3 × 3) showing the crystal structure. **e** Network of Ni–Ni bond paths in heazlewoodite Ni_3S_2 crystallites [272]. **f** Schematic representation of the in situ cathodic activation (ISCA) of the VS/Ni_xS_y/NF. **g**–**j** SEM and TEM images of the VS/Ni_xS_y/NF [276]

of the electrode. Here, the effect of the incorporation of V can be observed through the obtained SEM and TEM images in which the triangle-like nanosheets transformed to nanowires (Fig. 18g–j). And because of this change in morphology, the electrocatalytic performance of NiS greatly improved. The ISCA process is illustrated in Fig. 18f.

As for molybdenum–nickel disulphides, synergetic effects can be observed between Mo and Ni in which nickel sites can act as an excellent water dissociation centre, and Mo can provide decent adsorption capability towards hydrogen [279–281]. These synergetic effects on the interface of Ni–Mo–S are helpful in promoting catalytic kinetics, resulting in improved catalytic activities. Key issues with Ni-based chalcogenide catalysts are activity loss and morphology collapse during the catalytic process, and it is still challenging to synthesize stable and catalytically active Ni-based chalcogenide catalysts [282, 283].

3.1.2.4 Co-Based Phosphides Like Ni-based phosphides, Co-based phosphides also have the potential to be used as HER catalysts [277, 278, 284–290]. For example, Li et al. [289] conducted the synthesis of CoP nanocrystals embedded in carbon matrixes without the use of any harsh conditions or harmful organic reagents. Here, the use of a conductive carbon as the support assisted in improving the conductivity of the hybrid as well as provided more active sites as a result of the dispersion of active phases. Both SEM and TEM images and the schematic diagram of the resulting carbon are shown in Fig. 19b–j, and from these, it can be seen that the mesoporous structure of the carbon support is also helpful in hindering the aggregation of CoP nanoparticles. Because of all these factors, the resulting catalyst demonstrated a low Tafel slope value of 56.67 mV dec^{-1} and an overpotential of 112.18 mV at a current density of 10 mA cm^{-2}. The entire process for the synthesis is shown in Fig. 19a.

Cobalt phosphides are inferior to Pt catalysts for HER in alkaline media in terms of catalytic activity. However, metal (hydroxide) oxide interfaces have emerged recently as an effective method to enhance catalytic performances. As an example, Zhang et al. [290] conducted the selective phosphidation of CoP–CeO_2 hybrids on Ti mesh (CoP–CeO_2/Ti), and their resulting catalyst produced high catalytic activities. Here, the researchers assumed that the water dissociation process can be enhanced by CeO_2, therefore improving formation rates of H* adsorption intermediates. SEM micrographs confirm the formation of nanosheets as shown in Fig. 19j–l. In electrochemical testing in a 1 M KOH solution, the catalyst demonstrated high stability and a low overpotential value of 43 mV to deliver 10 mA cm^{-2}. A schematic illustration of the synthesis process is shown in Fig. 19m.

Hybrid compounds composed of carbon materials and metal compounds can have immense influences on HER performance in which the synergetic effects between the high intrinsic conductivity of carbon materials and the large exposed surface area of metal compounds collectively increase catalytic activities [293–295]. For example, Lin et al. [283] synthesized an efficient hybrid compound composed of N, P co-doped carbon nanoflakes (NPCFs) and CoP nanorods (NRs) through the direct pyrolysis of a mixture of biomass macromolecule sodium alginate and ammonium hypophosphite. [285] The obtained catalyst, because of the synergistic effects, produced a high electrocatalytic activity with a low Tafel slope value of 67 mV dec^{-1} and an overpotential of only 45 mV (Fig. 19o–r).

In recent years, Co-based phosphides with different morphologies such as nanowires, nanosheets, nanoparticles [287, 288], urchin-like CoP nanowires [289, 290], CoP nanowires arrays [277] and CoP nanotubes [153] have been successfully synthesized and show promising HER performances in alkaline media. They can also be used as supports or in combination with other materials to enhance electrocatalytic activities [296, 297].

3.1.2.5 Co-Based Chalcogenides Cobalt-based chalcogenides (sulphides and selenides) can catalyse HER processes in alkaline electrolysis [298–302], and Co sulphides have been proven to be efficient electrocatalysts. However, two issues are present in these cobalt-based chalcogenides, including low active surface areas and agglomeration of catalysts during HER operations [298]. An effective solution to these issues is to tune catalyst morphologies to enhance performance, and based on this, Kim et al. [298] prepared a 1D array of CoS_2 on the surface of carbon fibre paper (CFP) as an efficient electrocatalyst [300] which demonstrated high catalytic activities. As shown in Fig. 20a–j, SEM images revealed a pine tree-like nanocolumn structure for the CoS_2/CFP (Fig. 20a–j) in which the observed high catalytic activity can be attributed to. This special morphology is thought to be helpful in exposing more active sites for HER. In another study, Wang et al. [300] fabricated $CoSe_2$/CFP nanowires with a necklace-like morphology (Fig. 20k–n) and the resulting catalyst showed a high electrocatalytic activity, providing a low Tafel slope value of 34 mV dec^{-1} and a stability of up to 5000 cycles. The possible reason for this increased performance was attributed to the special nanostructure, which can ensure high contact areas with the electrolyte and increase the release of hydrogen gas bubbles from the surface.

Further improvements in the catalytic performance of cobalt-based chalcogenides can be made through synthesizing hybrid materials, such as Co_9S_8–MoS_x, Co_9S_8/GO and Co_9S_8–Ni_S/Ni foams. For example, Zhou et al. [297] prepared a hybrid catalyst containing cubic Co_9S_8 and nanocrystalline MoS_x that displayed a high catalytic activity with an overpotential value of just 98 mV at a current

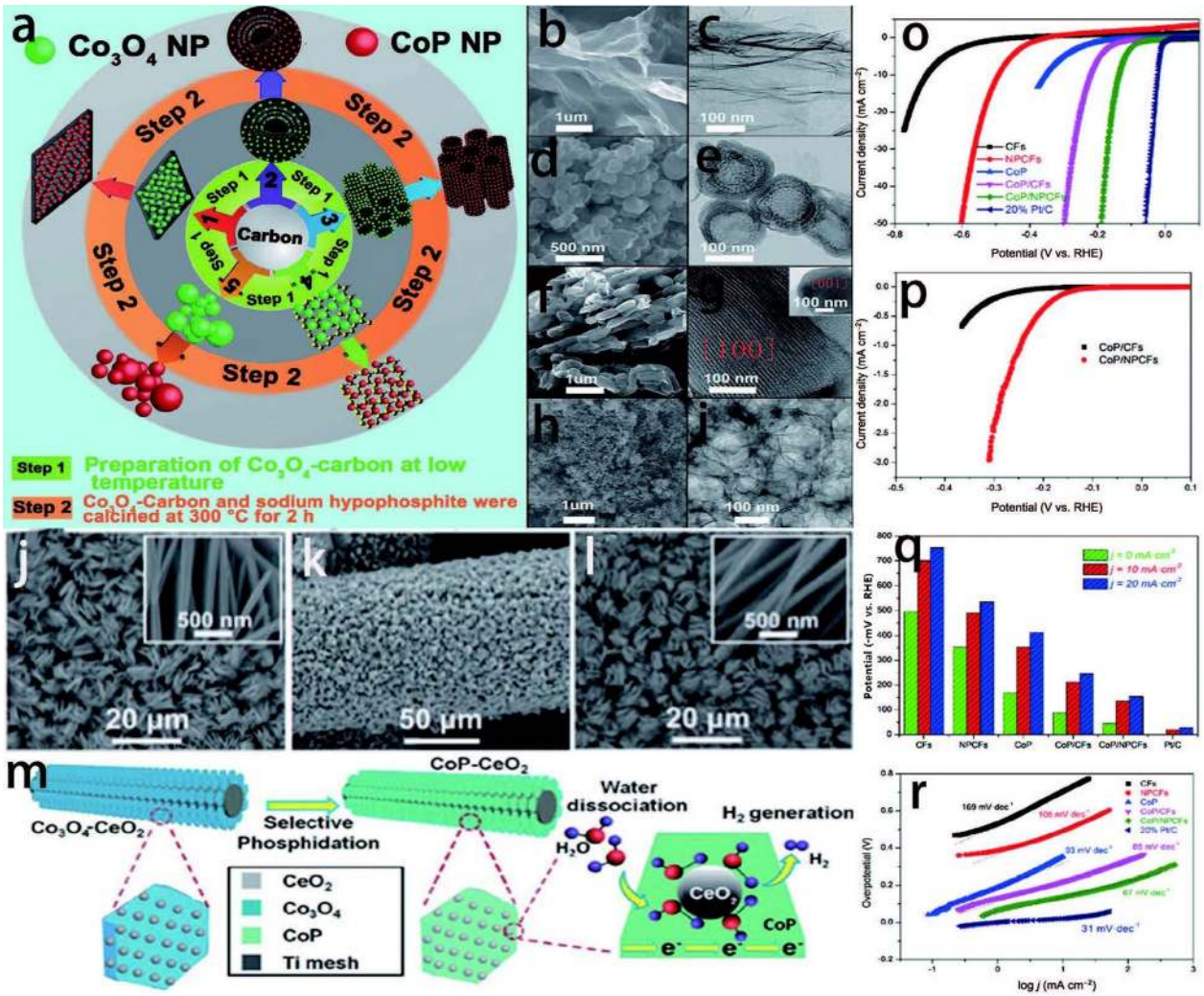

Fig. 19 **a** Illustration of the preparation procedures for free CoP NPs, Co. **b–j** SEM and TEM images of the RGO, mesoporous carbon vesicles, ordered mesoporous carbon, and macroporous carbon [291]. **j–l** SEM images of the Co_3O_4–CeO_2/Ti and the CoP–CeO_2/Ti. **m** Schematic illustration of selective phosphidation in the catalyst synthesis and catalytic process [292]. **o–r** LSV, histogram, BET surface area normalized LSV and Tafel slope of the CoP/NPCFs hybrid catalyst [285]

density of 10 mA cm^{-2} in a 1 M alkaline solution. In addition, the introduction of heteroatom dopants (N, B, S, P, F, etc.) to these composites can greatly enhance catalytic performances as well. For example, Gong et al. [301] found in their study that elemental N was the most effective dopant to be introduced into these hybrid materials in the improvement of catalytic activity. The researchers here suggest that this is because of the similar atomic sizes of nitrogen atoms and carbon atoms in the graphene and graphitic carbon, resulting in the efficient donation of electron pairs from the N atom to the sp^2-hybridized carbon atom [303, 304]. In another example, Li et al. [298] reported the synthesis of Co_9S_8 nanoparticles embedded in a N, S Co-doped graphene-unzipped carbon nanotube composite as a high-performance electrocatalyst for HERs. In this study, the as-synthesized catalyst outperformed many binary and ternary carbon-based composites in the literature and the excellent HER performances were attributed to the combined effects of abundant HER active sites created by Co_9S_8 NPs, structural defects in the carbon support induced by N and S doping, and increased conductivity because of the 3D structure.

Recently, many important developments have been made in Co-based sulphides and selenides as HER electrocatalysts, but there is still room for further development. This is because the HER, being a surface process, requires more exposed active sites and the prevention of the agglomeration of electrocatalysts during the HER.

3.1.2.6 Mo Sulphides Molybdenum disulphides (such as MoS_2) have been extensively used as HER catalysts because

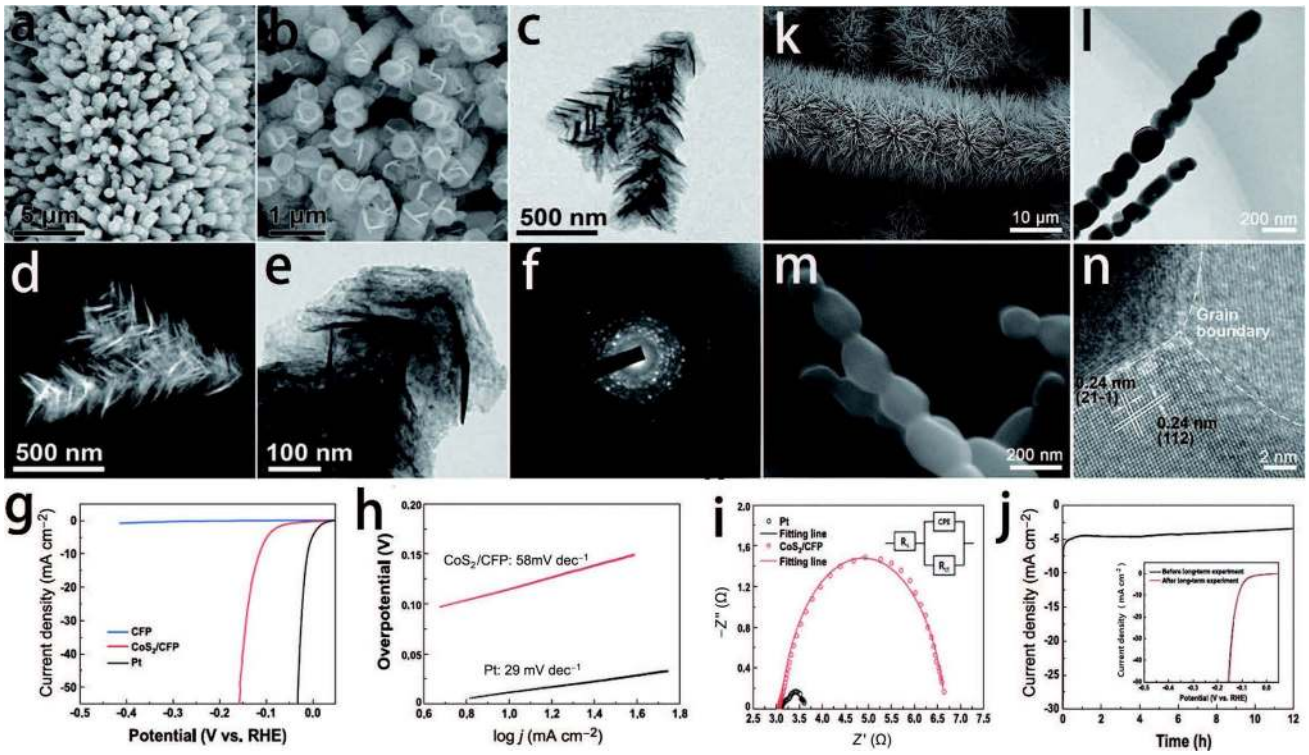

Fig. 20 **a**–**f** SEM, TEM and SAED patterns of CoS_2 nanopine tree array. **g**–**j** Polarization curve, Tafel slope, EIS spectra and long-term stability test of CoS_2 [300]. **k**–**n** SEM images and TEM images of the necklace-like $CoSe_2$ NWs on CFP (selenized at 450 °C) [302]

of their special structural and electronic properties in which the electrocatalytic properties of MoS_2 are highly dependent on the exposed edges [305–311]. For example, Yan et al. [306] reported the synthesis of ultrathin MoS_2 nanoplates with rich active sites through a facile solvent dependent control route. The formation of the ultrathin nanoplates was confirmed by the SEM and the TEM (Fig. 21a–d), and the researchers found that this highly novel synthesis route offered three advantages: (1) the resulting ultrathin MoS_2 nanoplates were rich with basal edges, leading to increased active sites; (2) the introduction of active S ligands into the ultrathin plate-like MoS_2 structure led to a more efficient MoS_2 catalyst for HERs than simple MoS_2; and (3) the direct growth of ultrathin MoS_2 nanoplates through the solvent dependent method with only source precursors is facile and controllable. In this study, the resulting catalyst achieved a high catalytic activity with an overpotential value of 90 mV and a Tafel slope value of 53 mV dec^{-1} (Fig. 21m–p). In another study, Shi et al. [307] grew MoS_2 nanosheets on the surface of commercially available Ti plates and found that the as-synthesized catalyst worked under all pH values.

The morphology of MoS_2 is crucial for HER catalysis [312, 313], and in a recent study, Cao et al. [310] reported an amorphous MoS_2 composite with highly active carbon black (CB) that was synthesized through a one-pot hydrothermal method. Here, the obtained porous MoS_2 displayed more active sites and a higher intrinsic activity than crystalline MoS_2. An ultrathin MoS_2/C_3N_4 nanosheet composite was also fabricated by Li et al. [311] using graphitic carbon nitride (Fig. 21i–l), and the researchers found that C_3N_4 can provide more metal coordination sites and offer more active sites that resulted in higher catalytic activities. Other MoS_2 composites possessing carbon or graphene also presented similar effects because of the intrinsically high electrical conductivity of carbon materials [312].

Overall, molybdenum sulphides, including crystalline MoS_2 and amorphous MoS_2, are gaining enormous attention from researchers because of their low costs, high earth abundance, increased electrical conductivity and better stability. These nanostructured materials are generally synthesized through mechanical exfoliation [314], chemical exfoliation [315, 316], chemical vapour deposition (CVD) [317–319], solvothermal [320, 321] and electrodeposition methods [322] in preparation for employment as HER catalysts. However, despite these developments, there is still a need for strategies to prevent the agglomeration of amorphous MoS_2 to expose more active sites.

3.1.2.7 Mo Phosphides Mo phosphides are also potential candidates for HERs in alkaline electrolysis because the high electrical conductivity of these phosphides gives them an edge over other Mo compounds, and many different meth-

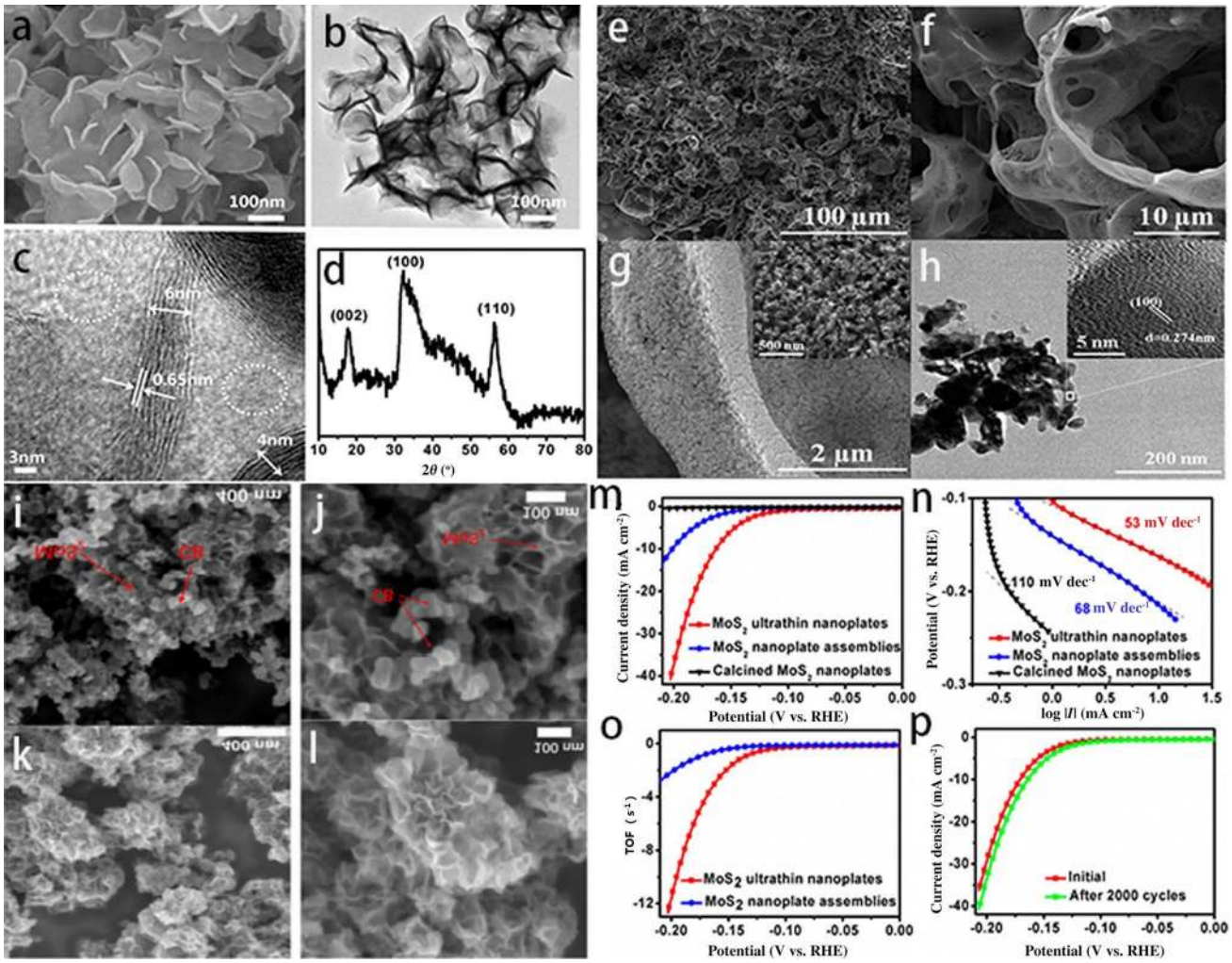

Fig. 21 **a–d** FESEM, TEM, high-resolution (HR) TEM and XRD patterns of ultrathin MoS_2 nanoplates. **m–p** Polarization curves, corresponding Tafel plots, calculated turnover frequencies of various samples and stability test for the ultrathin MoS_2 nanoplates [306]. **i–l** SEM images of different samples of MoS_2 [312]. **e–f** SEM images of 3D MoP-650 at different magnifications. **g–h** TEM images of 3D MoP-650, the insets show HRTEM images [327]

ods have been adopted to enhance the electrocatalytic performance of these phosphides, including the binder-free approach and templated synthesis towards flexible phosphides [323–326]. In one example, Deng et al. [327] reported the synthesis of a high-performing 3D MoP sponge as a non-precious metal electrocatalyst for HERs in alkaline media in which the 3D sponge-like morphology was obtained by using a template-assisted route. Usually, template synthesis methods increase catalyst costs, however, in this study, an inexpensive sponge polyurethane (PU) was used as the template, which made this process cost-effective. The resulting catalyst subsequently was found to possess a large surface area and a porous channel-rich structure, in which the side walls of the pores were composed of nanoparticles (Fig. 21e–h). These desirable characteristics allowed the catalyst to achieve a current density of 10 mA cm^{-2} with an overpotential value of only 105 mV and a Tafel slope of 126 mV dec^{-1}.

As discussed in earlier sections, hybrid materials with the RGO, the CB and the GC possess high electrocatalytic activities; therefore, hybrid materials of Mo phosphides are also promising candidates for HERs [328]. For example, Ojha et al. [321] reported a composite of reduced graphene oxide (RGO) and MoP that displayed highly efficient HER catalytic activities in both acidic and basic media in which the reported catalyst proved a good electrocatalytic performance in terms of overpotential and stability with an overpotential of 80 mV and a Tafel slope of 51 mV dec^{-1} in the alkaline medium.

3.1.2.8 Mo Carbides Molybdenum carbides (Mo_2C) are interstitial alloys which are generally produced by the incorporation of carbon atoms into the lattices of the transition metal Mo [329–332]. And despite recent advancements in Mo_2C, it

is still challenging to develop facile, controllable methods for the synthesis of Mo_2C. To address this challenge, Liu et al. [333] reported the synthesis of Mo_2C with 3D ultrafine Mo_2C nanocrystals well distributed in carbon nanofibres through a facile electrospinning and pyrolysis route. Here, SEM and TEM images revealed a 1D interconnected structure for the as-prepared hybrid of C–Mo_2C/C and the resulting catalyst achieved an overpotential value of 92 mV and a Tafel slope value of 63 mV dec^{-1} in 1 M KOH solution.

To further improve the performance of Mo_2C, nitrogen doping has been shown to enhance HER performance in several studies [333–337]. In a recent study, Jiang et al. [334] synthesized N-doped Mo_2C nanoparticle catalysts through a one-step solid-state electrocatalytic reduction of well-mixed MoS_2 and polypyrrole nanofibres in molten $CaCl_2$ at 850 °C (Fig. 22a). Here, the N-doping was found to increase the exposure of active sites and modify the electronic structure of Mo_2C, resulting in a catalyst that can operate under all pH values (0~14) and achieve a current density of 10 mA cm^{-2} with an overpotential value of 73 mV and a Tafel slope value of 59.6 mV dec^{-1}. From these promising results, it can be seen that molybdenum carbides and doped molybdenum carbides have the potential as HER catalysts in alkaline media.

Recent developments in molybdenum-based compounds (including sulphides, phosphides and carbides) have significant impacts on HER electrocatalytic performances because of their unique conductivity, chemical and thermal stability as well as their comparable catalytic property to state-of-the-art Pt group metals. However, despite the numerous enhancements in Mo-based compounds as HER catalysts, the development of facile and reliable techniques for controlled synthesis of nanostructured materials is still required.

3.2 Catalysts for HER in PEM Electrolysis

3.2.1 Noble Metals

Hydrogen evolution reactions (HERs) in PEM electrolysis are a crucial process, and in general, noble metals (Pt and Pd) are used as cathode catalysts. However, because of the scarcity and high cost of these noble metals, they are unsuitable for commercial applications. Therefore, to decrease the

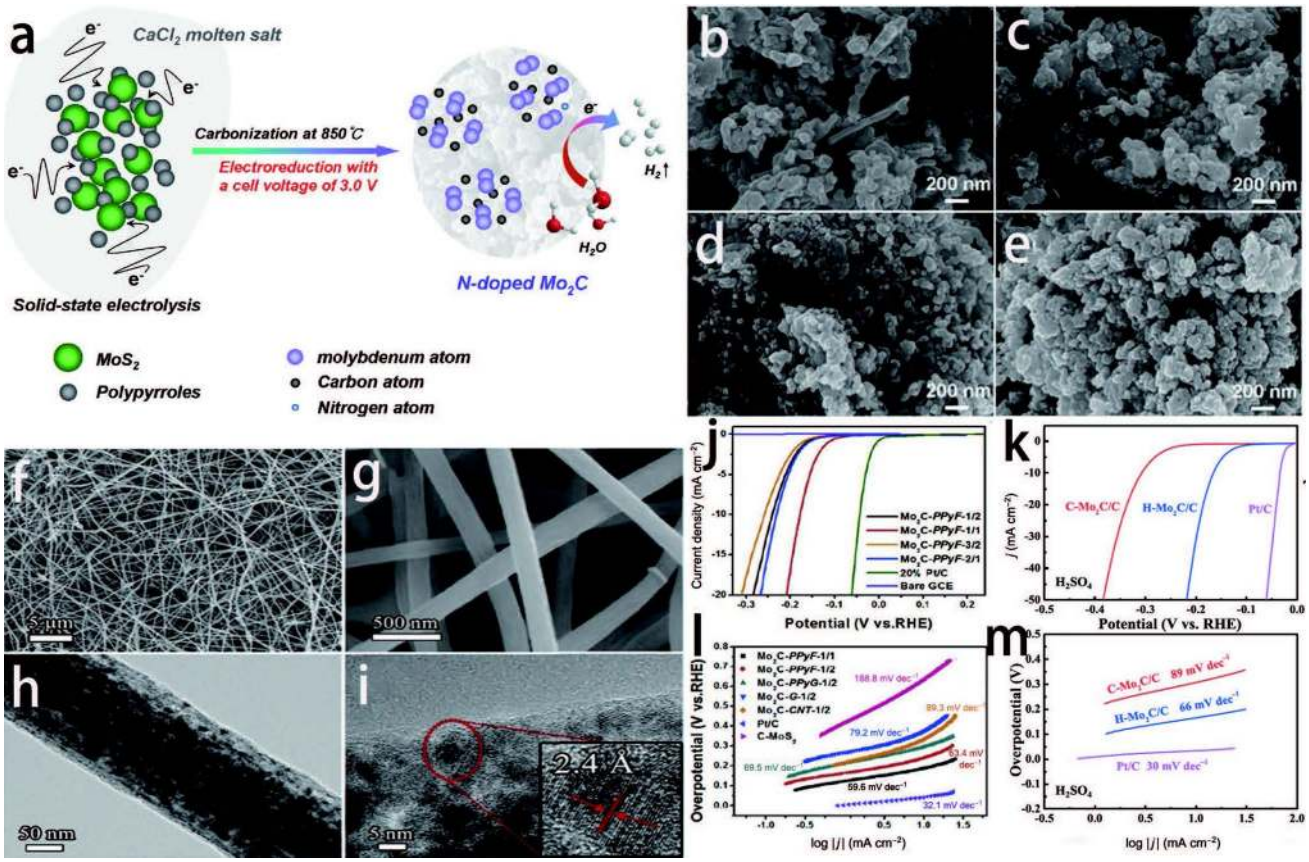

Fig. 22 **a** Synthetic process of N-doped Mo_2C catalysts. **b–e** SEM images of different Mo_2C. **j–m** Polarization curve, Tafel slope and Nyquist plot of different Mo_2C samples [336]. **f–i** SEM and TEM images of C–Mo_2C/C [333]

operational cost of PEM electrolysis, three different strategies have been adopted: (1) reducing noble metal loading; (2) using less expensive noble metals; and (3) developing alternative low-cost non-noble metal electrocatalysts.

In an example of noble metal catalysts for PEM electrolysis, Grigoriev et al. [338] synthesized Pt and Pd nanoparticles on the surface of graphitic nanofibres (GNFs) using chemical vaporization techniques (CVD). Here, TEM images confirmed the homogeneous deposition of Pt nanoparticles on the surface of the graphitic carbon and in comparison, with Vulcan X72 as a support for Pt nanoparticles, the nanoparticles synthesized on GNFs were relatively thinner and possessed a facetted structure which provided long-term stability in PEM electrolysis. Furthermore, strong interactions between the nanoparticles and the support material were also observed in the reported catalyst and the catalyst demonstrated better performances with the same Pt loading (40 wt%) than that of the Pt/XC-72 [338, 339].

Various forms of carbon, such as carbon nanotubes (CNTs), fullerenes, carbon back (CB) and graphenes can also be used as supports for noble metals in PEM electrolysis [340, 341]. This is because these carbon materials possess high electrical conductivities, large surface areas, high stabilities and are inexpensive. In addition, further improvements to the carbon materials can be achieved through doping them with nitrogen to form nitrogen-doped carbon nanotubes (NCNTs). This strategy has been proven to be successful due to the excellent electrical conductivity of the resulting product [342]. In a recent study, Ramakrishna et al. [341] supported Pd electrocatalysts onto the surface of nitrogen-doped CNTs and their resulting catalyst demonstrated enhanced catalytic activity towards HERs. In this study, SEM micrographs revealed that the NCNTs were 100 μm in length with diameters of 50~60 nm (Fig. 23a, b, e) and that the Pd catalysts were uniformly distributed on the surface of NCNTs with diameter sizes ranging from 40 to 60 nm. The researchers in this study attributed the enhanced catalytic activities of the resulting catalyst to the higher activity of the substrate.

3.2.2 Non-noble Metal

To allow PEM electrolysis to be more cost-effective, transition metal carbides (TMCs) are being explored to replace noble metal catalysts. This is because various transition metal carbides are known to possess similar electronic properties as Pt catalysts. In addition, the transition metals used in commonly explored TMC catalysts (Ti, V, Mo, Ta, W) are significantly more abundant and less expensive. TMCs cannot be used as electrocatalysts on their own because they showed a higher over potential of 200~300 mV compared to pore Pt. However, instead, they are used as support materials

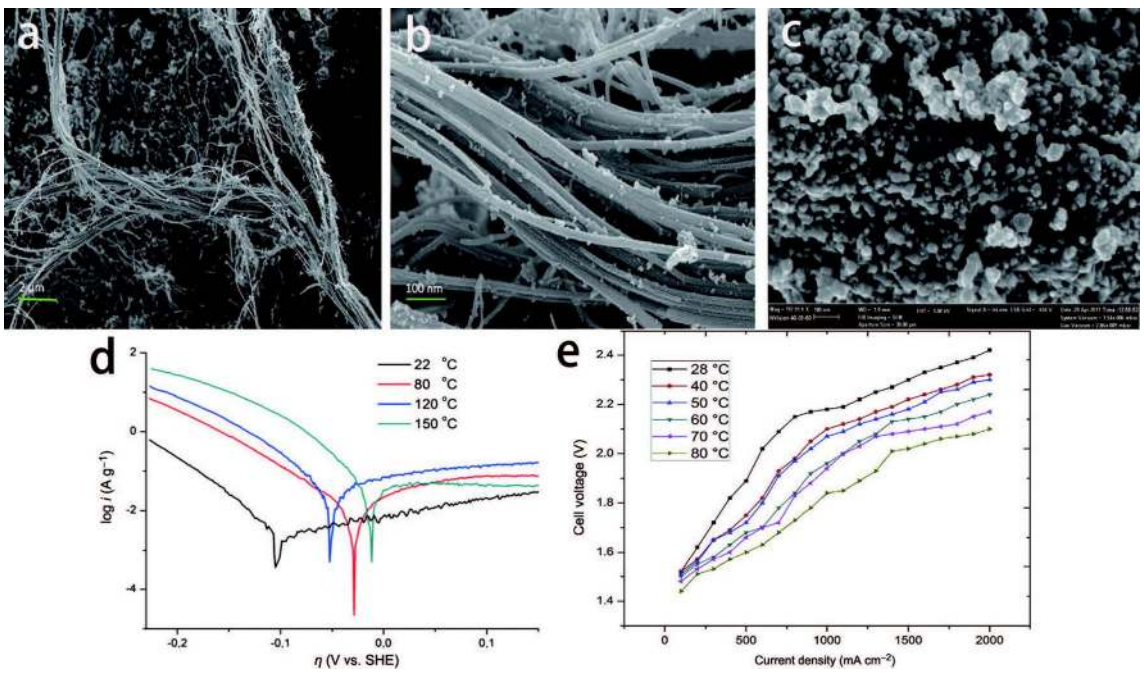

Fig. 23 **a**, **b** FESEM images of NCNTs. **e** Current voltage polarizations of 30 wt% Pd/NCNTs MEA in a 1 cm^2 area single-cell assembly at various temperatures [343]. **c** SEM image of WC powder, produced in a plasma reactor after carburization. **d** Tafel curves obtained for platinum electrodes at different temperatures in 85% phosphoric acid at a scan speed of 1 mV s^{-1} [344]

for noble metals, which reduce Pt loading and subsequently decrease PEM electrolysis operational costs [343, 345–349].

In a study conducted by Kelly et al. [345], Pd supported on tungsten carbide (WC) and molybdenum carbide (Mo_2C) was evaluated for the HER activity. As identified, Pd is less expensive than Pt and they share similar electronic and catalytic properties. And by using Mo_2C and WC as support materials, a monolayer Pd catalyst layer was formed which decreased metal loading and therefore costs. In another study conducted by Meyers et al. [346], a comparative study was carried for Pt, Pd and gold (Au) supported on metal carbides which showed promising results.

In another study, Nikiforov et al. [343] attempted to replace Pt catalysts with tungsten carbide (WC) through synthesis using the plasma synthesis method followed by carbonization. Here, SEM and TEM images confirmed the formation of nanopowders with a maximum particle size of 20 nm and the effects of temperature on the electrocatalytic property of the catalysts (both Pt and WC) were investigated. In the obtained results, the researchers found that temperature had a profound effect on the performance of WC, in which maximum HER activities were observed at 150 °C (Fig. 23c, d).

3.3 HER Catalysts in SOECs

3.3.1 Noble Metals

For HERs in SOECs, the most commonly used noble metal catalysts are Pt and Pt/C because they are regarded as the most electrocatalytically active. However, aside from the high cost of Pt, extreme sensitivity to Pt poisoning is a major drawback of Pt catalysts in SOECs [350–352]. Therefore, as an alternative, Pd catalysts have been investigated by researchers [353] and in recent years, attention has also been given to IrO_2 and RuO_2 catalysts. Further improvements in noble metal catalysts can also be made by using carbon as a support material. This is because the use of carbon supported metals presents several advantages, including increased triple phase boundaries for electrochemical reactions, easier release of hydrogen gas because of the porous nature of metal catalyst and increased intrinsic conductivity of metals. In 2010, Cheng et al. [354] synthesized carbon supported IrO_2 and RuO_2 and studied its use for the HER in SOECs and performed the TEM to investigate the physical properties of the catalyst. However, aside from this, there has not been much exploration in this field for SOECs, and very little work has been done in this direction.

3.3.2 Non-noble Metals

The SOEC is the reverse of the SOFC; therefore, the anode/cathode of SOFCs can be used as the cathode/anode for SOECs. For example, Ni–YSZ is commonly used as an anode in SOFCs and is also a common hydrogen electrode of SOECs. Despite this, this catalyst possesses poor redox stabilities and requires a high concentration of H_2 to protect the Ni from oxidation. The cause for this is the agglomeration of Ni particles during long-term high-temperature operations [355–357]. This issue can be minimized, however, by using redox stable perovskite oxides as the hydrogen electrode. For example, Cao et al. [358] reported the use of $La_{0.3}Sr_{0.7}Ti_{0.3}Fe_{0.7}O_{3-\sigma}$ (LSTF) as a novel symmetrical electrode coated on an SDC ($Sm_{0.2}Ce_{0.8}O_{1.9}$)–YSZ (yttria-stabilized zirconia)–SDC electrolyte. In their results, the LSTF demonstrated a good redox stability and excellent electrocatalytic activities in both anodic and cathodic conditions with maximum power densities of 215, 293 and 374 mW cm^{-2} being achieved at 800, 850 and 900 °C, respectively. The LSTF also demonstrated good short-term stability and reliable redox stability. Based on this, it is expected that LSTF can be a promising electrode material for SOECs.

$SrFeO_{3-\sigma}$-based ABO_3-type perovskites, despite their low redox stabilities, are also being explored as hydrogen electrodes for both SOFCs and SOECs in which the electrocatalytic performance of ABO_3 type perovskites can be enhanced by A site or B site doping, which can affect crystal lattice and physical properties. In a study conducted by Liu et al. [359], the effects of the substitution of Ti for Fe on the phase structure, electrical conductivity, chemical compatibility with electrolytes and electrochemical performance of $SrFe_{1-x}Ti_xO_{3-\sigma}$ were investigated. Here, it was found that the presence of Ti^{3+}/Ti^{4+} ions in the B site stabilized the neighbouring oxygen octahedral (BO_6), leading to structural stability. An increase in thermal expansion and decrease in conductivity and electrochemical performance were also observed with increasing Ti content.

Therefore, perovskites, double perovskites and substituted ABO_3 type perovskites are potential candidates for application as cathodes in SOECs operating at high or intermediate temperatures with important cathode materials studied in recent years being composed of $Sr_2Fe_{1.5}Mo_{0.5}O_{6-\delta}$ [360], $La_{0.4}Sr_{0.6}Co_{0.2}Fe_{0.7}Nb_{0.1}O_{3-\delta}$ [361], $La_{0.7}Sr_{0.3}Fe_{0.7}Ga_{0.3}O_{3-\delta}$ [362], $La_{0.6}Sr_{0.4}Co_{0.8}Fe_{0.2}O_3$ [363], CeO_2–$LaFeO_3$ [364], $SrFe_{0.75}M_{0.25}O_{3-\delta}$ (M = Ti, Zr, V, Nb, Cr, Mo, W) [365], $LaSr_2Fe_2CrO_{9-\delta}$ [366] and Pr-substituted $SrTiO_3$ [367, 368].

4 Summary, Challenges and Future Aspects

4.1 Summary

Water electrolysis, seen as an efficient process to generate hydrogen and pure oxygen, is an emerging field of research for energy storage and conversion. Presently, alkaline and PEM electrolysis are considered mature technologies,

whereas the SOEC is still at the laboratory scale. To increase water electrolysis energy efficiencies, both HER and OER processes, the two necessary reactions in water electrolysis, must be improved kinetically. Here, noble metals are considered to be the best electrocatalysts, however, associated issues such as high cost and low abundance of noble metals hinder the commercialization of water electrolysis technologies. And although improvements have been made to reduce noble metal loading through the modification of material compositions and morphologies or through the replacement of noble metals with non-noble metal-based catalysts, significant progresses have been insufficient.

In the case of alkaline electrolysis, various transition metal compounds, such as Ni-, Co-, Mn- and Fe-based compounds as well as their oxides (MO_x), phosphides (MP_x), sulphides (MS_x) and alloys (MM′), have been extensively studied in recent years in an attempt to replace noble metal catalysts for both OERs and HERs in water electrolysis. Here, catalytic performance enhancements have been carried out by using several different approaches, including the increase of electrical conductivity through alloying, the improvement of stability and conductivity through synthesizing bimetallic compounds, and the creation of synergetic effects by using hybrid compounds through combining intrinsically conductive carbon with chemically reactive metal compounds. In addition, the effects of morphology on electrocatalytic performance were extensively reviewed in literature by using template-assisted and template-less fabrication techniques. Furthermore, the role of electrodes (substrate) in enhancing electrocatalytic performances has also been explored by using different substrates such as carbon cloth, graphitic carbon, carbon black and nickel foam (NF). Promising 3D materials can be obtained by using the nickel foam (NF) as a substrate, which possesses long-range porous structures that can facilitate charge transfer and mass transport.

In the case of PEM electrolysis, non-noble metal catalysts that are capable of providing efficient performances have not yet been discovered. This is because very few non-noble metal catalysts are tolerant of the acid electrolytes used in PEM electrolysis. However, although pure non-noble metals are not suitable as catalysts for OER, they can be used as dopants or supports for noble metals. Non-precious transition metal oxides or carbides such as niobium oxide (Nb_2O_2), tin oxide (SnO_2), tantalum oxide (Ta_2O_5), titanium oxide (TiO_2), WC and TiC can be used as electrode materials to reduce noble metal loading and decrease overall operational costs, but these supports do not show any activity for OER in PEM electrolysis. Therefore, noble metals are still necessary for PEM electrolysis with the replacement of noble metals with non-noble metal catalysts for OERs being still unattainable. Because of this, more stable non-noble metal-based electrocatalysts need to be designed and created, such as Fe–N–C and Co–N–C.

In general, OER and HER catalysts for SOECs operating at high temperatures are unstable. In addition, the active surface area of electrodes needs to be enlarged and three key factors, including ionic conductivity, electronic conductivity and catalytic activity, need to be studied. SOFCs and SOECs are the reverse processes of one another, and therefore, the anode material of SOFCs can be used as the cathode material of SOECs and vice versa, and in general, noble metals are efficient catalysts for anodic and cathodic processes in SOECs operating at high temperatures. Therefore, to make the SOEC process more cost-effective for practical applications, the cost of the catalyst must be reduced and to achieve this, various non-precious catalysts have been studied. For OERs, non-noble metal catalysts include two different types of materials: (1) Ceramic materials that possess good ionic and electrical conductivities such as SFM, LSV, LSCM, LSM. These materials suffer from issues such as low electrocatalytic activity and stability, however. (2) Composite electrodes, such as Ni–YSZ, Ni–SDC, LSC–YSZ and LSM–YSZ possess enhanced catalytic activities and thermal expansion matching with electrolytes. As for the HER process in SOECs, perovskites, double perovskites and substituted ABO_3-type perovskites have been explored as potential candidates for application as cathodes operating at high or intermediate temperatures.

There has been extensive research into noble metal-based and non-noble metal-based catalysts for HERs and OERs in the three different technologies of water electrolysis in recent years, and although these studies have provided many innovative ideas to develop efficient, inexpensive and stable catalysts for water electrolysis in different systems, many technical challenges remain and are discussed as follows.

4.2 Challenges in Water Electrolysis Catalysts

Because of the high cost of noble metal-based catalysts, non-noble metal catalysts for OER and HER processes have been extensively studied in the past few years in an attempt to reduce or replacement noble metal usage and recent developments have shown promise towards commercialization. However, several challenges remain in the production of low-cost non-noble electrocatalysts, including: (1) low electrical conductivity of transition metal compounds for OERs and HERs; (2) fundamental problem of corrosion for carbon-based hybrid catalysts in the electrolysis process for both alkaline and acidic media; (3) non-active nature of transition metal oxides for PEM electrolysis; (4) limited knowledge of catalytic mechanisms of non-noble metal catalysts employed in alkaline media; (5) corrosion of proton ion membranes caused by transitional metals (Fe and Cu); (6) insufficient stability of ceramic catalyst materials for OERs and HERs in SOECs operating at high temperatures; and (7) a potential drop due to excessive loading of non-noble

metal at the anode. (8) Development of bifunctional catalysts for both OER and HER catalysts is still a challenge as the synthesis process is complicated. (9) Up to this point many catalysts have been synthesized with better performance than noble metals in one aspect only; the problem is to develop a catalyst which can surpass noble metals in all aspects. (10) Synthesis method has a direct relation with the catalysis performance, as it affects the structure of catalysts.

4.3 Possible Research Directions

Despite the numerous challenges faced by water electrolysis catalysts, there are many new research opportunities for scientists to develop new, highly efficient catalysts for OER and HER processes. Research directions that can be explored in the future include:

1. *The development of new, facile and cost-effective methods for the synthesis of non-precious metal-based catalysts for OERs and HERs with high electrocatalytic performances.* These new electrocatalyst synthesis methods can be either template or template-less methods, but they need to be inexpensive and be capable of producing catalysts with special structures that possess highly active surface area. Other than this, the development of novel techniques for the design/preparation/fabrication of catalysts is needed, which should be helpful in controlling catalyst morphologies.
2. *The fundamental understanding of catalytic mechanisms to select and design new OERs and HERs catalysts*. Here, catalytic reaction mechanisms of transition metal-based catalysts under different pH and temperature conditions require further exploration. Presently, not only are the mechanisms of water electrolysis electrocatalytic reactions in alkaline media unclear, the active centre cannot be identified with accuracy either. Further improvements in performance can be made with deeper understandings of the complete mechanism, which can lead to improved synthesis methods and doping strategies. Therefore, both theoretical calculations and experimental validations of catalytic mechanisms, such as DFT calculations on atomic levels, need to be carried out to gain deeper understandings of the catalytic process.
3. *The further exploration of low-/non-noble metal-based catalysts for OERs and HERs in PEM electrolysis.* There is a need to develop low-/non-noble metal catalysts that can operate in strong acidic conditions (pH < 3). In addition, these catalysts should also ideally possess high electrocatalytic performances comparable to state-of-the-art noble metal catalysts along with high stabilities.
4. *The development of low-/non-noble metal-based catalyst materials for OERs and HERs in SOECs.* Because electrode material degradation is a major challenge in SOECs, a thorough understanding of the degradation mechanisms of ceramic-based catalysts is necessary. This understanding can pave pathways towards the development of new catalytic materials for SOECs.

Overall, these future research directions will hopefully address current challenges in the development of effective and widely applicable strategies for non-noble metal-based catalysts for water electrolysis.

Acknowledgements We gratefully acknowledge the financial support from the National Key Research and Development Program of China (2017YFB0102900) and Shanghai Pujiang Program (17PJD016).

Compliance with Ethical Standards

Conflict of interest The authors declare that they have no conflicts of interest.

References

1. Nikolaidis, P., Poullikkas, A.: A comparative overview of hydrogen production processes. Renew. Sustain. Energy Rev. **67**, 597–611 (2017)
2. Singh, S., Jain, S., Venkateswaran, P.S., et al.: Hydrogen: a sustainable fuel for future of the transport sector. Renew. Sustain. Energy Rev. **51**, 623–633 (2015)
3. Hassmann, K., Kühne, H.M.: Primary energy sources for hydrogen production. Int. J. Hydrog. Energy **18**, 635–640 (1993)
4. López Ortiz, A., Meléndez Zaragoza, M.J., Collins-Martínez, V.: Hydrogen production research in Mexico: a review. Int. J. Hydrog. Energy **41**, 23363–23379 (2016)
5. Sharma, S., Ghoshal, S.K.: Hydrogen the future transportation fuel: from production to applications. Renew. Sustain. Energy Rev. **43**, 1151–1158 (2015)
6. Veziroğlu, T.N., Sahin, S.: 21st Century's energy: Hydrogen energy system. Energy Convers. Manag. **49**, 1820–1831 (2008)
7. Marbán, G., Valdés-Solís, T.: Towards the hydrogen economy? Int. J. Hydrog. Energy **32**, 1625–1637 (2007)
8. Sobrino, F.H., Monroy, C.R., Pérez, J.L.H.: Critical analysis on hydrogen as an alternative to fossil fuels and biofuels for vehicles in Europe. Renew. Sustain. Energy Rev. **14**, 772–780 (2010)
9. Mori, D., Hirose, K.: Recent challenges of hydrogen storage technologies for fuel cell vehicles. Int. J. Hydrog. Energy **34**, 4569–4574 (2009)
10. Ball, M., Wietschel, M.: The future of hydrogen—opportunities and challenges. Int. J. Hydrog. Energy **34**, 615–627 (2009)
11. Züttel, A.: Hydrogen storage methods. Naturwissenschaften **91**, 157–172 (2004)
12. Barbir, F.: Transition to renewable energy systems with hydrogen as an energy carrier. Energy **34**, 308–312 (2009)
13. Ahmed, A., Al-Amin, A.Q., Ambrose, A.F., et al.: Hydrogen fuel and transport system: a sustainable and environmental future. Int. J. Hydrog. Energy **41**, 1369–1380 (2016)
14. Milazzo, M.F., Spina, F., Primerano, P., et al.: Soy biodiesel pathways: global prospects. Renew. Sustain. Energy Rev. **26**, 579–624 (2013)

15. Achten, W.M.J., Verchot, L., Franken, Y.J., et al.: Jatropha biodiesel production and use. Biomass Bioenergy **32**, 1063–1084 (2008)
16. Balat, M., Balat, M.: Political, economic and environmental impacts of biomass-based hydrogen. Int. J. Hydrog. Energy **34**, 3589–3603 (2009)
17. Hosseini, S.E., Wahid, M.A.: Hydrogen production from renewable and sustainable energy resources: promising green energy carrier for clean development. Renew. Sustain. Energy Rev. **57**, 850–866 (2016)
18. Balat, M.: Hydrogen in fueled systems and the significance of hydrogen in vehicular transportation. Energy Source Part B **2**, 49–61 (2007)
19. Muradov, N., Veziroğlu, T.N.: From hydrocarbon to hydrogen–carbon to hydrogen economy. Int. J. Hydrog. Energy **30**, 225–237 (2005)
20. Caldwell, D.L.: Production of chlorine. In: Bockris, J.O., Conway, B.E., Yeager, E., et al. (eds.) Comprehensive Treatise of Electrochemistry, pp. 105–166. Springer, Boston (1981)
21. Balat, M.: Potential importance of hydrogen as a future solution to environmental and transportation problems. Int. J. Hydrog. Energy **33**, 4013–4029 (2008)
22. Blasi, A., Fiorenza, G., Freda, C., et al.: 6-Steam reforming of biofuels for the production of hydrogen-rich gas. In: Gugliuzza, A., Basile, A. (eds.) Membranes for Clean and Renewable Power Applications, pp. 145–181. Woodhead Publishing, Cambridge (2014)
23. Serban, M., Lewis, M.A., Marshall, C.L., et al.: Hydrogen production by direct contact pyrolysis of natural gas. Energy & Fuels **17**, 705–713 (2003)
24. Schlapbach, L., Züttel, A.: Hydrogen-storage materials for mobile applications. Nature **414**, 353–358 (2001)
25. Carmo, M., Fritz, D.L., Mergel, J., et al.: A comprehensive review on PEM water electrolysis. Int. J. Hydrog. Energy **38**, 4901–4934 (2013)
26. Trasatti, S.: Water electrolysis: who first? J. Electroanal. Chem. **476**, 90–91 (1999)
27. Choi, P., Bessarabov, D.G., Datta, R.: A simple model for solid polymer electrolyte (SPE) water electrolysis. Solid State Ion. **175**, 535–539 (2004)
28. Ursua, A., Gandía, L.M., Sanchis, P.: Hydrogen production from water electrolysis: current status and future trends. Proc. IEEE **100**, 410–426 (2012)
29. Holladay, J.D., Hu, J., King, D.L., et al.: An overview of hydrogen production technologies. Catal. Today **139**, 244–260 (2009)
30. Tahir, M., Pan, L., Idrees, F., et al.: Electrocatalytic oxygen evolution reaction for energy conversion and storage: a comprehensive review. Nano Energy **37**, 136–157 (2017)
31. Laguna-Bercero, M.A.: Recent advances in high temperature electrolysis using solid oxide fuel cells: a review. J. Power Sources **203**, 4–16 (2012)
32. Zha, Y., Disabb-Miller, M.L., Johnson, Z.D., et al.: Metal-cation-based anion exchange membranes. Chem. Soc. Rev. **134**, 4493–4496 (2012)
33. Beainy, A., Karami, N., Moubayed, N.: Simulink model for a PEM electrolyzer based on an equivalent electrical circuit (2015). In: International conference on renewable energies for developing countries 2014, Beirut, Lebanon, 26–27 Nov 2014
34. Nuttall, L.J., Fickett, A.P., Titterington, W.A.: Hydrogen generation by solid polymer electrolyte water electrolysis. In: Veziroğlu, T.N. (ed.) Hydrogen Energy: Part A, pp. 441–455. Springer, Boston (1975)
35. Gong, M., Wang, D.Y., Chen, C.C., et al.: A mini review on nickel-based electrocatalysts for alkaline hydrogen evolution reaction. Nano Res. **9**, 28–46 (2016)
36. Zhang, C., Wang, B., Shen, X., et al.: A nitrogen-doped ordered mesoporous carbon/graphene framework as bifunctional electrocatalyst for oxygen reduction and evolution reactions. Nano Energy **30**, 503–510 (2016)
37. Oh, J., Mee Lee, J., Yoo, Y., et al.: New insight of the photocatalytic behaviors of graphitic carbon nitrides for hydrogen evolution and their associations with grain size, porosity, and photophysical properties. Appl. Catal. B **218**, 349–358 (2017)
38. Busch, M., Halck, N.B., Kramm, U.I., et al.: Beyond the top of the volcano?—a unified approach to electrocatalytic oxygen reduction and oxygen evolution. Nano Energy **29**, 126–135 (2016)
39. Wang, J., Liu, J., Zhang, B., et al.: Synergistic effect of two actions sites on cobalt oxides towards electrochemical water-oxidation. Nano Energy **42**, 98–105 (2017)
40. Birss, V.I., Damjanovic, A., Hudson, P.G.: Oxygen evolution at platinum electrodes in alkaline solutions II. Mechanism of the reaction. J. Electrochem. Soc. **133**, 1621–1625 (1986)
41. Conway, B.E., Liu, T.C.: Characterization of electrocatalysis in the oxygen evolution reaction at platinum by evaluation of behavior of surface intermediate states at the oxide film. Langmuir **6**, 268–276 (1990)
42. Zheng, J.: Pt-free NiCo electrocatalysts for oxygen evolution by seawater splitting. Electrochim. Acta **247**, 381–391 (2017)
43. Makarova, M.V., Jirkovský, J., Klementová, M., et al.: The electrocatalytic behavior of $Ru_{0.8}Co_{0.2}O_{2-x}$—the effect of particle shape and surface composition. Electrochim. Acta **53**, 2656–2664 (2008)
44. Lewis, N.S., Nocera, D.G.: Powering the planet: Chemical challenges in solar energy utilization. Proc. Natl. Acad. Sci. U. S. A. **103**, 15729–15735 (2006)
45. Li, H., Tang, Q., He, B., et al.: Robust electrocatalysts from an alloyed Pt–Ru–M (M = Cr, Fe Co, Ni, Mo)-decorated Ti mesh for hydrogen evolution by seawater splitting. J. Mater. Chem. A **4**, 6513–6520 (2016)
46. Liu, X., Wang, X., Yuan, X., et al.: Rational composition and structural design of in situ grown nickel-based electrocatalysts for efficient water electrolysis. J. Mater. Chem. A **4**, 167–172 (2016)
47. Hammes-Schiffer, S.: Theory of proton-coupled electron transfer in energy conversion processes. Acc. Chem. Res. **42**, 1881–1889 (2009)
48. Stojić, D.L., Marčeta, M.P., Sovilj, S.P., et al.: Hydrogen generation from water electrolysis—possibilities of energy saving. J. Power Sources **118**, 315–319 (2003)
49. Luo, B., Yan, X., Xu, S., et al.: Synthesis of worm-like PtCo nanotubes for methanol oxidation. Electrochem. Commun. **30**, 71–74 (2013)
50. Man, I., Su, H.Y., Calle-Vallejo, F., et al.: Universality in oxygen evolution electrocatalysis on oxide surfaces. ChemCatChem **3**, 1159–1165 (2011)
51. Liu, J., Wang, J., Zhang, B., et al.: Hierarchical $NiCo_2S_4$@NiFe LDH heterostructures supported on nickel foam for enhanced overall-water-splitting activity. ACS Appl. Mater. Interfaces **9**, 15364–15372 (2017)
52. Norskov, J.K., Christensen, C.H.: Toward efficient hydrogen production at surfaces. Science **312**, 1322 (2006)
53. Lee, S.H., Lee, H., Cho, M., et al.: A layered hollow sphere architecture of iridium-decorated carbon electrode for oxygen evolution catalysis. Carbon **115**, 50–58 (2017)
54. Cherevko, S., Geiger, S., Kasian, O.: Oxygen and hydrogen evolution reactions on Ru, RuO_2, Ir, and IrO_2 thin film electrodes in acidic and alkaline electrolytes: a comparative study on activity and stability. Catal. Today **262**, 170–180 (2016)
55. Danilovic, N., Subbaraman, R., Chang, K.C., et al.: Activity–stability trends for the oxygen evolution reaction on monometallic

oxides in acidic environments. J. Phys. Chem. Lett. **5**, 2474–2478 (2014)
56. Pi, Y., Zhang, N., Guo, S., et al.: Ultrathin laminar Ir superstructure as highly efficient oxygen evolution electrocatalyst in broad pH range. Nano Lett. **16**, 4424–4430 (2016)
57. Jiao, Y., Zheng, Y., Jaroniec, M., et al.: Design of electrocatalysts for oxygen- and hydrogen-involving energy conversion reactions. Chem. Soc. Rev. **44**, 2060–2086 (2015)
58. Li, G., Li, S., Ge, J., et al.: Discontinuously covered IrO_2–RuO_2@Ru electrocatalysts for the oxygen evolution reaction: how high activity and long-term durability can be simultaneously realized in the synergistic and hybrid nano-structure. J. Mater. Chem. A **5**, 17221–17229 (2017)
59. Liyanage, D.R., Li, D., Cheek, Q.B., et al.: Synthesis and oxygen evolution reaction (OER) catalytic performance of $Ni_{2-x}Ru_xP$ nanocrystals: enhancing activity by dilution of the noble metal. J. Mater. Chem. A **5**, 17609–17618 (2017)
60. Huang, H., Yu, C., Zhao, C., et al.: Iron-tuned super nickel phosphide microstructures with high activity for electrochemical overall water splitting. Nano Energy **34**, 472–480 (2017)
61. Jiang, F., Zheng, T., Yang, Y.: Preparation and electrochromic properties of tungsten oxide and iridium oxide porous films. J. NonCryst. Solids **354**, 1290–1293 (2008)
62. Arciga-Duran, E., Meas, Y., Pérez-Bueno, J.J., et al.: Effect of oxygen vacancies in electrodeposited NiO towards the oxygen evolution reaction: role of Ni–glycine complexes. Electrochim. Acta **268**, 49–58 (2018)
63. Babar, P.T., Lokhande, A.C., Gang, M.G., et al.: Thermally oxidized porous NiO as an efficient oxygen evolution reaction (OER) electrocatalyst for electrochemical water splitting application. J. Ind. Eng. Chem. **60**, 493–497 (2018)
64. Zhang, T., Wu, M.Y., Yan, D.Y.: Engineering oxygen vacancy on NiO nanorod arrays for alkaline hydrogen evolution. Nano Energy **43**, 103–109 (2018)
65. Wu, Z., Zou, Z., Huang, J., et al.: Fe-doped NiO mesoporous nanosheets array for highly efficient overall water splitting. J. Catal. **358**, 243–252 (2018)
66. Zheng, Z., Geng, W., Wang, Y., et al.: $NiCo_2O_4$ nanoflakes supported on titanium suboxide as a highly efficient electrocatalyst towards oxygen evolution reaction. Int. J. Hydrog. Energy **42**, 119–124 (2017)
67. Chen, R., Wang, H.Y., Miao, J., et al.: A flexible high-performance oxygen evolution electrode with three-dimensional NiCo2O4 core–shell nanowires. Nano Energy **11**, 333–340 (2015)
68. Yan, K.L., Shang, X., Li, Z., et al.: Ternary mixed metal Fe-doped $NiCo_2O_4$ nanowires as efficient electrocatalysts for oxygen evolution reaction. Appl. Surf. Sci. **416**, 371–378 (2017)
69. Schoeberl, C., Manolova, M., Freudenberger, R.: Sol–gel-deposited cobalt and nickel oxide as an oxygen evolution catalyst in alkaline media. Int. J. Hydrog. Energy **40**, 11773–11778 (2015)
70. Xiao, Y., Feng, L., Hu, C., et al.: $NiCo_2O_4$ 3-dimensional nanosheet as effective and robust catalyst for oxygen evolution reaction. RSC Adv. **5**, 61900–61905 (2015)
71. Zeng, L., Zhao, T.S., Zhang, R.H., et al.: $NiCo_2O_4$ nanowires@MnO_x nanoflakes supported on stainless steel mesh with superior electrocatalytic performance for anion exchange membrane water splitting. Electrochem. Commun. **87**, 66–70 (2018)
72. Chanda, D., Hnát, J., Bystron, T., et al.: Optimization of synthesis of the nickel–cobalt oxide based anode electrocatalyst and of the related membrane-electrode assembly for alkaline water electrolysis. J. Power Sources **347**, 247–258 (2017)
73. Cheng, H., Su, Y.Z., Kuang, P.Y., et al.: Hierarchical $NiCo_2O_4$ nanosheet-decorated carbon nanotubes towards highly efficient electrocatalyst for water oxidation. J. Mater. Chem. A **3**, 19314–19321 (2015)
74. Ning, Y., Ma, D., Shen, Y., et al.: Constructing hierarchical mushroom-like bifunctional $NiCo/NiCo_2S_4$@NiCo/Ni foam electrocatalysts for efficient overall water splitting in alkaline media. Electrochim. Acta **265**, 19–31 (2018)
75. Yang, Y., Zhou, M., Guo, W., et al.: $NiCoO_2$ nanowires grown on carbon fiber paper for highly efficient water oxidation. Electrochim. Acta **174**, 246–253 (2015)
76. Shao, Y., Zheng, M., Cai, M., et al.: improved electrocatalytic performance of core–shell $NiCo/NiCoO_x$ with amorphous FeOOH for oxygen-evolution reaction. Electrochim. Acta **257**, 1–8 (2017)
77. Yan, K.L., Shang, X., Gao, W.K., et al.: Ternary MnO_2/$NiCo_2O_4$/NF with hierarchical structure and synergistic interaction as efficient electrocatalysts for oxygen evolution reaction. J. Alloys Compd. **719**, 314–321 (2017)
78. Zhang, Y., Zhang, H., Fang, L., et al.: Facile synthesis of nickel manganese composite oxide nanomesh for efficient oxygen evolution reaction and supercapacitors. Electrochim. Acta **245**, 32–40 (2017)
79. Zhang, D., Meng, L., Shi, J., et al.: One-step preparation of optically transparent Ni–Fe oxide film electrocatalyst for oxygen evolution reaction. Electrochim. Acta **169**, 402–408 (2015)
80. Liu, G., Gao, X., Wang, K., et al.: Uniformly mesoporous NiO/$NiFe_2O_4$ biphasic nanorods as efficient oxygen evolving catalyst for water splitting. Int. J. Hydrog. Energy **41**, 17976–17986 (2016)
81. Browne, M.P., Stafford, S., O'Brien, M., et al.: The goldilocks electrolyte: examining the performance of iron/nickel oxide thin films as catalysts for electrochemical water splitting in various aqueous NaOH solutions. J. Mater. Chem. A **4**, 11397–11407 (2016)
82. Hwang, G.J., Gil, B.M., Ryu, C.H.: Preparation of the electrode using $NiFe_2O_4$ powder for the alkaline water electrolysis. J. Ind. Eng. Chem. **48**, 242–248 (2017)
83. Xie, Y., Wang, X., Tang, K., et al.: Blending Fe_3O_4 into a Ni/NiO composite for efficient and stable bifunctional electrocatalyst. Electrochim. Acta **264**, 225–232 (2018)
84. Görlin, M., Gliech, M., de Araújo, J.F.: Dynamical changes of a Ni–Fe oxide water splitting catalyst investigated at different pH. Catal. Today **262**, 65–73 (2016)
85. Jiang, J., Zhang, C., Ai, L.: Hierarchical iron nickel oxide architectures derived from metal–organic frameworks as efficient electrocatalysts for oxygen evolution reaction. Electrochim. Acta **208**, 17–24 (2016)
86. Banerjee, S., Debata, S., Madhuri, R., et al.: Electrocatalytic behavior of transition metal (Ni, Fe, Cr) doped metal oxide nanocomposites for oxygen evolution reaction. Appl. Surf. Sci. **449**, 660–668 (2018)
87. Liu, H., Wang, Y., Lu, X., et al.: The effects of Al substitution and partial dissolution on ultrathin NiFeAl trinary layered double hydroxide nanosheets for oxygen evolution reaction in alkaline solution. Nano Energy **35**, 350–357 (2017)
88. Yan, K., Lafleur, T., Chai, J., et al.: Facile synthesis of thin NiFe-layered double hydroxides nanosheets efficient for oxygen evolution. Electrochem. Commun. **62**, 24–28 (2016)
89. Li, X., Zai, J., Liu, Y., et al.: Atomically thin layered NiFe double hydroxides assembled 3D microspheres with promoted electrochemical performances. J. Power Sources **325**, 675–681 (2016)
90. Zhang, K., Wang, W., Kuai, L., et al.: A facile and efficient strategy to gram-scale preparation of composition-controllable Ni–Fe LDHs nanosheets for superior OER catalysis. Electrochim. Acta **225**, 303–309 (2017)

91. Youn, D.H., Park, Y.B., Kim, J.Y., et al.: One-pot synthesis of NiFe layered double hydroxide/reduced graphene oxide composite as an efficient electrocatalyst for electrochemical and photoelectrochemical water oxidation. J. Power Sources **294**, 437–443 (2015)
92. Zhan, T., Liu, X., Lu, S., et al.: Nitrogen doped NiFe layered double hydroxide/reduced graphene oxide mesoporous nanosphere as an effective bifunctional electrocatalyst for oxygen reduction and evolution reactions. Appl. Catal. B Environ. **205**, 551–558 (2017)
93. Lee, E., Park, A.H., Park, H.U., et al.: Facile sonochemical synthesis of amorphous NiFe-(oxy)hydroxide nanoparticles as superior electrocatalysts for oxygen evolution reaction. Ultrason. Sonochem. **40**, 552–557 (2018)
94. Xia, D.C., Zhou, L., Qiao, S., et al.: Graphene/Ni–Fe layered double-hydroxide composite as highly active electrocatalyst for water oxidation. Mater. Res. Bull. **74**, 441–446 (2016)
95. Stern, L.A., Feng, L., Song, F., et al.: Ni_2P as a Janus catalyst for water splitting: the oxygen evolution activity of Ni2P nanoparticles. Energy Environ. Sci. **8**, 2347–2351 (2015)
96. Liu, G., He, D., Yao, R., et al.: Enhancing the water oxidation activity of Ni_2P nanocatalysts by iron-doping and electrochemical activation. Electrochim. Acta **253**, 498–505 (2017)
97. Pu, Z., Xue, Y., Li, W., et al.: Efficient water splitting catalyzed by flexible NiP_2 nanosheet array electrodes under both neutral and alkaline solutions. New J. Chem. **41**, 2156–2159 (2017)
98. Wang, X., Li, W., Xiong, D., et al.: Fast fabrication of self-supported porous nickel phosphide foam for efficient, durable oxygen evolution and overall water splitting. J. Mater. Chem. A **4**, 5639–5646 (2016)
99. Ren, J., Hu, Z., Chen, C., et al.: Integrated Ni_2P nanosheet arrays on three-dimensional Ni foam for highly efficient water reduction and oxidation. J. Energy Chem. **26**, 1196–1202 (2017)
100. Zhang, B., Lui, Y.H., Ni, H., et al.: Bimetallic $(Fe_xNi_{1-x})_2P$ nanoarrays as exceptionally efficient electrocatalysts for oxygen evolution in alkaline and neutral media. Nano Energy **38**, 553–560 (2017)
101. Jin, L., Xia, H., Huang, Z., et al.: Phase separation synthesis of trinickel monophosphide porous hollow nanospheres for efficient hydrogen evolution. J. Mater. Chem. A **4**, 10925–10932 (2016)
102. Barwe, S., Andronescu, C., Vasile, E., et al.: Influence of Ni to Co ratio in mixed Co and Ni phosphides on their electrocatalytic oxygen evolution activity. Electrochem. Commun. **79**, 41–45 (2017)
103. Xiao, C., Zhang, B., Li, D.: Partial-sacrificial-template synthesis of Fe/Ni phosphides on ni foam: a strongly stabilized and efficient catalyst for electrochemical water splitting. Electrochim. Acta **242**, 260–267 (2017)
104. Zhang, C., Xie, Y., Deng, H., et al.: Ternary nickel iron phosphide supported on nickel foam as a high-efficiency electrocatalyst for overall water splitting. Int. J. Hydrog. Energy **43**, 7299–7306 (2018)
105. Bandal, H.A., Jadhav, A.R., Kim, H.: Facile synthesis of bicontinuous Ni_3Fe alloy for efficient electrocatalytic oxygen evolution reaction. J. Alloys Compd. **726**, 875–884 (2017)
106. Flis-Kabulska, I., Flis, J.: Electroactivity of Ni–Fe cathodes in alkaline water electrolysis and effect of corrosion. Corros. Sci. **112**, 255–263 (2016)
107. Yang, Y., Zhuang, L., Lin, R., et al.: A facile method to synthesize boron-doped Ni/Fe alloy nano-chains as electrocatalyst for water oxidation. J. Power Sources **349**, 68–74 (2017)
108. Zhu, Y., Wang, Y., Liu, S., et al.: Facile and controllable synthesis at an ionic layer level of high-performance NiFe-based nanofilm electrocatalysts for the oxygen evolution reaction in alkaline electrolyte. Electrochem. Commun. **86**, 38–42 (2018)
109. Fu, Y., Yu, H.Y., Jiang, C., et al.: NiCo alloy nanoparticles decorated on n-doped carbon nanofibers as highly active and durable oxygen electrocatalyst. Adv. Funct. Mater. **28**, 1705094 (2018)
110. Du, L., Luo, L., Feng, Z., et al.: Nitrogen-doped graphitized carbon shell encapsulated NiFe nanoparticles: a highly durable oxygen evolution catalyst. Nano Energy **39**, 245–252 (2017)
111. Fu, S., Song, J., Zhu, C., et al.: Ultrafine and highly disordered Ni_2Fe nanofoams enabled highly efficient oxygen evolution reaction in alkaline electrolyte. Nano Energy **44**, 319–326 (2018)
112. Shetty, S., Mohamed Jaffer Sadiq, M., Bhat, D.K., et al.: Electrodeposition and characterization of Ni–Mo alloy as an electrocatalyst for alkaline water electrolysis. J. Electroanal. Chem. **796**, 57–65 (2017)
113. Rosalbino, F., Delsante, S., Borzone, G., et al.: Electrocatalytic activity of crystalline Ni–Co–M (M = Cr, Mn, Cu) alloys on the oxygen evolution reaction in an alkaline environment. Int. J. Hydrog. Energy **38**, 10170–10177 (2013)
114. Su, X., Sun, Q., Bai, J., et al.: Electrodeposition of porous MoO_2-doped NiFe nanosheets for highly efficient electrocatalytic oxygen evolution reactions. Electrochim. Acta **260**, 477–482 (2018)
115. Wu, L.K., Wu, W.Y., Xia, J., et al.: A nanostructured nickel–cobalt alloy with an oxide layer for an efficient oxygen evolution reaction. J. Mater. Chem. A **5**, 10669–10677 (2017)
116. Edison, T.N.J.I., Atchudan, R., Karthik, N., et al.: Ultrasonic synthesis, characterization and energy applications of Ni–B alloy nanorods. J. Taiwan Inst. Chem. Eng. **80**, 901–907 (2017)
117. Vishnu Prataap, R.K., Mohan, S.: Electrodeposited-hydroxide surface-covered porous nickel-cobalt alloy electrodes for efficient oxygen evolution reaction. Chem. Commun. **53**, 3365–3368 (2017)
118. Hu, C.C., Wu, Y.R.: Bipolar performance of the electroplated iron-nickel deposits for water electrolysis. Mater. Chem. Phys. **82**, 588–596 (2003)
119. Chen, J., Chen, J., Yu, D., et al.: Carbon nanofiber-supported PdNi alloy nanoparticles as highly efficient bifunctional catalysts for hydrogen and oxygen evolution reactions. Electrochim. Acta **246**, 17–26 (2017)
120. Yu, J., Zhong, Y., Zhou, W., et al.: Facile synthesis of nitrogen-doped carbon nanotubes encapsulating nickel cobalt alloys 3D networks for oxygen evolution reaction in an alkaline solution. J. Power Sources **338**, 26–33 (2017)
121. Du, J., Zou, Z., Liu, C., et al.: Hierarchical Fe-doped Ni_3Se_4 ultrathin nanosheets as an efficient electrocatalyst for oxygen evolution reaction. Nanoscale **10**, 5163–5170 (2018)
122. Xu, Y.Z., Yuan, C.Z., Chen, X.P.: Co-doped NiSe nanowires on nickel foam via a cation exchange approach as efficient electrocatalyst for enhanced oxygen evolution reaction. RSC Adv. **6**, 106832–106836 (2016)
123. Hao, J., Yang, W., Hou, J., et al.: Nitrogen doped NiS_2 nanoarrays with enhanced electrocatalytic activity for water oxidation. J. Mater. Chem. A **5**, 17811–17816 (2017)
124. Feng, L.L., Yu, G., Wu, Y., et al.: High-index faceted Ni_3S_2 nanosheet arrays as highly active and ultrastable electrocatalysts for water splitting. Chem. Soc. Rev. **137**, 14023–14026 (2015)
125. Zhou, W., Wu, X.J., Cao, X., et al.: Ni_3S_2 nanorods/Ni foam composite electrode with low overpotential for electrocatalytic oxygen evolution. Energy Environ. Sci. **6**, 2921–2924 (2013)
126. Li, X., Han, G.Q., Liu, Y.R., et al.: NiSe@NiOOH core–shell hyacinth-like nanostructures on nickel foam synthesized by in situ electrochemical oxidation as an efficient electrocatalyst for the oxygen evolution reaction. ACS Appl. Mater. Interfaces **8**, 20057–20066 (2016)

127. Koza, J.A., He, Z., Miller, A.S., et al.: Electrodeposition of crystalline Co_3O_4—a catalyst for the oxygen evolution reaction. Chem. Mater. **24**, 3567–3573 (2012)
128. Casella, I.G.: Electrodeposition of cobalt oxide films from carbonate solutions containing Co(II)–tartrate complexes. J. Electroanal. Chem. **520**, 119–125 (2002)
129. Sun, Y., Gao, S., Lei, F., et al.: Atomically-thin non-layered cobalt oxide porous sheets for highly efficient oxygen-evolving electrocatalysts. Chem. Sci. **5**, 3976–3982 (2014)
130. Ranaweera, C.K., Zhang, C., Bhoyate, S., et al.: Flower-shaped cobalt oxide nano-structures as an efficient, flexible and stable electrocatalyst for the oxygen evolution reaction. Mater. Chem. Front. **1**, 1580–1584 (2017)
131. Wang, X., Li, T.T., Zheng, Y.Q.: Co_3O_4 nanosheet arrays treated by defect engineering for enhanced electrocatalytic water oxidation. Int. J. Hydrog. Energy **43**, 2009–2017 (2018)
132. Natarajan, S., Anantharaj, S., Tayade, R.J., et al.: Recovered spinel $MnCo_2O_4$ from spent lithium-ion batteries for enhanced electrocatalytic oxygen evolution in alkaline medium. Dalton Trans. **46**, 14382–14392 (2017)
133. Sagu, J.S., Mehta, D., Wijayantha, K.G.U.: Electrocatalytic activity of $CoFe_2O_4$ thin films prepared by AACVD towards the oxygen evolution reaction in alkaline media. Electrochem. Commun. **87**, 1–4 (2018)
134. AlShehri, S., Ahmed, J., Ahamad, T., et al.: Bifunctional electrocatalytic performances of $CoWO_4$ nanocubes for water redox reactions (OER/ORR). RSC Adv. **7**, 45615–45623 (2017)
135. Zhu, G., Ge, R., Qu, F., et al.: In situ surface derivation of an Fe–Co–Bi layer on an Fe-doped Co_3O_4 nanoarray for efficient water oxidation electrocatalysis under near-neutral conditions. J. Mater. Chem. A **5**, 6388–6392 (2017)
136. Zhang, L., Yang, C., Xie, Z., et al.: Cobalt manganese spinel as an effective cocatalyst for photocatalytic water oxidation. Appl. Catal. B Environ. **224**, 886–894 (2018)
137. Xu, W., Lyu, F., Bai, Y., et al.: Porous cobalt oxide nanoplates enriched with oxygen vacancies for oxygen evolution reaction. Nano Energy **43**, 110–116 (2018)
138. Deng, S., Shen, S., Zhong, Y., et al.: Assembling Co_9S_8 nanoflakes on Co_3O_4 nanowires as advanced core/shell electrocatalysts for oxygen evolution reaction. J. Energy Chem. **26**, 1203–1209 (2017)
139. Zhang, J., Zhang, D., Yang, Y., et al.: Facile synthesis of $ZnCo_2O_4$ mesoporous structures with enhanced electrocatalytic oxygen evolution reaction properties. RSC Adv. **6**, 92699–92704 (2016)
140. Suryanto, B.H.R., Lu, X., Zhao, C.: Layer-by-layer assembly of transparent amorphous Co_3O_4 nanoparticles/graphene composite electrodes for sustained oxygen evolution reaction. J. Mater. Chem. A **1**, 12726–12731 (2013)
141. Sun, X., Gao, L., Guo, C., et al.: Sulfur incorporated $CoFe_2O_4$/multiwalled carbon nanotubes toward enhanced oxygen evolution reaction. Electrochim. Acta **247**, 843–850 (2017)
142. Hu, W., Wang, Q., Wu, S., et al.: Facile one-pot synthesis of a nitrogen-doped mesoporous carbon architecture with cobalt oxides encapsulated in graphitic layers as a robust bicatalyst for oxygen reduction and evolution reactions. J. Mater. Chem. A **4**, 16920–16927 (2016)
143. Zhang, L., Mi, T., Ziaee, M.A., et al.: Hollow POM@MOF hybrid-derived porous Co_3O_4/$CoMoO_4$ nanocages for enhanced electrocatalytic water oxidation. J. Mater. Chem. A **6**, 1639–1647 (2018)
144. Zhang, Y.X., Guo, X., Zhai, X., et al.: Diethylenetriamine (DETA)-assisted anchoring of Co_3O_4 nanorods on carbon nanotubes as efficient electrocatalysts for the oxygen evolution reaction. J. Mater. Chem. A **3**, 1761–1768 (2015)
145. Qi, C., Zhang, L., Xu, G., et al.: Co@Co_3O_4 nanoparticle embedded nitrogen-doped carbon architectures as efficient bicatalysts for oxygen reduction and evolution reactions. Appl. Surf. Sci. **427**, 319–327 (2018)
146. Long, J., Gong, Y., Lin, J.: Metal–organic framework-derived Co_9S_8@CoS@CoO@C nanoparticles as efficient electro- and photo-catalysts for the oxygen evolution reaction. J. Mater. Chem. A **5**, 10495–10509 (2017)
147. Wei, Y., Ren, X., Ma, H., et al.: $CoC_2O_4{\cdot}2H_2O$ derived Co_3O_4 nanorods array: a high-efficiency 1D electrocatalyst for alkaline oxygen evolution reaction. Chem. Commun. **54**, 1533–1536 (2018)
148. Liu, M., Li, J.: Cobalt phosphide hollow polyhedron as efficient bifunctional electrocatalysts for the evolution reaction of hydrogen and oxygen. ACS Appl. Mater. Interfaces **8**, 2158–2165 (2016)
149. Dutta, A., Samantara, A.K., Dutta, S.K., et al.: Surface-oxidized dicobalt phosphide nanoneedles as a nonprecious, durable, and efficient OER catalyst. ACS Energy Lett. **1**, 169–174 (2016)
150. Jin, Z., Li, P., Xiao, D.: Metallic Co_2P ultrathin nanowires distinguished from CoP as robust electrocatalysts for overall water-splitting. Green Chem. **18**, 1459–1464 (2016)
151. Huang, Z., Chen, Z., Chen, Z., et al.: Cobalt phosphide nanorods as an efficient electrocatalyst for the hydrogen evolution reaction. Nano Energy **9**, 373–382 (2014)
152. Pu, Z., Liu, Q., Jiang, P., et al.: CoP nanosheet arrays supported on a Ti Plate: an efficient cathode for electrochemical hydrogen evolution. Chem. Mater. **26**, 4326–4329 (2014)
153. Tian, J., Liu, Q., Asiri, A.M., et al.: Self-supported nanoporous cobalt phosphide nanowire arrays: an efficient 3D hydrogen-evolving cathode over the wide range of pH 0–14. Chem. Soc. Rev. **136**, 7587–7590 (2014)
154. Fu, S., Zhu, C., Song, J., et al.: Highly ordered mesoporous bimetallic phosphides as efficient oxygen evolution electrocatalysts. ACS Energy Lett. **1**, 792–796 (2016)
155. Cao, Z., Zhou, T., Xi, W., et al.: Bimetal metal–organic frameworks derived $Co_{0.4}Fe_{0.28}P$ and $Co_{0.37}Fe_{0.26}S$ nanocubes for enhanced oxygen evolution reaction. Electrochim. Acta **263**, 576–584 (2018)
156. Yin, D., Jin, Z., Liu, M., et al.: Microwave-assisted synthesis of the cobalt-iron phosphates nanosheets as an efficient electrocatalyst for water oxidation. Electrochim. Acta **260**, 420–429 (2018)
157. Li, D., Baydoun, H., Verani, C.N., et al.: Efficient water oxidation using CoMnP nanoparticles. Chem. Soc. Rev. **138**, 4006–4009 (2016)
158. Wang, J., Yang, W., Liu, J.: CoP_2 nanoparticles on reduced graphene oxide sheets as a super-efficient bifunctional electrocatalyst for full water splitting. J. Mater. Chem. A **4**, 4686–4690 (2016)
159. Bai, Y., Zhang, H., Feng, Y., et al.: Sandwich-like CoP/C nanocomposites as efficient and stable oxygen evolution catalysts. J. Mater. Chem. A **4**, 9072–9079 (2016)
160. Xiong, X., Ji, Y., Xie, M., et al.: MnO_2–CoP_3 nanowires array: an efficient electrocatalyst for alkaline oxygen evolution reaction with enhanced activity. Electrochem. Commun. **86**, 161–165 (2018)
161. Jiang, H., Li, C., Shen, H., et al.: Supramolecular gel-assisted synthesis Co_2P particles anchored in multielement co-doped graphene as efficient bifunctional electrocatalysts for oxygen reduction and evolution. Electrochim. Acta **231**, 344–353 (2017)
162. Wu, R., Wang, D.P., Zhou, K., et al.: Porous cobalt phosphide/graphitic carbon polyhedral hybrid composites for efficient oxygen evolution reactions. J. Mater. Chem. A **4**, 13742–13745 (2016)

163. Zhao, X., Jiang, J., Xue, Z., et al.: An ambient temperature, CO_2-assisted solution processing of amorphous cobalt sulfide in a thiol/amine based quasi-ionic liquid for oxygen evolution catalysis. Chem. Commun. **53**, 9418–9421 (2017)
164. Guo, M., Xu, K., Qu, Y., et al.: Porous Co_3O_4/CoS_2 nanosheet-assembled hierarchical microspheres as superior electrocatalyst towards oxygen evolution reaction. Electrochim. Acta **268**, 10–19 (2018)
165. Wu, C., Zhang, Y., Dong, D., et al.: Co_9S_8 nanoparticles anchored on nitrogen and sulfur dual-doped carbon nanosheets as highly efficient bifunctional electrocatalyst for oxygen evolution and reduction reactions. Nanoscale **9**, 12432–12440 (2017)
166. Chen, P., Xu, K., Tong, Y., et al.: Cobalt nitrides as a class of metallic electrocatalysts for the oxygen evolution reaction. Inorg. Chem. Front. **3**, 236–242 (2016)
167. Gao, T., Jin, Z., Zhang, Y., et al.: Coupling cobalt–iron bimetallic nitrides and N-doped multi-walled carbon nanotubes as high-performance bifunctional catalysts for oxygen evolution and reduction reaction. Electrochim. Acta **258**, 51–60 (2017)
168. Sun, Y., Zhang, T., Li, X., et al.: Mn doped porous cobalt nitride nanowires with high activity for water oxidation under both alkaline and neutral conditions. Chem. Commun. **53**, 13237–13240 (2017)
169. Xue, Y., Ren, Z., Xie, Y., et al.: $CoSe_x$ nanocrystalline-dotted CoCo layered double hydroxide nanosheets: a synergetic engineering process for enhanced electrocatalytic water oxidation. Nanoscale **9**, 16256–16263 (2017)
170. Li, J., Liu, G., Liu, B., et al.: Fe-doped $CoSe_2$ nanoparticles encapsulated in N-doped bamboo-like carbon nanotubes as an efficient electrocatalyst for oxygen evolution reaction. Electrochim. Acta **265**, 577–585 (2018)
171. Zhou, Y., Luo, M., Zhang, Z., et al.: Iron doped cobalt sulfide derived boosted electrocatalyst for water oxidation. Appl. Surf. Sci. **448**, 9–15 (2018)
172. Yang, J., Yang, Z., Li, L.H., et al.: Highly efficient oxygen evolution from CoS_2/CNT nanocomposites via a one-step electrochemical deposition and dissolution method. Nanoscale **9**, 6886–6894 (2017)
173. Luo, X.F., Wang, J., Liang, Z.S., et al.: Manganese oxide with different morphology as efficient electrocatalyst for oxygen evolution reaction. Int. J. Hydrog. Energy **42**, 7151–7157 (2017)
174. Indra, A., Menezes, P.W., Zaharieva, I., et al.: Active mixed-valent MnO_x water oxidation catalysts through partial oxidation (corrosion) of nanostructured MnO particles. Angew. Chem. Int. Ed. **52**, 13206–13210 (2013)
175. Kölbach, M., Fiechter, S., van de Krol, R., et al.: Evaluation of electrodeposited α-Mn_2O_3 as a catalyst for the oxygen evolution reaction. Catal. Today **290**, 2–9 (2017)
176. Hazarika, K.K., Goswami, C., Saikia, H., et al.: Cubic Mn_2O_3 nanoparticles on carbon as bifunctional electrocatalyst for oxygen reduction and oxygen evolution reactions. Mol. Catal. **451**, 153–160 (2018)
177. Lian, S., Browne, M.P., Dominguez, C., et al.: Template-free synthesis of mesoporous manganese oxides with catalytic activity in the oxygen evolution reaction. Sustain. Energy Fuels **1**, 780–788 (2017)
178. Meng, Y., Song, W., Huang, H., et al.: Structure–property relationship of bifunctional MnO_2 nanostructures: highly efficient, ultra-stable electrochemical water oxidation and oxygen reduction reaction catalysts identified in alkaline media. Chem. Soc. Rev. **136**, 11452–11464 (2014)
179. Bhandary, N., Ingole, P.P., Basu, S.: Electrosynthesis of Mn–Fe oxide nanopetals on carbon paper as bi-functional electrocatalyst for oxygen reduction and oxygen evolution reaction. Int. J. Hydrog. Energy **43**, 3165–3171 (2018)
180. Maruthapandian, V., Pandiarajan, T., Saraswathy, V., et al.: Oxygen evolution catalytic behaviour of Ni doped Mn_3O_4 in alkaline medium. RSC Adv. **6**, 48995–49002 (2016)
181. Song, X., Yang, T., Du, H., et al.: New binary Mn and Cr mixed oxide electrocatalysts for the oxygen evolution reaction. J. Electroanal. Chem. **760**, 59–63 (2016)
182. Hosseini-Benhangi, P., Kung, C.H., Alfantazi, A., et al.: Controlling the interfacial environment in the electrosynthesis of MnO_x nanostructures for high-performance oxygen reduction/evolution electrocatalysis. ACS Appl. Mater. Interfaces **9**, 26771–26785 (2017)
183. Zhang, J.H., Feng, J.Y., Zhu, T., et al.: Pd-doped urchin-like MnO_2-carbon sphere three-dimensional (3D) material for oxygen evolution reaction. Electrochim. Acta **196**, 661–669 (2016)
184. Seitz, L.C., Hersbach, T.J.P., Nordlund, D., et al.: Enhancement effect of noble metals on manganese oxide for the oxygen evolution reaction. J. Phys. Chem. Lett. **6**, 4178–4183 (2015)
185. Qian, M., Liu, X., Cui, S., et al.: Copper oxide nanosheets prepared by molten salt method for efficient electrocatalytic oxygen evolution reaction with low catalyst loading. Electrochim. Acta **263**, 318–327 (2018)
186. Yan, Y., Zhao, B., Yi, S.C., et al.: Assembling pore-rich FeP nanorods on the CNT backbone as an advanced electrocatalyst for oxygen evolution. J. Mater. Chem. A **4**, 13005–13010 (2016)
187. Li, X., Li, C., Yoshida, A., et al.: Facile fabrication of CuO microcube@Fe–Co_3O_4 nanosheet array as a high-performance electrocatalyst for the oxygen evolution reaction. J. Mater. Chem. A **5**, 21740–21749 (2017)
188. Zhang, X., Zhang, B., Liu, S., et al.: RGO modified Ni doped FeOOH for enhanced electrochemical and photoelectrochemical water oxidation. Appl. Surf. Sci. **436**, 974–980 (2018)
189. Zhang, R., Zhang, C., Chen, W.: FeP embedded in N, P dual-doped porous carbon nanosheets: an efficient and durable bifunctional catalyst for oxygen reduction and evolution reactions. J. Mater. Chem. A **4**, 18723–18729 (2016)
190. Siracusano, S., Van Dijk, N., Payne-Johnson, E., et al.: Nanosized IrO_x and $IrRuO_x$ electrocatalysts for the O_2 evolution reaction in PEM water electrolysers. Appl. Catal. B Environ. **164**, 488–495 (2015)
191. Song, S., Zhang, H., Xiaoping, M., et al.: Electrochemical investigation of electrocatalysts for the oxygen evolution reaction in PEM water electrolyzers. Int. J. Hydrog. Energy **33**, 4955–4961 (2008)
192. Slavcheva, E., Radev, I., Bliznakov, S., et al.: Sputtered iridium oxide films as electrocatalysts for water splitting via PEM electrolysis. Electrochim. Acta **52**, 3889–3894 (2007)
193. Siracusano, S., Baglio, V., Grigoriev, S.A., et al.: The influence of iridium chemical oxidation state on the performance and durability of oxygen evolution catalysts in PEM electrolysis. J. Power Sources **366**, 105–114 (2017)
194. Li, G., Yu, H., Yang, D., et al.: Iridium–tin oxide solid-solution nanocatalysts with enhanced activity and stability for oxygen evolution. J. Power Sources **325**, 15–24 (2016)
195. Kadakia, K.S., Jampani, P.H., Velikokhatnyi, O.I., et al.: Nanostructured F doped IrO_2 electro-catalyst powders for PEM based water electrolysis. J. Power Sources **269**, 855–865 (2014)
196. Kadakia, K.S., Jampani, P.H., Velikokhatnyi, O.I., et al.: Study of fluorine doped (Nb, Ir)O_2 solid solution electro-catalyst powders for proton exchange membrane based oxygen evolution reaction. Mater. Sci. Eng. B **212**, 101–108 (2016)
197. Kadakia, K., Datta, M.K., Velikokhatnyi, O.I., et al.: High performance fluorine doped (Sn, Ru)O_2 oxygen evolution reaction electro-catalysts for proton exchange membrane based water electrolysis. J. Power Sources **245**, 362–370 (2014)

198. Mayousse, E., Maillard, F., Fouda-Onana, F., et al.: Synthesis and characterization of electrocatalysts for the oxygen evolution in PEM water electrolysis. Int. J. Hydrog. Energy **36**, 10474–10481 (2011)
199. Kadakia, K., Datta, M.K., Velikokhatnyi, O.I., et al.: Novel (Ir, Sn, Nb)O_2 anode electrocatalysts with reduced noble metal content for PEM based water electrolysis. Int. J. Hydrog. Energy **37**, 3001–3013 (2012)
200. Puthiyapura, V.K., Mamlouk, M., Pasupathi, S., et al.: Physical and electrochemical evaluation of ATO supported IrO_2 catalyst for proton exchange membrane water electrolyser. J. Power Sources **269**, 451–460 (2014)
201. Marshall, A.T., Sunde, S., Tsypkin, M., et al.: Performance of a PEM water electrolysis cell using $Ir_xRu_yTa_zO_2$ electrocatalysts for the oxygen evolution electrode. Int. J. Hydrog. Energy **32**, 2320–2324 (2007)
202. Wu, X., Tayal, J., Basu, S., et al.: Nano-crystalline $Ru_xSn_{1-x}O_2$ powder catalysts for oxygen evolution reaction in proton exchange membrane water electrolysers. Int. J. Hydrog. Energy **36**, 14796–14804 (2011)
203. Fernández, J.L., Gennero De Chialvo, M.R., Chialvo, A.C.: Preparation and electrochemical characterization of Ti/Ru_x $Mn_{1-x}O_2$ electrodes. J. Appl. Electrochem. **32**, 513–520 (2002)
204. Wu, X., Scott, K.: RuO_2 supported on Sb-doped SnO_2 nanoparticles for polymer electrolyte membrane water electrolysers. Int. J. Hydrog. Energy **36**, 5806–5810 (2011)
205. Slavcheva, E., Borisov, G., Lefterova, E., et al.: Ebonex supported iridium as anode catalyst for PEM water electrolysis. Int. J. Hydrog. Energy **40**, 11356–11361 (2015)
206. Stoyanova, A., Borisov, G., Lefterova, E., et al.: Oxygen evolution on Ebonex-supported Pt-based binary compounds in PEM water electrolysis. Int. J. Hydrog. Energy **37**, 16515–16521 (2012)
207. Xu, J., Liu, G., Li, J., et al.: The electrocatalytic properties of an IrO_2/SnO_2 catalyst using SnO_2 as a support and an assisting reagent for the oxygen evolution reaction. Electrochim. Acta **59**, 105–112 (2012)
208. Karimi, F., Peppley, B.A.: Metal carbide and oxide supports for iridium-based oxygen evolution reaction electrocatalysts for polymer-electrolyte-membrane water electrolysis. Electrochim. Acta **246**, 654–670 (2017)
209. Polonský, J., Petrushina, I.M., Christensen, E., et al.: Tantalum carbide as a novel support material for anode electrocatalysts in polymer electrolyte membrane water electrolysers. Int. J. Hydrog. Energy **37**, 2173–2181 (2012)
210. Ye, F., Li, J., Wang, X., et al.: Electrocatalytic properties of Ti/Pt–IrO_2 anode for oxygen evolution in PEM water electrolysis. Int. J. Hydrog. Energy **35**, 8049–8055 (2010)
211. Lagarteira, T., Han, F., Morawietz, T., et.al.: Highly active screen-printed $IrTi_4O_7$ anodes for proton exchange membrane electrolyzers. In: Hyceltec 2017–VI Symposium on Hydrogen, Fuel Cells and Advanced Batteries, Porto, Portugal, 19–23 June 2017
212. Erning, J.W., Hauber, T., Stimming, U., et al.: Catalysis of the electrochemical processes on solid oxide fuel cell cathodes. J. Power Sources **61**, 205–211 (1996)
213. Sahibzada, M., Benson, S.J., Rudkin, R.A., et al.: Pd-promoted $La_{0.6}Sr_{0.4}Co_{0.2}Fe_{0.8}O_3$ cathodes. Solid State Ion. **113–115**, 285–290 (1998)
214. Haanappel, V.A.C., Rutenbeck, D., Mai, A., et al.: The influence of noble-metal-containing cathodes on the electrochemical performance of anode-supported SOFCs. J. Power Sources **130**, 119–128 (2004)
215. Yu, B., Zhang, W., Xu, J. et al.: Microstructural characterization and electrochemical properties of $Ba_{0.5}Sr_{0.5}Co_{0.8}Fe_{0.2}O_{3-\delta}$ and its application for anode of SOEC. Int. J. Hydrog. Energy **33**, 6873–6877 (2008)
216. Chrzan, A., Karczewski, J., Gazda, M., et al.: $La_{0.6}Sr_{0.4}Co_{0.2}Fe_{0.8}O_{3-\delta}$ oxygen electrodes for solid oxide cells prepared by polymer precursor and nitrates solution infiltration into gadolinium doped ceria backbone. J. Eur. Ceram. Soc. **37**, 3559–3564 (2017)
217. Gao, C., Liu, Y., Xi, K., et al.: Improve the catalytic property of $La_{0.6}Sr_{0.4}Co_{0.2}Fe_{0.8}O_3/Ce_{0.9}Gd_{0.1}O_2$ (LSCF/CGO) cathodes with CuO nanoparticles infiltration. Electrochim. Acta **246**, 148–155 (2017)
218. Kim, S.J., Kim, K.J., Dayaghi, A.M., et al.: Polarization and stability of $La_2NiO_{4+\delta}$ in comparison with $La_{0.6}Sr_{0.4}Co_{0.2}Fe_{0.8}O_{3-\delta}$ as air electrode of solid oxide electrolysis cell. Int. J. Hydrog. Energy **41**, 14498–14506 (2016)
219. Fan, H., Keane, M., Li, N., et al.: Electrochemical stability of $La_{0.6}Sr_{0.4}Co_{0.2}Fe_{0.8}O_{3-\delta}$ infiltrated YSZ oxygen electrode for reversible solid oxide fuel cells. Int. J. Hydrog. Energy **39**, 14071–14078 (2014)
220. Meng, X., Shen, Y., Xie, M., et al.: Novel solid oxide cells with $SrCo_{0.8}Fe_{0.1}Ga_{0.1}O_{3-\delta}$ oxygen electrode for flexible power generation and hydrogen production. J. Power Sources **306**, 226–232 (2016)
221. Boulfrad, S., Cassidy, M., Djurado, E., et al.: Pre-coating of LSCM perovskite with metal catalyst for scalable high performance anodes. Int. J. Hydrog. Energy **38**, 9519–9524 (2013)
222. Chrzan, A., Ovtar, S., Jasinski, P., et al.: High performance $LaNi_{1-x}Co_xO_{3-\delta}$ ($x = 0.4$–0.7) infiltrated oxygen electrodes for reversible solid oxide cells. J. Power Sources **353**, 67–76 (2017)
223. Egger, A., Schrödl, N., Gspan, C., et al.: $La_2NiO_{4+\delta}$ as electrode material for solid oxide fuel cells and electrolyzer cells. Solid State Ion. **299**, 18–25 (2017)
224. Ai, N., Li, N., He, S., et al.: Highly active and stable $Er_{0.4}Bi_{1.6}O_3$ decorated $La_{0.76}Sr_{0.19}MnO_{3+\sigma}$ nanostructured oxygen electrodes for reversible solid oxide cells. J. Mater. Chem. A **5**, 12149–12157 (2017)
225. Tan, Y., Wang, A., Jia, L., et al.: High-performance oxygen electrode for reversible solid oxide cells with power generation and hydrogen production at intermediate temperature. Int. J. Hydrog. Energy **42**, 4456–4464 (2017)
226. Zhou, N., Yin, Y.M., Li, J., et al.: A robust high performance cobalt-free oxygen electrode $La_{0.5}Sr_{0.5}Fe_{0.8}Cu_{0.15}Nb_{0.05}O_{3-\delta}$ for reversible solid oxide electrochemical cell. J. Power Sources **340**, 373–379 (2017)
227. Mahata, A., Datta, P., Basu, R.N.: Synthesis and characterization of Ca doped $LaMnO_3$ as potential anode material for solid oxide electrolysis cells. Ceram. Int. **43**, 433–438 (2017)
228. Chen, K., Ai, N., Jiang, S.P.: Enhanced electrochemical performance and stability of (La, Sr)MnO_3–(Gd, Ce)O_2 oxygen electrodes of solid oxide electrolysis cells by palladium infiltration. Int. J. Hydrog. Energy **37**, 1301–1310 (2012)
229. Tong, X., Zhou, F., Yang, S., et al.: Performance and stability of Ruddlesden–Popper $La_2NiO_{4+\delta}$ oxygen electrodes under solid oxide electrolysis cell operation conditions. Ceram. Int. **43**, 10927–10933 (2017)
230. Yan, J., Zhao, Z., Shang, L., et al.: Co-synthesized Y-stabilized Bi_2O_3 and Sr-substituted $LaMnO_3$ composite anode for high performance solid oxide electrolysis cell. J. Power Sources **319**, 124–130 (2016)
231. Cheng, X., Li, Y., Zheng, L., et al.: Highly active, stable oxidized platinum clusters as electrocatalysts for the hydrogen evolution reaction. Energy Environ. Sci. **10**, 2450–2458 (2017)
232. Lima, D.W., Fiegenbaum, F., Trombetta, F., et al.: PtNi and PtMo nanoparticles as efficient catalysts using TEA-PS.BF_4 ionic

liquid as electrolyte towards HER. Int. J. Hydrog. Energy **42**, 5676–5683 (2017)
233. Ren, F., Zhou, W., Du, Y., et al.: High efficient electrocatalytic oxidation of formic acid at Pt dispersed on porous poly(o-methoxyaniline). Int. J. Hydrog. Energy **36**, 6414–6421 (2011)
234. Zheng, J.: Binary platinum alloy electrodes for hydrogen and oxygen evolutions by seawater splitting. Appl. Surf. Sci. **413**, 72–82 (2017)
235. Gabler, A., Müller, C.I., Rauscher, T., et al.: Ultrashort-pulse laser structured titanium surfaces with sputter-coated platinum catalyst as hydrogen evolution electrodes for alkaline water electrolysis. Int. J. Hydrog. Energy **43**, 7216–7226 (2018)
236. Luo, B., Yan, X., Chen, J., et al.: PtFe nanotubes/graphene hybrid: facile synthesis and its electrochemical properties. Int. J. Hydrog. Energy **38**, 13011–13016 (2013)
237. Ma, R., Zhou, Y., Wang, F., et al.: Efficient electrocatalysis of hydrogen evolution by ultralow-Pt-loading bamboo-like nitrogen-doped carbon nanotubes. Mater. Today **6**, 173–180 (2017)
238. Deng, J., Ren, P., Deng, D., et al.: Highly active and durable non-precious-metal catalysts encapsulated in carbon nanotubes for hydrogen evolution reaction. Energy Environ. Sci. **7**, 1919–1923 (2014)
239. Wang, Z.L., Hao, X.F., Jiang, Z., et al.: C and N hybrid coordination derived Co–C–N complex as a highly efficient electrocatalyst for hydrogen evolution reaction. Chem. Soc. Rev. **137**, 15070–15073 (2015)
240. Guan, H., Lin, J., Qiao, B., et al.: Catalytically active Rh subnanoclusters on TiO_2 for CO oxidation at cryogenic temperatures. Angew. Chem. Int. Ed. **55**, 2820–2824 (2016)
241. Wang, S., Gao, X., Hang, X., et al.: Ultrafine pt nanoclusters confined in a calixarene-based Ni_{24} coordination cage for high-efficient hydrogen evolution reaction. J. Am. Chem. Soc. **138**, 16236–16239 (2016)
242. Fang, M., Gao, W., Dong, G., et al.: Hierarchical NiMo-based 3D electrocatalysts for highly-efficient hydrogen evolution in alkaline conditions. Nano Energy **27**, 247–254 (2016)
243. Sun, T., Cao, J., Dong, J., et al.: Ordered mesoporous NiCo alloys for highly efficient electrocatalytic hydrogen evolution reaction. Int. J. Hydrog. Energy **42**, 6637–6645 (2017)
244. Guo, H., Youliwasi, N., Zhao, L., et al.: Carbon-encapsulated nickel–cobalt alloys nanoparticles fabricated via new post-treatment strategy for hydrogen evolution in alkaline media. Appl. Surf. Sci. **435**, 237–246 (2018)
245. Schalenbach, M., Speck, F.D., Ledendecker, M., et al.: Nickel-molybdenum alloy catalysts for the hydrogen evolution reaction: activity and stability revised. Electrochim. Acta **259**, 1154–1161 (2018)
246. Rauscher, T., Müller, C.I., Schmidt, A., et al.: Ni–Mo–B alloys as cathode material for alkaline water electrolysis. Int. J. Hydrog. Energy **41**, 2165–2176 (2016)
247. Yüce, A.O., Döner, A., Kardaş, G.: NiMn composite electrodes as cathode material for hydrogen evolution reaction in alkaline solution. Int. J. Hydrog. Energy **38**, 4466–4473 (2013)
248. Yang, Q., Lv, C., Huang, Z., et al.: Amorphous film of ternary NiCoP alloy on Ni foam for efficient hydrogen evolution by electroless deposition. Int. J. Hydrog. Energy **43**, 7872–7880 (2018)
249. Wang, X., Su, R., Aslan, H., et al.: Tweaking the composition of NiMoZn alloy electrocatalyst for enhanced hydrogen evolution reaction performance. Nano Energy **12**, 9–18 (2015)
250. Zhu, Y., Zhang, X., Song, J., et al.: Microstructure and hydrogen evolution catalytic properties of Ni–Sn alloys prepared by electrodeposition method. Appl. Catal. A Gen. **500**, 51–57 (2015)
251. He, X.D., Xu, F., Li, F., et al.: Composition–performance relationship of Ni_xCu_y nanoalloys as hydrogen evolution electrocatalyst. J. Electroanal. Chem. **799**, 235–241 (2017)
252. Hong, S.H., Ahn, S.H., Choi, J., et al.: High-activity electrodeposited NiW catalysts for hydrogen evolution in alkaline water electrolysis. Appl. Surf. Sci. **349**, 629–635 (2015)
253. Yin, Z., Chen, F.: A facile electrochemical fabrication of hierarchically structured nickel–copper composite electrodes on nickel foam for hydrogen evolution reaction. J. Power Sources **265**, 273–281 (2014)
254. Zhang, J., Baro, M.D., Pellicer, E., et al.: Electrodeposition of magnetic, superhydrophobic, non-stick, two-phase Cu–Ni foam films and their enhanced performance for hydrogen evolution reaction in alkaline water media. Nanoscale **6**, 12490–12499 (2014)
255. Wu, Y., He, H.: Direct-current electrodeposition of Ni–S–Fe alloy for hydrogen evolution reaction in alkaline solution. Int. J. Hydrog. Energy **43**, 1989–1997 (2018)
256. McArthur, M.A., Jorge, L., Coulombe, S., et al.: Synthesis and characterization of 3D Ni nanoparticle/carbon nanotube cathodes for hydrogen evolution in alkaline electrolyte. J. Power Sources **266**, 365–373 (2014)
257. Damian, A., Omanovic, S.: Ni and NiMo hydrogen evolution electrocatalysts electrodeposited in a polyaniline matrix. J. Power Sources **158**, 464–476 (2006)
258. Bai, Y., Zhang, H., Li, X., et al.: Novel peapod-like Ni_2P nanoparticles with improved electrochemical properties for hydrogen evolution and lithium storage. Nanoscale **7**, 1446–1453 (2015)
259. Jiang, P., Liu, Q., Sun, X.: NiP_2 nanosheet arrays supported on carbon cloth: an efficient 3D hydrogen evolution cathode in both acidic and alkaline solutions. Nanoscale **6**, 13440–13445 (2014)
260. Jeoung, S., Seo, B., Hwang, J.M., et al.: Direct conversion of coordination compounds into Ni_2P nanoparticles entrapped in 3D mesoporous graphene for an efficient hydrogen evolution reaction. Mater. Chem. Front. **1**, 973–978 (2017)
261. Pu, Z., Liu, Q., Tang, C., et al.: Ni_2P nanoparticle films supported on a Ti plate as an efficient hydrogen evolution cathode. Nanoscale **6**, 11031–11034 (2014)
262. Hansen, M.H., Stern, L.A., Feng, L., et al.: Widely available active sites on Ni_2P for electrochemical hydrogen evolution—insights from first principles calculations. Phys. Chem. Chem. Phys. **17**, 10823–10829 (2015)
263. Wang, X., Zhou, H., Zhang, D., et al.: Mn-doped NiP_2 nanosheets as an efficient electrocatalyst for enhanced hydrogen evolution reaction at all pH values. J. Power Sources **387**, 1–8 (2018)
264. Ma, Z., Li, R., Wang, M., et al.: Self-supported porous Ni–Fe–P composite as an efficient electrocatalyst for hydrogen evolution reaction in both acidic and alkaline medium. Electrochim. Acta **219**, 194–203 (2016)
265. Ledendecker, M., Krick Calderon, S., Papp, C., et al.: The synthesis of nanostructured Ni5P4 films and their use as a non-noble bifunctional electrocatalyst for full water splitting. Angew. Chem. **54**, 12538–12542 (2015)
266. Zhang, J., Cui, R., Li, X.A., et al.: A nanohybrid consisting of $NiPS_3$ nanoparticles coupled with defective graphene as a pH-universal electrocatalyst for efficient hydrogen evolution. J. Mater. Chem. A **5**, 23536–23542 (2017)
267. Jin, Z., Li, P., Huang, X., et al.: Three-dimensional amorphous tungsten-doped nickel phosphide microsphere as an efficient electrocatalyst for hydrogen evolution. J. Mater. Chem. A **2**, 18593–18599 (2014)
268. Li, Y., Jiang, Z., Huang, J., et al.: Template-synthesis and electrochemical properties of urchin-like NiCoP electrocatalyst for hydrogen evolution reaction. Electrochim. Acta **249**, 301–307 (2017)
269. Wu, J., Ge, X., Li, Z., et al.: Highly dispersed NiCoP nanoparticles on carbon nanotubes modified nickel foam for efficient electrocatalytic hydrogen production. Electrochim. Acta **252**, 101–108 (2017)

270. Liu, T., Yan, X., Xi, P., et al.: Nickel–cobalt phosphide nanowires supported on Ni foam as a highly efficient catalyst for electrochemical hydrogen evolution reaction. Int. J. Hydrog. Energy **42**, 14124–14132 (2017)
271. Tang, C., Pu, Z., Liu, Q., et al.: NiS_2 nanosheets array grown on carbon cloth as an efficient 3D hydrogen evolution cathode. Electrochim. Acta **153**, 508–514 (2015)
272. Yang, C., Gao, M.Y., Zhang, Q.B., et al.: In-situ activation of self-supported 3D hierarchically porous Ni_3S_2 films grown on nanoporous copper as excellent pH-universal electrocatalysts for hydrogen evolution reaction. Nano Energy **36**, 85–94 (2017)
273. Ouyang, C., Wang, X., Wang, C., et al.: Hierarchically porous Ni_3S_2 nanorod array foam as highly efficient electrocatalyst for hydrogen evolution reaction and oxygen evolution reaction. Electrochim. Acta **174**, 297–301 (2015)
274. Tao, K., Gong, Y., Lin, J.: Low-temperature synthesis of NiS/MoS_2/C nanowires/nanoflakes as electrocatalyst for hydrogen evolution reaction in alkaline medium via calcining/sulfurizing metal–organic frameworks. Electrochim. Acta **274**, 74–83 (2018)
275. Liu, Z.Z., Shang, X., Dong, B., et al.: Triple Ni–Co–Mo metal sulfides with one-dimensional and hierarchical nanostructures towards highly efficient hydrogen evolution reaction. J. Catal. **361**, 204–213 (2018)
276. Shang, X., Yan, K.L., Rao, Y., et al.: In situ cathodic activation of V-incorporated Ni_xS_y nanowires for enhanced hydrogen evolution. Nanoscale **9**, 12353–12363 (2017)
277. Du, H., Liu, Q., Cheng, N., et al.: Template-assisted synthesis of CoP nanotubes to efficiently catalyze hydrogen-evolving reaction. J. Mater. Chem. A **2**, 14812–14816 (2014)
278. Gu, S., Du, H., Asiri, A.M., et al.: Three-dimensional interconnected network of nanoporous CoP nanowires as an efficient hydrogen evolution cathode. Phys. Chem. Chem. Phys. **16**, 16909–16913 (2014)
279. Luo, P., Zhang, H., Liu, L., et al.: Targeted synthesis of unique nickel sulfide (NiS, NiS_2) microarchitectures and the applications for the enhanced water splitting system. ACS Appl. Mater. Interfaces **9**, 2500–2508 (2017)
280. Kuang, P., Tong, T., Fan, K., et al.: In situ fabrication of Ni–Mo bimetal sulfide hybrid as an efficient electrocatalyst for hydrogen evolution over a wide pH range. ACS Catal. **7**, 6179–6187 (2017)
281. Yu, X.Y., Feng, Y., Jeon, Y., et al.: Formation of Ni–Co–MoS_2 nanoboxes with enhanced electrocatalytic activity for hydrogen evolution. Adv. Mater. **28**, 9006–9011 (2016)
282. Zhu, H., Zhang, J., Ruoping, Y., et al.: When cubic cobalt sulfide meets layered molybdenum disulfide: a core–shell system toward synergetic electrocatalytic water splitting. Adv. Mater. **27**, 4752–4759 (2015)
283. Wu, Z., Guo, J., Wang, J., et al.: Hierarchically porous electrocatalyst with vertically aligned defect-rich CoMoS nanosheets for the hydrogen evolution reaction in an alkaline medium. ACS Appl. Mater. Interfaces **9**, 5288–5294 (2017)
284. Yan, X.Y., Devaramani, S., Chen, J., et al.: Self-supported rectangular CoP nanosheet arrays grown on a carbon cloth as an efficient electrocatalyst for the hydrogen evolution reaction over a variety of pH values. New J. Chem. **41**, 2436–2442 (2017)
285. Lin, Y., Pan, Y., Zhang, J.: CoP nanorods decorated biomass derived N, P co-doped carbon flakes as an efficient hybrid catalyst for electrochemical hydrogen evolution. Electrochim. Acta **232**, 561–569 (2017)
286. Jin, J., Zhu, Y., Liu, Y., et al.: CoP nanoparticles combined with WS_2 nanosheets as efficient electrocatalytic hydrogen evolution reaction catalyst. Int. J. Hydrog. Energy **42**, 3947–3954 (2017)
287. Jiang, P., Liu, Q., Ge, C., et al.: CoP nanostructures with different morphologies: synthesis, characterization and a study of their electrocatalytic performance toward the hydrogen evolution reaction. J. Mater. Chem. A **2**, 14634–14640 (2014)
288. Popczun, E.J., Read, C.G., Roske, C.W., et al.: Highly active electrocatalysis of the hydrogen evolution reaction by cobalt phosphide nanoparticles. Angew. Chem. Int. Ed. **53**, 5427–5430 (2014)
289. Yang, H., Zhang, Y., Hu, F., et al.: Urchin-like CoP nanocrystals as hydrogen evolution reaction and oxygen reduction reaction dual-electrocatalyst with superior stability. Nano Lett. **15**, 7616–7620 (2015)
290. Zhou, D., He, L., Zhu, W., et al.: Interconnected urchin-like cobalt phosphide microspheres film for highly efficient electrochemical hydrogen evolution in both acidic and basic media. J. Mater. Chem. A **4**, 10114–10117 (2016)
291. Li, M., Liu, X., Xiong, Y., et al.: Facile synthesis of various highly dispersive CoP nanocrystal embedded carbon matrices as efficient electrocatalysts for the hydrogen evolution reaction. J. Mater. Chem. A **3**, 4255–4265 (2015)
292. Zhang, R., Ren, X., Hao, S., et al.: Selective phosphidation: an effective strategy toward CoP/CeO_2 interface engineering for superior alkaline hydrogen evolution electrocatalysis. J. Mater. Chem. A **6**, 1985–1990 (2018)
293. Jintao, Z., Liangti, Q., Gaoquan, S., et al.: N, P-codoped carbon networks as efficient metal-free bifunctional catalysts for oxygen reduction and hydrogen evolution reactions. Angew. Chem. **128**, 2270–2274 (2016)
294. Zhou, W., Jia, J., Lu, J., et al.: Recent developments of carbon-based electrocatalysts for hydrogen evolution reaction. Nano Energy **28**, 29–43 (2016)
295. Yan, D., Dou, S., Tao, L., et al.: Electropolymerized supermolecule derived N, P co-doped carbon nanofiber networks as a highly efficient metal-free electrocatalyst for the hydrogen evolution reaction. J. Mater. Chem. A **4**, 13726–13730 (2016)
296. Ma, L., Shen, X., Zhou, H., et al.: CoP nanoparticles deposited on reduced graphene oxide sheets as an active electrocatalyst for the hydrogen evolution reaction. J. Mater. Chem. A **3**, 5337–5343 (2015)
297. Qian, L., Jingqi, T., Wei, C., et al.: Carbon nanotubes decorated with CoP nanocrystals: a highly active non-noble-metal nanohybrid electrocatalyst for hydrogen evolution. Angew. Chem. Int. Ed. **53**, 6710–6714 (2014)
298. Li, M., Zhou, H., Yang, W., et al.: Co_9S_8 nanoparticles embedded in a N, S co-doped graphene-unzipped carbon nanotube composite as a high performance electrocatalyst for the hydrogen evolution reaction. J. Mater. Chem. A **5**, 1014–1021 (2017)
299. Zhou, X., Yang, X., Hedhili, M.N., et al.: Symmetrical synergy of hybrid Co_9S_8–MoS_x electrocatalysts for hydrogen evolution reaction. Nano Energy **32**, 470–478 (2017)
300. Kim, J.Y., Han, S., Bang, J.H.: Cobalt disulfide nano-pine-tree array as a platinum alternative electrocatalyst for hydrogen evolution reaction. Mater. Lett. **189**, 97–100 (2017)
301. Ansovini, D., Jun Lee, C.J., Chua, C.S., et al.: A highly active hydrogen evolution electrocatalyst based on a cobalt-nickel sulfide composite electrode. J. Mater. Chem. A **4**, 9744–9749 (2016)
302. Wang, K., Xi, D., Zhou, C., et al.: $CoSe_2$ necklace-like nanowires supported by carbon fiber paper: a 3D integrated electrode for the hydrogen evolution reaction. J. Mater. Chem. A **3**, 9415–9420 (2015)
303. Gong, K., Du, F., Xia, Z., et al.: Nitrogen-doped carbon nanotube arrays with high electrocatalytic activity for oxygen reduction. Science **323**, 760 (2009)
304. Dai, L., Xue, Y., Qu, L., et al.: Metal-free catalysts for oxygen reduction reaction. Chem. Rev. **115**, 4823–4892 (2015)

305. Xie, J., Zhang, H., Li, S., et al.: Defect-rich MoS_2 ultrathin nanosheets with additional active edge sites for enhanced electrocatalytic hydrogen evolution. Adv. Mater. **25**, 5807–5813 (2013)
306. Yan, Y., Xia, B., Ge, X., et al.: Ultrathin MoS_2 nanoplates with rich active sites as highly efficient catalyst for hydrogen evolution. ACS Appl. Mater. Interfaces **5**, 12794–12798 (2013)
307. Xia, X., Zheng, Z., Zhang, Y., et al.: Synthesis of MoS_2–carbon composites with different morphologies and their application in hydrogen evolution reaction. Int. J. Hydrog. Energy **39**, 9638–9650 (2014)
308. Wang, F., Sun, Y., He, Y., et al.: Highly efficient and durable MoNiNC catalyst for hydrogen evolution reaction. Nano Energy **37**, 1–6 (2017)
309. Shi, J., Hu, J.: Molybdenum sulfide nanosheet arrays supported on Ti plate: an efficient hydrogen-evolving cathode over the whole pH range. Electrochim. Acta **168**, 256–260 (2015)
310. Qian, X., Ding, J., Zhang, J., et al.: Ultrathin molybdenum disulfide/carbon nitride nanosheets with abundant active sites for enhanced hydrogen evolution. Nanoscale **10**, 1766–1773 (2018)
311. Guo, M., Wu, Q., Yu, M., et al.: One-step liquid phase chemical method to prepare carbon-based amorphous molybdenum sulfides: as the effective hydrogen evolution reaction catalysts. Electrochim. Acta **236**, 280–287 (2017)
312. Cao, P., Peng, J., Li, J., et al.: Highly conductive carbon black supported amorphousmolybdenum disulfide for efficient hydrogen evolution reaction. J. Power Sources **347**, 210–219 (2017)
313. Li, R., Yang, L., Xiong, T., et al.: Nitrogen doped MoS_2 nanosheets synthesized via a low-temperature process as electrocatalysts with enhanced activity for hydrogen evolution reaction. J. Power Sources **356**, 133–139 (2017)
314. Mak, K.F., He, K., Lee, C., et al.: Tightly bound trions in monolayer MoS_2. Nat. Mater. **12**, 207 (2012)
315. Joensen, P., Frindt, R.F., Morrison, S.R.: Single-layer MoS_2. Mater. Res. Bull. **21**, 457–461 (1986)
316. Eda, G., Yamaguchi, H., Voiry, D., et al.: Photoluminescence from chemically exfoliated MoS_2. Nano Lett. **11**, 5111–5116 (2011)
317. Liu, K.K., Zhang, W., Lee, Y.H., et al.: Growth of large-area and highly crystalline MoS_2 thin layers on insulating substrates. Nano Lett. **12**, 1538–1544 (2012)
318. Wang, X., Feng, H., Wu, Y., et al.: Controlled synthesis of highly crystalline MoS_2 flakes by chemical vapor deposition. Chem. Soc. Rev. **135**, 5304–5307 (2013)
319. Yongjie, Z., Zheng, L., Sina, N., et al.: Large-area vapor-phase growth and characterization of MoS_2 atomic layers on a SiO_2 substrate. Small **8**, 966–971 (2012)
320. Xie, J., Zhang, J., Li, S., et al.: Controllable disorder engineering in oxygen-incorporated MoS_2 ultrathin nanosheets for efficient hydrogen evolution. Chem. Soc. Rev. **135**, 17881–17888 (2013)
321. Li, Y., Wang, H., Xie, L., et al.: MoS_2 nanoparticles grown on graphene: an advanced catalyst for the hydrogen evolution reaction. Chem. Soc. Rev. **133**, 7296–7299 (2011)
322. Merki, D., Fierro, S., Vrubel, H., et al.: Amorphous molybdenum sulfide films as catalysts for electrochemical hydrogen production in water. Chem. Sci. **2**, 1262–1267 (2011)
323. Ojha, K., Sharma, M., Kolev, H., et al.: Reduced graphene oxide and MoP composite as highly efficient and durable electrocatalyst for hydrogen evolution in both acidic and alkaline media. Catal. Sci. Technol. **7**, 668–676 (2017)
324. Pu, Z., Saana Amiinu, I., Wang, M., et al.: Semimetallic MoP_2: an active and stable hydrogen evolution electrocatalyst over the whole pH range. Nanoscale **8**, 8500–8504 (2016)
325. Deng, C., Xie, J., Xue, Y., et al.: Synthesis of MoP decorated carbon cloth as a binder-free electrode for hydrogen evolution. RSC Adv. **6**, 68568–68573 (2016)
326. Xiao, P., Sk, M.A., Thia, L., et al.: Molybdenum phosphide as an efficient electrocatalyst for the hydrogen evolution reaction. Energy Environ. Sci. **7**, 2624–2629 (2014)
327. Deng, C., Ding, F., Li, X., et al.: Templated-preparation of a three-dimensional molybdenum phosphide sponge as a high performance electrode for hydrogen evolution. J. Mater. Chem. A **4**, 59–66 (2016)
328. Pu, Z., Wei, S., Chen, Z., et al.: Flexible molybdenum phosphide nanosheet array electrodes for hydrogen evolution reaction in a wide pH range. Appl. Catal. B Environ. **196**, 193–198 (2016)
329. Chen, X., Qi, J., Wang, P., et al.: Polyvinyl alcohol protected Mo_2C/Mo_2N multicomponent electrocatalysts with controlled morphology for hydrogen evolution reaction in acid and alkaline medium. Electrochim. Acta **273**, 239–247 (2018)
330. Lv, C., Huang, Z., Yang, Q., et al.: Nanocomposite of MoO_2 and MoC loaded on porous carbon as an efficient electrocatalyst for hydrogen evolution reaction. Inorg. Chem. Front. **5**, 446–453 (2018)
331. Xie, X., Lin, L., Liu, R.Y., et al.: The synergistic effect of metallic molybdenum dioxide nanoparticle decorated graphene as an active electrocatalyst for an enhanced hydrogen evolution reaction. J. Mater. Chem. A **3**, 8055–8061 (2015)
332. Bukola, S., Merzougui, B., Creager, S.E., et al.: Nanostructured cobalt-modified molybdenum carbides electrocatalysts for hydrogen evolution reaction. Int. J. Hydrog. Energy **41**, 22899–22912 (2016)
333. Liu, X., Zhang, L., Lan, X., et al.: Paragenesis of Mo_2C nanocrystals in mesoporous carbon nanofibers for electrocatalytic hydrogen evolution. Electrochim. Acta **274**, 23–30 (2018)
334. Wang, H., Sun, C., Cao, Y., et al.: Molybdenum carbide nanoparticles embedded in nitrogen-doped porous carbon nanofibers as a dual catalyst for hydrogen evolution and oxygen reduction reactions. Carbon **114**, 628–634 (2017)
335. Jing, S., Zhang, L., Luo, L., et al.: N-doped porous molybdenum carbide nanobelts as efficient catalysts for hydrogen evolution reaction. Appl. Catal. B Environ. **224**, 533–540 (2018)
336. Jiang, R., Fan, J., Hu, L., et al.: Electrochemically synthesized N-doped molybdenum carbide nanoparticles for efficient catalysis of hydrogen evolution reaction. Electrochim. Acta **261**, 578–587 (2018)
337. Jin, Y., Shen, P.K.: Nanoflower-like metallic conductive MoO_2 as a high-performance non-precious metal electrocatalyst for the hydrogen evolution reaction. J. Mater. Chem. A **3**, 20080–20085 (2015)
338. Grigoriev, S.A., Mamat, M.S., Dzhus, K.A., et al.: Platinum and palladium nano-particles supported by graphitic nano-fibers as catalysts for PEM water electrolysis. Int. J. Hydrog. Energy **36**, 4143–4147 (2011)
339. Grigoriev, S.A., Millet, P., Fateev, V.N.: Evaluation of carbon-supported Pt and Pd nanoparticles for the hydrogen evolution reaction in PEM water electrolysers. J. Power Sources **177**, 281–285 (2008)
340. Su, D.S., Centi, G.: A perspective on carbon materials for future energy application. J. Energy Chem. **22**, 151–173 (2013)
341. Pushkarev, A.S., Pushkareva, I.V., Grigoriev, S.A., et al.: Electrocatalytic layers modified by reduced graphene oxide for PEM fuel cells. Int. J. Hydrog. Energy **40**, 14492–14497 (2015)

342. Terrones, M., Ajayan, P.M., Banhart, F., et al.: N-doping and coalescence of carbon nanotubes: synthesis and electronic properties. Appl. Phys. A **74**, 355–361 (2002)
343. Esposito, D.V., Hunt, S.T., Kimmel, Y.C., et al.: A new class of electrocatalysts for hydrogen production from water electrolysis: metal monolayers supported on low-cost transition metal carbides. Chem. Soc. Rev. **134**, 3025–3033 (2012)
344. Nikiforov, A.V., Petrushina, I.M., Christensen, E., et al.: WC as a non-platinum hydrogen evolution electrocatalyst for high temperature PEM water electrolysers. Int. J. Hydrog. Energy **37**, 18591–18597 (2012)
345. Kelly, T.G., Hunt, S.T., Esposito, D.V., et al.: Monolayer palladium supported on molybdenum and tungsten carbide substrates as low-cost hydrogen evolution reaction (HER) electrocatalysts. Int. J. Hydrog. Energy **38**, 5638–5644 (2013)
346. Esposito, D.V., Hunt, S.T., Stottlemyer, A.L., et al.: Low-cost hydrogen-evolution catalysts based on monolayer platinum on tungsten monocarbide substrates. Angew. Chem. Int. Ed. **49**, 9859–9862 (2010)
347. Meyer, S., Nikiforov, A.V., Petrushina, I.M., et al.: Transition metal carbides (WC, Mo_2C, TaC, NbC) as potential electrocatalysts for the hydrogen evolution reaction (HER) at medium temperatures. Int. J. Hydrog. Energy **40**, 2905–2911 (2015)
348. Tang, C., Sun, A., Xu, Y., et al.: High specific surface area Mo_2C nanoparticles as an efficient electrocatalyst for hydrogen evolution. J. Power Sources **296**, 18–22 (2015)
349. Ramakrishna, S.U.B., Srinivasulu Reddy, D., Shiva Kumar, S., et al.: Nitrogen doped CNTs supported palladium electrocatalyst for hydrogen evolution reaction in PEM water electrolyser. Int. J. Hydrog. Energy **41**, 20447–20454 (2016)
350. Sedlak, J.M., Lawrance, R.J., Enos, J.F.: Advances in oxygen evolution catalysis in solid polymer electrolyte water electrolysis. Int. J. Hydrog. Energy **6**, 159–165 (1981)
351. Takenaka, H., Torikai, E., Kawami, Y., et al.: Solid polymer electrolyte water electrolysis. Int. J. Hydrog. Energy **7**, 397–403 (1982)
352. Millet, P., Durand, R., Pineri, M.: Preparation of new solid polymer electrolyte composites for water electrolysis. Int. J. Hydrog. Energy **15**, 245–253 (1990)
353. Pantani, O., Anxolabéhère-Mallart, E., Aukauloo, A., et al.: Electroactivity of cobalt and nickel glyoximes with regard to the electro-reduction of protons into molecular hydrogen in acidic media. Electrochem. Commun. **9**, 54–58 (2007)
354. Cheng, J., Zhang, H., Ma, H., et al.: Study of carbon-supported IrO_2 and RuO_2 for use in the hydrogen evolution reaction in a solid polymer electrolyte electrolyzer. Electrochim. Acta **55**, 1855–1861 (2010)
355. Yan, J., Chen, H., Dogdibegovic, E., et al.: High-efficiency intermediate temperature solid oxide electrolyzer cells for the conversion of carbon dioxide to fuels. J. Power Sources **252**, 79–84 (2014)
356. Zhan, Z., Zhao, L.: Electrochemical reduction of CO_2 in solid oxide electrolysis cells. J. Power Sources **195**, 7250–7254 (2010)
357. Singh, V., Muroyama, H., Matsui, T., et al.: Feasibility of alternative electrode materials for high temperature CO_2 reduction on solid oxide electrolysis cell. J. Power Sources **293**, 642–648 (2015)
358. Cao, Z., Zhang, Y., Miao, J., et al.: Titanium-substituted lanthanum strontium ferrite as a novel electrode material for symmetrical solid oxide fuel cell. Int. J. Hydrog. Energy **40**, 16572–16577 (2015)
359. Yu, X., Long, W., Jin, F., et al.: Cobalt-free perovskite cathode materials $SrFe_{1-x}Ti_xO_{3-\delta}$ and performance optimization for intermediate-temperature solid oxide fuel cells. Electrochim. Acta **123**, 426–434 (2014)
360. Liu, Q., Dong, X., Xiao, G., et al.: A novel electrode material for symmetrical SOFCs. Adv. Mater. **22**, 5478–5482 (2010)
361. Yang, Z., Xu, N., Han, M., et al.: Performance evaluation of $La_{0.4}Sr_{0.6}Co_{0.2}Fe_{0.7}Nb_{0.1}O_{3-\delta}$ as both anode and cathode material in solid oxide fuel cells. Int. J. Hydrog. Energy **39**, 7402–7406 (2014)
362. Yang, Z., Chen, Y., Jin, C., et al.: $La_{0.7}Sr_{0.3}Fe_{0.7}Ga_{0.3}O_{3-\sigma}$ as electrode material for a symmetrical solid oxide fuel cell. RSC Adv. **5**, 2702–2705 (2015)
363. Lai, B.K., Kerman, K., Ramanathan, S.: Nanostructured $La_{0.6}Sr_{0.4}Co_{0.8}Fe_{0.2}O_3/Y_{0.08}Zr_{0.92}O_{1.96}/La_{0.6}Sr_{0.4}Co_{0.8}Fe_{0.2}O_3$ (LSCF/YSZ/LSCF) symmetric thin film solid oxide fuel cells. J. Power Sources **196**, 1826–1832 (2011)
364. Liu, L., Sun, K., Li, X., et al.: A novel doped CeO_2–$LaFeO_3$ composite oxide as both anode and cathode for solid oxide fuel cells. Int. J. Hydrog. Energy **37**, 12574–12579 (2012)
365. Fernández-Ropero, A.J., Porras-Vázquez, J.M., Cabeza, A., et al.: High valence transition metal doped strontium ferrites for electrode materials in symmetrical SOFCs. J. Power Sources **249**, 405–413 (2014)
366. Zhou, Q., Yuan, C., Han, D., et al.: Evaluation of $LaSr_2Fe_2CrO_{9-\delta}$ as a potential electrode for symmetrical solid oxide fuel cells. Electrochim. Acta **133**, 453–458 (2014)
367. Yaremchenko, A.A., Patrício, S.G., Frade, J.R.: Thermochemical behavior and transport properties of Pr-substituted $SrTiO_3$ as potential solid oxide fuel cell anode. J. Power Sources **245**, 557–569 (2014)
368. Wang, X., Zhang, C., Zang, G., et al.: Effect of doping content of Pr ions on oxygen vacancies in $SrTiO_3$ films. J. Alloys Compd. **637**, 277–280 (2015)

Muhammad Arif Khan received his Bachelor's degree in physical chemistry from the Institute of Chemical Sciences, University of Peshawar, Pakistan, and M.Phil. in physical chemistry from the NCE, University of Peshawar, Pakistan. Currently, he is working as a Ph.D. scholar under the supervision of associate Professor Hongbin Zhao at Shanghai University. His research interests are focused on electrode materials for energy storage devices and electrocatalysis.

Hongbin Zhao received his Ph.D. from Shanghai Jiaotong University in 2009 and completed his postdoctoral research in Shanghai University between 2009 and 2011. Since 2011, he has remained at Shanghai University in addition to working for a year in the Department of Chemical Engineering at the University of Waterloo, Canada, from 2014 to 2015 as a visiting scholar (Shanghai Pujiang Talent). He is currently an associate professor at Shanghai University, and his research interests focus on electrode materials for fuel cells, lithium-ion batteries, lithium–sulphur batteries and supercapacitors. He was awarded the "Shanghai Pujiang Talent" award and has published more than 70 academic papers, 1 edited book, 2 book chapters and 6 patents. In addition, he has also organized more than 5 academic research projects and one application project.

Wenwen Zou received his B.Sc. from the College of Engineering, Huzhou University, in 2017 and is currently a M.S. student at the College of Sciences, Shanghai University. His research interests include the synthesis of non-noble metal catalysts and their application in fuel cells and solid polymer electrolyte water-splitting techniques.

Zhe Chen received his B.Sc. from the College of Sciences, Shanghai University, in 2017 and is currently a M.S. student at the College of Sciences, Shanghai University. His research interests include the synthesis of non-noble metal catalysts and their application in fuel cells and solid polymer electrolyte water-splitting techniques.

Wenjuan Cao received her B.Sc. in 2016 majoring in chemical engineering and technology from the Zhengzhou University of Light Industry. Currently, she is pursuing her M.S. in the Department of Chemistry, Shanghai University. Her research interests focus on electrode materials for lithium-ion batteries, water-splitting catalysts and fuel cells.

Jianhui Fang started his career at the Shanghai University of Science and Technology in 1986 and received his Ph.D. from Shanghai University in 2006. Currently, he is a professor and supervisor at Shanghai University and his research field mainly involves the innovation and application of material chemistry, electrochemistry and water treatment technologies.

Jiaqiang Xu is professor and vice dean of the Department of Chemistry at Shanghai University. His research interests include controllable synthesis of nanostructured materials and their application in sensing, energy and environment. His accomplishments include over 200 peer-reviewed journal publications with 5700 citations and 42 H-Index, along with 6 provincial science and technology achievement awards and tens of patents. Currently, Jiaqiang Xu is also a director at the Special Committee on Gas and Humidity Sensor Technologies within China Electronics Society and an academic leader in the field of nanostructured materials and devices belonging to the Nanomaterials Chemistry Key Discipline of Shanghai Municipal Education Commission. He also is a member of the Council of Sensors and Actuators Technical Committee, China Instrument and Control Society and China Sensors Alliance.

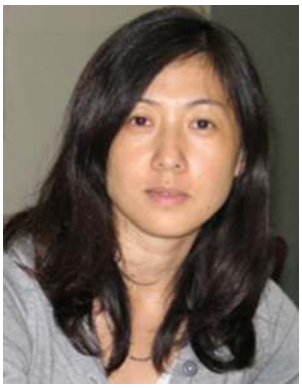

Lei Zhang is a senior research officer at the National Research Council Canada (NRC), a Fellow of the Royal Society of Chemistry (FRSC), an adjunct professor at Shanghai University, and the vice president of the International Academy of Electrochemical Energy Science (IAOEES). In 2004, she joined NRC to initiate the PEM Fuel Cell program and has also carried out R&D into other electrochemical energy technologies, such as supercapacitors, metal–air batteries and hybrid batteries. She has coauthored more than 170 publications (> 13000 citations), including over 80 referenced journal papers, 3 edited books, 4 book chapters, 5 patents and applications and over 50 technical reports. She is also a member of the NSERC Industrial R&D Fellowships College of Reviewers in Canada and an editorial board member of Electrochemical Energy Reviews (EER), Springer Nature. In addition, she is an active member of the Royal Society of Chemistry (RSC), the Canadian Society for Chemistry (CSC), the Canadian Society for Chemical Engineering (CSChE) and the International Academy of Electrochemical Energy Science (IAOEES).

Jiujun Zhang is a professor at Shanghai University and a principal research officer (Emeritus) and technical core competency leader at the National Research Council of Canada Energy (NRC). Dr. Zhang received his B.S. and M.Sc. in electrochemistry from Peking University in 1982 and 1985, respectively, and his Ph.D. in electrochemistry from Wuhan University in 1988. He then carried out three terms of postdoctoral research at the California Institute of Technology, York University, and the University of British Columbia. Dr. Zhang has over 30 years of scientific research experience, particularly in electrochemical energy storage and conversion. In addition, he is also an adjunct professor at the University of British Columbia and the University of Waterloo.